FISEVIER

Contents lists available at ScienceDirect

Palaeogeography, Palaeoclimatology, Palaeoecology

journal homepage: www.elsevier.com/locate/palaeo





New mammals from the Naskal intertrappean site and the age of India's earliest eutherians

Gregory P. Wilson Mantilla ^{a,*}, Paul R. Renne ^{b,c}, Bandana Samant ^d, Dhananjay M. Mohabey ^d, Anup Dhobale ^d, Andrew J. Tholt ^c, Thomas S. Tobin ^e, Mike Widdowson ^f, S. Anantharaman ^{g,h}, Dilip Chandra Dassarma ^g, Jeffrey A. Wilson Mantilla ^{i,*}

- ^a Burke Museum and Department of Biology, University of Washington, Seattle, WA 98195-1800, USA
- ^b Berkeley Geochronology Center, Berkeley, CA 94709, USA
- ^c Department of Earth and Planetary Science, University of California, Berkeley, CA 94709, USA
- ^d Department of Geology, RTM Nagpur University, Nagpur 440001, India
- ^e Department of Geological Sciences, University of Alabama, Tuscaloosa, AL 35487, USA
- f Department of Geology, School of Environmental Sciences, University of Hull, HU6 7RX, UK
- g Palaeontology Division, Geological Survey of India, Hyderabad, 500-068 India
- ^h Department of Geology, Presidency College, Chennai 600 005, India
- i Museum of Paleontology and Department of Earth & Environmental Sciences, University of Michigan, Ann Arbor, MI 48109-1085, USA

ARTICLE INFO

Editor: Howard Falcon-Lang

Keywords:
Deccan Traps
mammals
Cretaceous-Paleogene
palynology
geochronology
magnetostratigraphy
chemostratigraphy

ABSTRACT

The first Cretaceous mammals described from India were recovered from the Naskal locality, on the southeastern edge of the Deccan Traps Volcanic Province (DTVP), where it is preserved between two basalt flows. Because the DTVP eruptions spanned the Cretaceous-Paleogene boundary (KPB), it is often unknown whether trap-associated fossil sites are latest Cretaceous (Maastrichtian) or early Paleocene in age. The Naskal locality accounts for nearly half of published mammal records from DTVP-associated sediments as well as a host of other vertebrate microfossils. Its age takes on singular importance in the context of mammalian evolution in India and the effects of the end-Cretaceous mass extinction and subsequent evolutionary radiation of placentals. Here we describe two new mammal species, *Indoclemensia naskalensis* gen. et sp. nov. and *I. magnus* sp. nov., from Naskal and present evidence from 40 Ar/ 39 Ar geochronology, magnetostratigraphy, and chemostratigraphy of the over- and underlying basalt flows to refine the age of the Naskal locality and nearby Rangapur locality. In conjunction with palynostratigraphy and vertebrate biostratigraphy, these sites can be confidently restricted to a <100 kyr interval spanning the KPB. The most probable 40 Ar/ 39 Ar age is latest Cretaceous (66.136–66.056 Ma), but an earliest Paleogene age cannot be ruled out. We explore the implications of this age assignment for Deccan chemostratigraphy and Deccan volcanism, Cretaceous-Paleogene (K/Pg) mass extinction, Indian mammalian faunal evolution, and the timing of the origin of placental mammals.

1. Introduction

The first Cretaceous mammal specimens from India were reported by Prasad and Sahni (1988) from the Naskal locality in the south-central state of Telangana (Fig. 1). Attributed to the new genus and species *Deccanolestes hislopi*, the original materials (three isolated cheek teeth) were recovered from a vertebrate microfossil concentration intercalated between two flows of the Deccan Traps. As a result of continued bulk

sampling and screenwashing, the Naskal locality has yielded nearly half of all published Deccan Trap-associated mammalian specimens (22 out of 51 total specimens; Prasad and Sahni, 1988; Prasad et al., 1994; Prasad and Godinot, 1994; Krause et al., 1997; Prasad et al., 2007b; Wilson et al., 2007; Boyer et al., 2010). Thus, Naskal holds a central role in our understanding of this critical interval of mammalian evolution on the Indian subcontinent.

Like many other Deccan Trap-associated sedimentary deposits in

E-mail addresses: gpwilson@uw.edu (G.P. Wilson Mantilla), prenne@bgc.org (P.R. Renne), bandanabhu@gmail.com (B. Samant), dinomohabey@yahoo.com (D.M. Mohabey), anupdhobale@gmail.com (A. Dhobale), andytholt@gmail.com (A.J. Tholt), ttobin@ua.edu (T.S. Tobin), M.Widdowson@hull.ac.uk (M. Widdowson), gsi_sa@hotmail.com (S. Anantharaman), dilipchandra@yahoo.com (D.C. Dassarma), wilsonja@umich.edu (J.A. Wilson Mantilla).

^{*} Corresponding authors.

India, the Naskal locality is remote from the thick sequence of flows exposed on the Western Ghats (Fig. 1), which has previously been the focus for volcanological, chemostratigraphic, and geochronological studies (e.g., Beane et al., 1986; Devey and Lightfoot, 1986; Pande et al., 1988; Mitchell and Widdowson, 1991; Venkatesan et al., 1993; Jay and Widdowson, 2008; Jay et al., 2009; Sprain et al., 2019; Schoene et al., 2019). Like many Deccan Trap-associated fossil localities, Naskal has a limited thickness (<3 m) and restricted lateral exposure (<15 m) and areal distribution (<5 m²). The associated basalt flows provide geochronological data, and their geochemistry enables correlation to the Western Ghats chemostratigraphy. An informal field designation for Deccan Trap-associated fossil localities was established more than 150 years ago (e.g., Blanford, 1867a, 1867b), gained currency in nineteenth and early twentieth century descriptions of Indian geology and paleontology, and remains pervasive today. "Intertrappean" deposits like Naskal occur between two lava flows, whereas "infratrappean" deposits (e.g., Bara Simla) are only capped by a flow and are typically underlain by basement rocks. This field nomenclature often serves as a stand-in for age assessment—infratrappean horizons are considered older than intertrappean horizons, and most intertrappean horizons are considered

similar in age to one another. This assumption is incorrect because lava flows covered the basement at different times during the eruptive phase (Sahni et al., 1994). Unfortunately, these simplistic age proxies are typically unaccompanied by (and can preclude) deeper investigation of the age of deposition, and in some cases, they can even overturn actual sampling of age data. For example, important dinosaur-bearing infratrappean localities at Rahioli and Bara Simla (Jabalpur) have been considered to be the same age, even though they were deposited in different inland basins during different magnetic polarity chrons (C30n and C29r, respectively; Hansen et al., 1996, 2005; Mohabey and Samant, 2013).

Description of *Deccanolestes hislopi* by Prasad and Sahni (1988) led to more purposeful and intensive sampling for vertebrate microfossils in Deccan Trap-associated sedimentary deposits. The Geological Survey of India (Southern Region) led paleontological and geological exploration in infratrappean and intertrappean beds in the states of Telangana and Karnataka from 1992 to 1999. Underwater screenwashing of \sim 20,000 kg of matrix from several localities and fossil picking under 10x magnification led to the recovery of more than 70 mammalian specimens of isolated teeth, dentulous jaws, and postcranial elements. Some

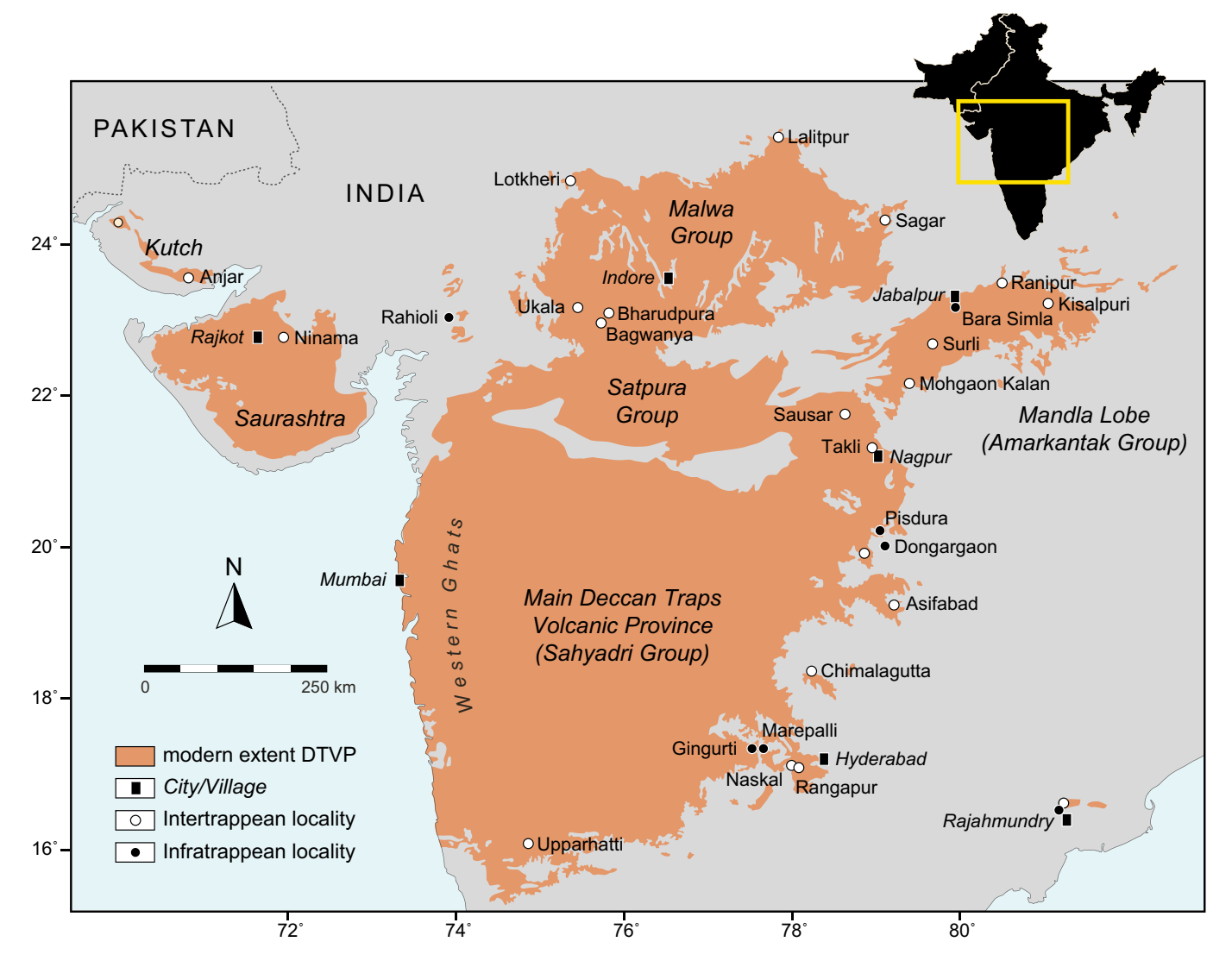


Fig. 1. Map of India showing vertebrate- and palynomorph-bearing fossil localities associated with the Deccan Traps Volcanic Province (DTVP). The lobes and subregions of the DTVP have distinct spatial and temporal signatures, and their outlines are based on Dasgupta et al. (1993) and labeled in larger-point italics type. Cities and villages (black-filled rectangles) are labeled in smaller-point italics type. Infratrappean localities (black-filled circles) and intertrappean localities (white-filled circles) that are discussed in the text are labeled; others are not. The map and tracing of the DTVP are modified from Wilson et al. (2019b:fig. 1). Note that the border between India and Pakistan in both the inset and enlarged maps is approximate and is not a political boundary.

specimens in the Geological Survey of India collection have been mentioned or tentatively identified in brief reports (Das Sarma et al., 1995; Anantharaman and Das Sarma, 1997), but detailed descriptions have been undertaken for only two taxa. Avashishta bacharamensis was the first mammaliaform reported from the infratrappean beds of India and provided a 90-million-year range extension for Haramiyida (Anantharaman et al., 2006). Dakshina jederi is a sudamericid gondwanatherian described from teeth recovered from the Naskal locality and the Upparhatti locality near Gokak, Karnataka (Wilson et al., 2007). This taxon has been suggested to be a junior synonym of Bharattherium bonapartei (Prasad et al., 2007b).

In this paper, we provide robust new age data for the Naskal intertrappean locality and the neighboring Rangapur locality, based on biostratigraphy, field mapping based physical volcanic stratigraphy, chemostratigraphy, magnetostratigraphy, and geochronology. We also describe two new eutherian mammal species based on four isolated upper and lower molars from the Naskal locality. We then discuss the implications of this important age assessment for Deccan chemostratigraphy and Deccan volcanism, extinctions at the Cretaceous-Paleogene boundary (KPB), the evolution of India's mammalian fauna, and the timing of the origin of placental mammals.

1.1. Institutional abbreviations

GSI, Geological Survey of India, Kolkata (Calcutta), India; GSI/PAL/SR, Geological Survey of India, Palaeontology Division, Southern Region, Hyderabad, India; RTMNU, RTM Nagpur University, Nagpur, India.

1.2. Dental measurements and conventions

We use the dental terminology of Bown and Kraus (1979), Nessov et al. (1998), and Kielan-Jaworowska et al. (2004). We refer to lower dentition with lower-case letters and upper dentition with upper-case letters (m and M, respectively, for molars); the number following the letter designates position in the dental series. Figure 2 provides a schematic representation and explanation for all dental measurements and their abbreviations. Measurements were taken to the nearest hundredth millimeter using ImageJ (Schneider et al., 2012) on standardized images in the views shown in Figure 2.

BL В C PAH PRH MEH DW MW PRL TAL PADH TRW TAH TAW PDH MDH **TRAng**

2. Geological setting

The Naskal and Rangapur sections are intertrappean exposures located on the southeastern portion of the main part of the Deccan Traps Volcanic Province (DTVP; Jay and Widdowson, 2008) in the state of Telangana (Fig. 1). There, basalt flows and associated infratrappean sediments rest unconformably over basement rocks. Previous work identified at least nine basalt flows, attaining a minimum thickness of ~150 m (Mitchell and Widdowson, 1991; Bilgrami, 1999; Jay and Widdowson, 2008). Jay and Widdowson (2008) demonstrated the presence of lavas in the southeastern DTVP whose geochemistry can be correlated with Wai Subgroup formations (viz. Poladpur, Ambenali, Mahabaleshwar) of the Western Ghats (Table 1), but they did not establish any flow stratigraphy or geochronology for these lavas. This chemostratigraphy provided our first indication that the Naskal and Rangapur intertrappeans might be younger than previously thought (Wilson et al., 2019a).

Geological Survey of India researchers (Dutt, 1975; Ahluwalia, 1990) established a local lava flow stratigraphy mapped at the 1:50,000 scale,

Table 1

Nomenclature and approximate maximum thicknesses of the major stratigraphical units of the DTVP from the Western Ghats. Packages of basalt flows with similar chemical and isotopic characteristics comprise the different subgroups and formations (see Beane et al., 1986; Devey and Lightfoot, 1986; Mitchell and Widdowson, 1991).

Group	Sub-Group	Formation	Maximum	
			Thickness (m)	
Topmost lavas				
	WAI	Panhala	175	
		Mahabaleshwar	280	
		Ambenali	500	
		Poladpur	400	
DECCAN TRAPS	LONAVALA	Bushe	325	
		Khandala	180	
	KALSUBAI	Bhimashankar	140	
		Thakurvadi	650	
		Neral	145	
		Igatpuri	150	
		Jawhar	700	
Lowermost lavas				

Fig. 2. Schematic representation for all measurements taken on eutherian molar teeth described herein. A Right upper molar in A, occlusal; B, buccal; and, C, mesial views. Right lower molar in D, occlusal; E, buccal; and F, lingual views. Most measurements and descriptions follow Butler (1990), but distal width and trigonid width follow Archibald (1982) and talonid height follows Archibald et al. (2001). Measurements were taken using conventional mesiodistal and horizontal axes. The mesiodistal axis for upper molars is oriented parallel to the line passing through the apices of the metacone and paracone, and that for lower molars is oriented parallel to the line passing through the apices of the entoconid and metaconid. The horizontal base line for both upper and lower molar crowns is placed at the cervical line of the tooth (i.e., the boundary between the enamel-covered crown and the root). Abbreviations: BL, buccal length; DW, distal width; L, length; MDH, metaconid height; MEH, metacone height; MW, mesial width; PAH, paracone height; PADH, paraconid height; PDH, protoconid height; PRH, protocone height; PRL, protoconal length; PRW, protoconal width; TAH, talonid height; TAL, talonid length; TAW, talonid width; TRAng, trigonid angle; TRL, trigonid length; and TRW, trigonid width.

based on the physical-volcanic characters of the flows, petrological and petrogenetic studies, and associated sediments and red boles (Fig. 3). Dutt (1975) and Ahluwalia (1990) differentiated nine flows, numbered sequentially, with thicknesses ranging from 7–30 m. In most places, the local tops of this flow sequence are substantially laterized, in some cases to a depth greater than 10 m. More details on flow architecture are provided below in Section 3.3.

There are up to three different sites that have produced vertebrate microfossils in the intertrappean sediments near Naskal village, indicating this area developed as a broad site of deposition during an eruptive hiatus in this area of the southeastern DTVP. Hereafter, we refer to them as: (1) the "Prasad Naskal site," for that explored by Prasad and various co-authors (Prasad and Sahni, 1988, 2014; Khajuria and Singh, 1992; Prasad et al., 1994; Khajuria and Prasad, 1998; Prasad and de Lapparent de Broin, 2002; Singh et al., 2006); (2) the "GSI Naskal quarry," for that explored by researchers of the GSI Southern Region in the 1990s (Das Sarma et al., 1995; Anantharaman and Das Sarma, 1997); and (3) the "2016 Naskal site," for that explored during our most recent field research in 2016, 2017, and 2019. The GSI Naskal quarry and the 2016 Naskal site are within meters of each other (Fig. 4) but at different stratigraphic levels (see Section 2.1). Regrettably, the imprecise nature of the published site descriptions of the Prasad Naskal site at the outcrop scale and the high rates of surficial weathering and erosion in the area have made direct comparison of that site with the other two localities challenging. Nevertheless, the available descriptions of these sites are lithologically similar to one another (see Section 2.1) and thus likely represent comparable, if not directly connected, depositional environments.

The Prasad Naskal site is described in all publications as located ~ 2 km northeast of the village of Naskal, in the Rangareddi District of Telangana (Fig. 3). This description is consistent with the location of the GSI Naskal quarry and 2016 Naskal site (Fig. 3), although insufficiently precise to definitively connect the sites. Despite including similar language describing the location of their site in their text, Prasad and de Lapparent de Broin (2002:fig. 1)) depicted their "Naskal" site to the southeast of Naskal, near the Rangapur fossil locality. Given the continuity of authorship with previous publications on the Prasad Naskal site, we believe this figure is likely in error and defer to their text description. The lack of precise location coordinates or site descriptions means that we cannot be certain that there is just one Prasad Naskal site, and inconsistencies in the names assigned to the basalts immediately bracketing the site create additional uncertainty.

The basalt flow stratigraphy of Dutt (1975) and Ahluwalia (1990) indicates that the mammal-bearing intertrappean sections at Naskal and Rangapur are bracketed by Flows 3 and 4 (Fig. 3), as reported in initial descriptions of the geology of the Prasad Naskal site (Prasad and Khajuria, 1990; Khajuria and Singh, 1992). However, subsequent work by these same authors interpreted the Naskal intertrappean exposure to be bracketed by Flows 4 and 5 without further elaboration (e.g., Prasad et al., 1994; Khajuria and Prasad, 1998). Although these workers seem to have followed the basalt flow stratigraphy of Dutt (1975) and Ahluwalia (1990), no geological maps with updated flow designations were included in these later studies. Nevertheless, it is a feature of lava stratigraphies for individual flow units within a single lava field eruption to terminate and to be overlain by renewed activity during the same eruptive phase (i.e., during development of a flow field). As such, we are unclear on whether this change in flow identification indicates reference to different intertrappean exposure, reflects a decision to revise the previously existing basalt stratigraphy, is a function of the lava complexity, or represents a mapping error.

This omission has resulted in ambiguity regarding the stratigraphic position of the Naskal exposure relative to nearby sites, including Rangapur. Whereas most previous work implicitly suggested that the Naskal intertrappean sediments are exposed along a single horizon, Venugopal Rao (1987) recorded two fossiliferous Naskal intertrappean sites — one between Flows 3 and 4 and the other between Flows 4 and 5 — but did

not specify whether vertebrate fossils had been found at both. Despite this uncertainty, and recognizing eruptive complexity at the very local scale, we will henceforth describe the Naskal intertrappean exposure studied herein as being located between Flows 3 and 4, based on mapping efforts by Dutt (1975) and Ahluwalia (1990).

The Rangapur fossil site has received less study than has Naskal (Rana, 1988, 1990a, 2005; Rana and Wilson, 2003), but previous work is consistent about its location. The Rangapur intertrappean lies 6 km south-southeast from the Naskal site and has generally been considered its lateral equivalent (Prasad et al., 1994) and mapped as such (Fig. 3). However, the Rangapur intertrappean differs lithologically from the Naskal intertrappean in being more calcareous and stratigraphically thinner, exposing just over 2 m of section. Likewise, the fossil content of these sites has been interpreted to indicate different ages for the sites, with Naskal fossils suggesting a Maastrichtian age (Prasad and Sahni, 1988; Prasad et al., 1994; Singh et al., 2006) and Rangapur fossils suggesting either a Maastrichtian (Rana and Wilson, 2003) or a Paleocene age (Rana, 2005). At Rangapur, as at Naskal, intertrappean sediments are described as bracketed by Flows 4 and 5 in older literature (Rana, 1988, 1990a), but field mapping suggests these are Flows 3 and 4 (Dutt, 1975; Ahluwalia, 1990). As discussed in Sections 3.3, 3.4, and 3.6, our results suggest that the overlying flow at both Naskal and Rangapur is Flow 4, but the underlying flows differ slightly geochemically and will be designated Flows 3a and 3b, respectively.

2.1. Naskal intertrappean: lithology and sampling

The intertrappean sediments of the GSI Naskal quarry/2016 Naskal site (17° 14' 21" N, 77° 53' 16" E) were deposited across an irregular basalt surface of Flow 3a at an elevation of 624 m above mean sea level (amsl), which has approximately 4 m of topographic relief (Fig. 3), a value consistent with that observed in modern basaltic flow fields (e.g., Zimbelman and Johnston, 2002). This paleotopographic irregularity may also partially account for the different measured thickness and lithologies recorded by previous researchers. The maximum stratigraphic thickness of this intertrappean (i.e., between Flows 3a and 4) is 3 m, although there is no single exposure that reveals the full thickness of the section.

The GSI Naskal quarry, which was excavated by the GSI Southern Region in the 1990s, is in the upper part of the described section (Figs. 4and 5). Approximately 18,000 kg of bulk sediment was collected from the white marlstone to mudstone, the loose, yellowish, shaly/carbonate mudstone to marlstone, and the hard, yellowish, shaly marlstone for screenwashing and vertebrate microfossil sorting. The vertebrate microfossils recovered were mostly from the white marlstone to mudstone. This lithology is similar to that described as the fossiliferous horizon at the Prasad Naskal site and suggests our site is located nearby or at the same location described in their studies. The GSI Naskal quarry terminated at an underlying ~20-cm-thick, black-to-gray cherty limestone (Fig. 5). By 2016, sediment within the upper part of the GSI Naskal quarry was no longer exposed or accessible by trenching because most of it already had been removed. However, deep (>2 m) trenching in 2019 did locate the lowest chert layer of the GSI Naskal quarry in direct superposition to the NSK-B Section of the 2016 Naskal site (Fig. 4), although no remaining original strata were preserved above this chert.

In 2016, we examined an exposure ~7 m to the west of the GSI Naskal quarry (NSK-A; Figs. 4 and 5) to describe the sedimentology from the stratigraphic interval sampled during original work there, although this section was no longer well exposed by 2019. We sampled for palynomorphs from several strata and across a lateral extent at NSK-A, but only two chert layers were productive (Fig. 5). A definitive connection between either chert layer from NSK-A and the chert layer at the top of NSK-B could not be made due to lack of exposure. Although the lower chert from NSK-A is at least 1.5 m higher in elevation than that exposed at NSK-B or the GSI Naskal quarry, the most likely depositional model is that these chert layers are laterally continuous. This stratum,

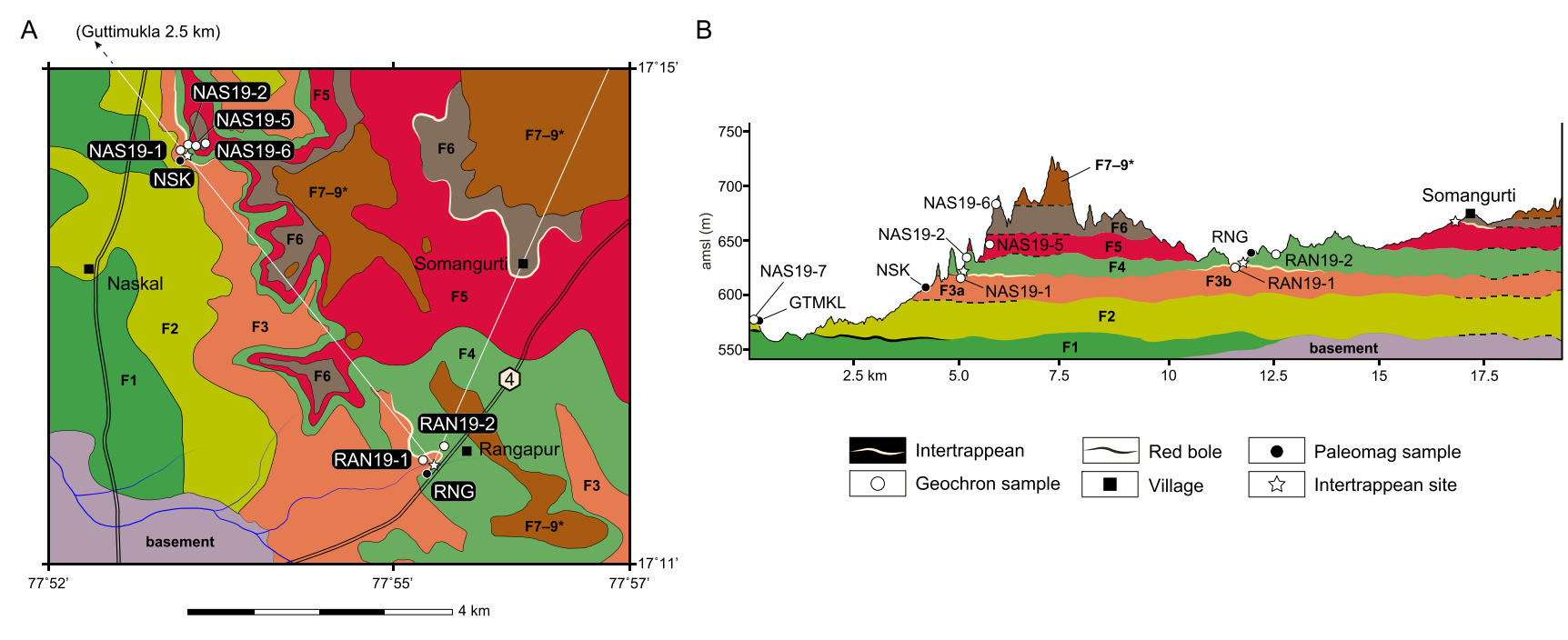


Fig. 3. Deccan Traps lava flow distributions at Naskal and Rangapur localities, based on mapping by Geological Survey of India at the 1:50,000 scale (modified from Dutt, 1975 and Ahluwalia, 1990). A, Map view and B, reconstructed cross-sectional view from northwest (Naskal site, NSK) to southeast (Rangapur site, RNG) to northeast (Somangurti), indicating lava flows (F1–9), fossil localities (stars), and location of samples collected for Ar-Ar dating (open circles) and paleomagnetic analysis (closed circles). The cross-sectional view was drawn based on the elevation profile from Google Earth connecting the points of interest (white line in A). The X and Y axes show distance in kilometers and elevation in meters, respectively. NSK and RAN/RNG numbers refer to geochronological samples taken at Naskal and Rangapur, respectively (see Table 5). Dashed lines indicate inferred contacts between flows.



Fig. 4. Photograph showing the relative proximity of the GSI Naskal quarry and the 2016 Naskal site. The GSI quarry is in the center, and the 2016 Naskal sedimentological logs were conducted to the right (NSK-B, lower) and left (NSK-A, upper). The GSI Naskal quarry and NSK-A are likely stratigraphically equivalent, and the lowermost chert from the GSI Naskal quarry can be traced directly to the uppermost chert from NSK-B. Vertebrate fossils were recovered from both GSI Naskal quarry and NSK-B, but only those from GSI Naskal quarry are included in this paper. Palynomorphs were recovered from NSK-A. Photograph by DMM.

from which NSKAP-3 and NSKAP-4 were collected (Fig. 5), is interpreted to be draped across original topographic relief. The upper chert layer also yielded identifiable palynomorphs (NSKAP-1; Fig. 5). An unproductive pollen sample was collected from a white marlstone in the GSI Naskal quarry section.

We collected bulk sediment samples for screenwashing and vertebrate microfossil sorting (NSK-B 2.1, 2.2) from this site in 2016, 2017, and 2019. Samples were recovered from a wavy-laminated to cmbedded, sandy clay interbedded/laminated with occasionally calcareous, siltstone (Figs. 4 and 5). This unit appears similar to ripplelaminated mudstones described in the lower exposures of the Prasad Naskal site, but those studies recovered fossil remains from higher in the section, from a calcareous mudstone below a basalt that we designate as Flow 4 (Prasad et al., 1994; Prasad and Sahni, 1988; Khajuria and Prasad, 1998). Vertebrate microfossils, including mammals, recovered from this sampling will be reported in future studies. Overall, the 2016 Naskal site section fines upwards and becomes less sandy with discontinuous organic laminae and the appearance of some thin (~1 cm) carbonate beds. The palynological samples, which are from the NSK-A section, are stratigraphically below and therefore very slightly older than most vertebrate microfossil samples collected at the GSI Naskal quarry (described in Section 4) and younger than those collected at the 2016 Naskal site, although all are preserved within the same intertrappean sequence (Fig. 5).

⁴⁰Ar/³⁹Ar geochronological samples were taken from the least weathered exposures of the two flows bracketing the Naskal intertrappean: Flow 3a (NAS19-1, elevation 614 m, 5.6 m below the top of flow); and Flow 4 (NAS19-2, elevation 632 m, 10.9 m above the lowest exposure of flow). Oriented blocks for paleomagnetic analysis were collected from Flow 3a (Table 2), at a level 10 m below the top of the flow (elevation 632 m).

2.2. Rangapur intertrappean: lithology and sampling

The Rangapur fossil site is exposed along a small river cut $(17^{\circ}\ 11^{\circ}\ 48^{\circ}\ N,\ 77^{\circ}\ 55^{\circ}\ 26^{\circ}\ E)$ northwest of the village of Rangapur and 6 km southeast of the Naskal site (Figs. 1 and 3). The intertrappean sediments are exposed along a greater lateral extent (>100 m) and over less

obvious depositional topography than the GSI Naskal quarry/2016 Naskal site. Most of the sediment is fine-grained and calcareous to some degree, ranging from marl to more pure micrite (Fig. 6). As at Naskal, samples were collected from several lithologies and across a lateral extent (>100 m) to find palynomorphs, but only one chert layer yielded useful palynomorphs (RNGP-2; Fig. 6).

We collected bulk sediment samples for vertebrate microfossil recovery from the marl horizon (varies laterally from white to brown) at $\sim\!60$ cm in the measured section (Fig. 6), which is the same horizon that was sampled previously (Rana, 1988, 1990a; Rana and Wilson, 2003). The vertebrate microfossil-rich Rangapur intertrappean exposure, which comprises $\sim\!200\text{-cm-thick}$ sediments, also shows draping contact with the lower and upper flows. The sediments are dominantly marly, with presence of thin partings of silicified shale, thin gray and black chert and tuffaceous clays. In some places, almost a meter of pervasively silicified limestone is exposed, but in other places the overlying flow (Flow 4) is also observed to be directly in contact with the marls below the capping chert (Fig. 6).

 40 Ar/ 39 Ar geochronological samples were taken from the two flows bracketing the Rangapur intertrappean: Flow 3b (RAN19-1, elevation 626 m); and Flow 4 (RAN19-2, elevation 638 m). Oriented blocks for paleomagnetic analysis were collected from Flow 4 (elevation 632 m; see Table 2).

3. Age of the Naskal and Rangapur intertrappean sites

Historically, general constraints for the age of the Deccan Traps were based on their stratigraphic position between the underlying Bagh beds, regarded as Cretaceous in age (Duncan, 1865), and overlying 'nummulitics' of Eocene age (Rogers, 1869). Early attempts at refining the age of Deccan Trap-associated sediments relied initially on invertebrate biostratigraphy and only later on vertebrate fossils. In an inversion of current practice, the age of the Deccan Trap-associated sediments was "principally of interest for the evidence it may give as to the age of the great volcanic formation with which it is so closely connected" (Medlicott, 1872:115).

Below we evaluate the biostratigraphic, chemostratigraphic, paleomagnetic, and geochronological data for the ages of the Naskal and

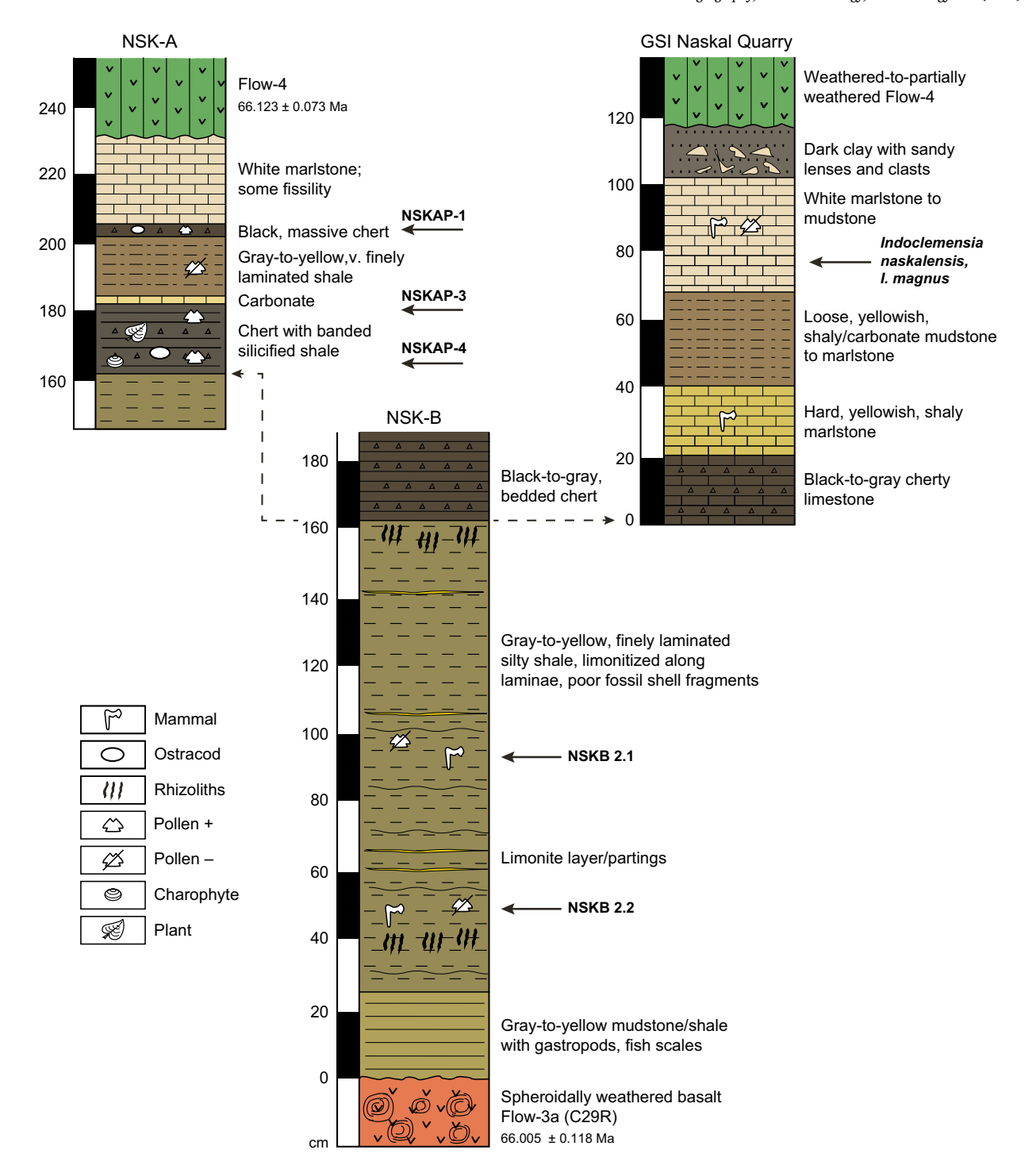


Fig. 5. Sedimentological log of GSI Naskal quarry and 2016 Naskal site. Strata from which successful (Pollen +, labeled) and unsuccessful (Pollen -, unlabeled) palynological samples were taken are marked. Main vertebrate microfossil-bearing levels are indicated. NSKB 2.1 and 2.2 represent collections for microfossil sorting made in 2019 but are not yet described. Stratum from which the new mammalian taxa (*Indoclemensia* spp.) described in this paper were recovered are marked. 40 Ar/ 39 Ar plateau age data for NAS19-1 (Flow 3a) and NAS19-2 (Flow 4) are from Table 5. However, note that application of Monte Carlo methods and Bayesian constraint to 40 Ar/ 39 Ar ages of the bounding lavas (see Section 3.6.1) indicates that the permissible age range of the Naskal intertrappean is between 66.136 and 66.056 Ma, at 68% confidence. Abbreviations: NSK, Naskal; NSKAP, Naskal-A section palynological sample; NSKB, Naskal-B section vertebrate fossil sample.

Rangapur intertrappean localities. In each subsection, we synthesize the previously published data and then present our new data and age assessment.

3.1. Vertebrate fossil biostratigraphy of Deccan Trap-associated deposits

Age estimates for Deccan Trap-associated fossiliferous deposits

diverged widely at first, including strong claims for Cretaceous and Eocene ages. Through time, these estimates each would ratchet upwards and downwards, respectively, towards the currently accepted Maastrichtian age for most intertrappean beds (but see Cripps et al., 2005). Fig. 1 shows a map of vertebrate-bearing fossil localities associated with the DTVP.

Table 2

Paleomagnetic data for localities in Rangapur (RNG), Naskal (NSK), and Guttimukla (GTMKL). Abbreviations: Alpha 95, circle of confidence with 95% probability level; D, declination; dm, the semi-axis of the 95% confidence ellipse perpendicular to the great-circle path; dp, the semi-axis of the 95% confidence ellipse along the great-circle path from site to pole; F, flow; I, inclination; k, precision parameter; n, number of specimens; N, normal polarity; R, reversed polarity; VGP, Virtual Geomagnetic Pole.

	RNG (F4)	NSK (F3a)	GTMKL (F2)
n	5	6	5
D	133.9°	172.7°	165.2°
I	69.9°	5.0°	26.6°
alpha95	4.8°	14.7°	10.2°
k	259.13	21.78	57
VGP lat	44	22.6	-55.5
VGP long	53.2	23.4	103.5
dp	7.0885	14.7964	6
dm	8.2492	20.857	11.1
Palaeolatitude	53.79	35.52	_
Polarity (N/R)	R	R	R

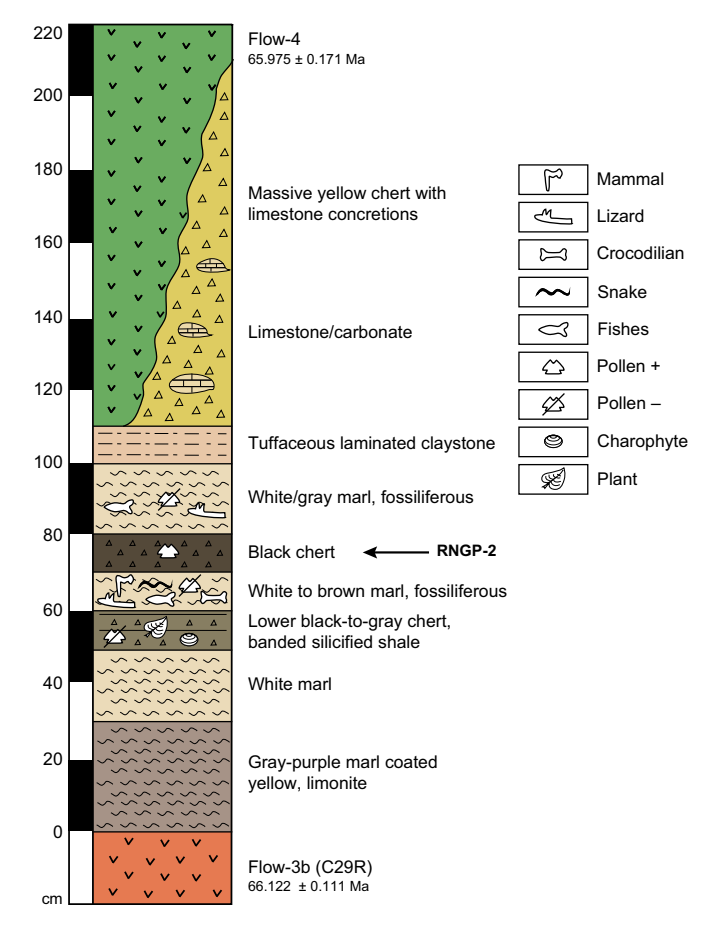


Fig. 6. Sedimentological log of Rangapur intertrappean section showing strata from which vertebrate microfossils have been recovered and where both successful (Pollen +, labeled) and unsuccessful (Pollen -, unlabeled) palynological samples were collected. 40 Ar/ 39 Ar plateau age data for RAN19-1 (Flow 3b) and RAN19-2 (Flow 4) are from Table 5. However, note that application of Monte Carlo methods and Bayesian constraint to 40 Ar/ 39 Ar ages of the bounding lavas (see Section 3.6.1) indicates that the permissible age range of the Rangapur intertrappean is between 66.184 and 66.075 Ma, at 68% confidence. Abbreviation: RNG, Rangapur; RNGP, Rangapur section palynological sample.

3.1.1. Dinosaurs

Evidence for a Cretaceous age for the Lameta infratrappean beds was suggested by its possible correlation with the Bagh beds, which were

considered to be Cretaceous in age based on fossil echinoderms (Duncan, 1865). The first reported dinosaur from India, a "Saurian closely allied to Pelorosaurus" collected from Jabalpur in 1828 (Sleeman, 1844), drew comparisons with fauna from the Wealden of England, and thus an Early Cretaceous age (Lydekker, 1877:40). This assessment would hold for a century, supported by new discoveries and intensive field work in central India by Matley (1921:159), who considered the carnivorous and herbivorous dinosaur fauna at Jabalpur consistent with an Early Cretaceous age. A century after Lydekker's initial report on Titanosaurus indicus, Chatterjee (1978) presented a reassessment of the Indian dinosaur fauna that implied a Late Cretaceous age for Jabalpur and other infratrappean sites in the Lameta Formation. This was based on links between titanosaur sauropods in Jabalpur and the Ariyalur Group (Cauvery Basin), which was considered Maastrichtian based on marine index fossils, as well as the re-interpretation of the Indian theropod Indosuchus as a tyrannosaurid (Walker, 1964), a group then considered to be restricted to the latest Cretaceous (see Chatterjee, 1978:571). Buffetaut (1987) likewise mentioned possible correlation between the Lameta Formation and the Maastrichtian Ariyalur Group based on dinosaur remains, but viewed the comparisons insufficiently detailed to warrant a definitive link. Instead, Buffetaut (1987) listed several lines of evidence that suggested a post-Turonian age for the Lameta Formation, including similarities with titanosaurs from Argentina and France, the re-interpretation of Indosuchus as a tyrannosaurid, as well as thenemerging evidence of the presence of the myliobatoid ray Igdabatis in the Lameta Formation (see Section 3.1.3).

The systematic assessments of the Indian dinosaur fauna by Huene (1933), Walker (1964), Chatterjee (1978), and Buffetaut (1987) are, to varying degrees, now considered invalid. All Indian theropods are now definitively included within Abelisauroidea, not Megalosauridae or Tyrannosauridae (e.g., Bonaparte et al., 1990; Molnar, 1990). All Indian titanosaurs are closely related to other Gondwanan forms, principally those of Madagascar and South America (see Wilson and Upchurch, 2003; Wilson et al., 2009, 2011; Wilson et al., 2019a, 2019b). Nevertheless, the inference of a latest Cretaceous age for the Lameta Formation remains.

The presence of non-avian dinosaurs in some Deccan Trap-associated sediments in India suggests deposition occurred prior to the Cretaceous-Paleogene (K/Pg) event, but these fossils are routinely inferred as Maastrichtian in age, regardless of biostratigraphic distribution of the individual taxon sampled. For example, titanosaur eggshell of the oogenus Megaloolithus is known to occur in slightly older Campanianaged sediments in Argentina (e.g., Dingus et al., 2000; Chiappe et al., 2001). There are even reports of Megaloolithus eggshells in the Middle Jurassic (Garcia et al., 2006). Theropod teeth, including those of abelisauroids, are occasionally diagnosable to the genus level (e.g., Masiakasaurus; Carrano et al., 2002) but most often are not, and so precise age assessments based on them are not possible. A further complication is that the conventional assumption that infratrappean horizons are everywhere equivalent in age and older than intertrappean horizons (which themselves are of similar age to one another) has allowed biostratigraphic indicators at one site to extend to other sites with similar relationships to the Deccan Traps.

3.1.2. Ray-finned fish

An Eocene age for the infratrappean Lameta Formation of central India was initially based on similarities of fossil plants, invertebrates, and actinopterygian fish with those of the London Clay (Hislop and Hunter, 1854). This early Tertiary age was supported in subsequent studies of Deccan Trap-associated ichthyofauna. Woodward (1908) described from Dongargaon, an infratrappean site in central India, three new fish species: Eoserranus hislopi, Lepidosteus indicus, and Pycnodus lametae. Based on the stratigraphic ranges of closely related fish, he suggested that "the age of the Lameta fish-fauna is therefore fixed between the Danian Cretaceous and the Upper Eocene" (Woodward, 1908:5). Hora (1938) followed with a detailed examination of fish from

the same infratrappean site (Dongargaon) and several intertrappean sites (Paharsingha, Takli, Deothan, Kheri). Based on a previous study of the biogeographic affinities of infratrappean and intertrappean fossil fish (Hora, 1937), he estimated "these beds were laid down in the early tertiaries when ... the land connection between India and Africa had disappeared" (Hora, 1938:372). He also distinguished their relative ages, asserting that infratrappeans are the oldest Deccan Trap-associated beds and that certain intertrappean horizons (Takli, Paharsingha) were older than others (Deothan, Kheri). Slightly tighter age constraints were suggested for new intertrappean sites of Ninama and Bamanbor in Saurashtra, western India by Borkar (1973), who suggested the fish fauna was of Paleocene-lower Eocene age. Much more recently, the Bamanbor intertrappean fish fauna was estimated to be older than 62 Ma, between Late Cretaceous and early Paleocene (Arratia et al., 2004:638). A similar age estimate was provided for the Rangapur intertrappean, based on otoliths pertaining to 16 fish species associated with freshwater ostracod and charophyte assemblages of latest Cretaceous-Paleocene age (Rana, 1988, 1996). In a subsequent revision of otoliths from Rangapur and other intertrappean sites (Naskal, Nagpur [Takli], Chemalgutta=Chimalagutta), Nolf et al. (2008:240) narrowed the inferred temporal range to Maastrichtian "not only based on the fishes, dinosaurs, ostracods, and palynofossils, but also because of the striking similarity between the fauna and flora of infra- and intertrappean beds."

3.1.3. Igdabatis

The convergence towards a Maastrichtian age for Deccan Trapassociated sediments in India may be tied to reliance on vertebrate biostratigraphic indicators, principally the myliobatoid ray Igdabatis sigmodon. Igdabatis was described by Cappetta (1972) on the basis of teeth collected from the deposits of the Iullemmeden Basin exposed at Mont Igdaman, Niger (now referred to as Mont Indamane; see Lapparent de Broin et al., 2020). Igdabatis sigmodon is diagnosed as a "Myliobatid with transversely arched median teeth, some with a distinct sigmoidal outline. High crown, of variable thickness, with fine honeycomb ornamentation. Two to three lateral articular facets. Root formed by alternating furrows and crests of variable length. Rectilinear lateral teeth, with a very asymmetrical crown." (Cappetta, 1972:215, translated from the French by JAWM). Igdabatis has been reported from both Mont Indamane and the nearby In Tahout site (Moody and Sutcliffe, 1991). Somewhat surprisingly, Igdabatis has not yet been reported from contemporaneous continental, nearshore, or marine deposits elsewhere in northern Africa (e.g., Maastrichtian-Paleocene Dakhla Formation of Egypt; Tantawy et al., 2001), but it has been reported in Spain and India.

Jain and Sahni (1983) first recognized Igdabatis from infratrappean horizons of the Lameta Formation exposed near Pisdura, in central India. This record was enlisted as part of the evidence supporting the claim that "The coastal fish faunas from the Cretaceous-Paleocene of Niger are identical at the generic level to taxa from the Indian peninsula"—which in turn was part of the evidence for a lack of Indian endemism (Sahni, 1984:442). Courtillot et al. (1986) also reported a myliobatid tooth from the dinosaur-bearing beds of Jabalpur, which they indicated was identical to Igdabatis teeth from the Maastrichtian of Niger. Prasad (1989) reported Igdabatis sigmodon from infratrappean Lameta deposits of Jabalpur, Pisdura, and Marepalli, as well as intertrappean deposits of Naskal, Nagpur (Takli), and Asifabad. Although these Indian specimens were originally thought to be conspecific with the Nigerienne form Igdabatis sigmodon (Cappetta, 1972), they were eventually placed within their own species, Igdabatis indicus (Prasad and Cappetta, 1993). I. indicus has also been identified from several sites in Spain (Soler-Gijón and López-Martínez, 1998). More recently, a third Igdabatis species, I. marmii has been described from Spain (Blanco, 2019).

There remains confusion surrounding the taxonomic specificity of the various *Igdabatis* records within India, in large part because reference is not often made to the diagnostic characteristics of the taxon. Specimens referred to *Igdabatis indicus* or *Igdabatis* sp. have been

reported from infratrappean horizons of Pisdura, Marepalli, and Jabalpur, intertrappean horizons of Asifabad, Naskal, Lotkheri, and Kisalpuri, and the Fatehgarh Formation of Rajasthan (see Mathur et al., 2005, 2006; Verma et al., 2017:260, table 4). This latter occurrence is of interest because it represents the only potential *Igdabatis*-bearing locality in India that is not associated with the Deccan Traps. The Fatehgarh specimens, however, are either poorly preserved or not diagnostic of *Igdabatis* (Mathur et al., 2006: pl. 1, figs. 1-5). Rana et al. (2006) described additional fish specimens from Fatehgarh that include better preserved material. Although Rana et al. (2006) reported myliobatoid chondrichthyans, they did not find specimens they could attribute to *Igdabatis*; rather, the chondrichthyan assemblage is consistent with a Paleocene age for the Fatehgarh Formation, from which dinosaur bones have not been reported.

Beyond concerns about the identity of specimens attributed to *Igdabatis*, the Fatehgarh Formation vertebrate assemblage raises an important point about biostratigraphic ranges. The relative dearth of earliest Paleocene vertebrate microfossil sites deposited under similar conditions to those at Deccan Trap-associated sites means that there is limited opportunity to record the presence or absence of *Igdabatis* outside the Maastrichtian. If such sites are also rare in Spain and Niger, then the last appearance datum for *Igdabatis* species is poorly constrained

3.1.4. New assessment: vertebrate fossil biostratigraphy of the Naskal and Rangapur intertrappeans

The late Maastrichtian age originally inferred for *Deccanolestes hislopi* was based on "reports of dinosaur remains from a number of intertrappeans" (Prasad and Sahni, 1988:638). However, no definitive dinosaur fossils have been reported from Naskal, despite the presence of fishes, frogs, lizards, snakes, turtles, and crocodiles at the site (Prasad and Sahni, 1988). The Maastrichtian age for Naskal therefore rests on a presumption that Indian intertrappeans are coeval, which we now have reason to suspect is problematic.

Our sample of vertebrate microfossils (\sim 3,000 specimens) from the Naskal and Rangapur sites documents a taxonomically diverse assemblage, including fish, anurans, squamates, a sphenodontian, turtles, crocodilians, and mammals. We did not document a single definitive non-avian dinosaur eggshell, bone, or tooth from either site. This pattern is repeated in the similarly extensive collections by Prasad and colleagues from Naskal and by Rana and colleagues from Rangapur (e.g., Prasad, 2012; Rana, 1990b). The sole exception is a single non-avian dinosaur tooth ("cf. Theropoda") reported from Naskal in an early taxonomic compendium (e.g., Khajuria and Prasad, 1998:157, table 2). This specimen was neither described nor figured, and for this reason we were not able to confirm its identification. Importantly, we were not able to compare it with serrated teeth of ziphodont crocodiles, which subsequently were reported from the Naskal intertrappean site (Prasad and de Lapparent de Broin, 2002:pls. 3, 4, 7). If indeed this tooth is definitively attributable to a theropod dinosaur, then it underscores the extreme rarity of non-avian dinosaurs at these two sites. Our sample from Naskal and Rangapur also documents teeth of myliobatoid chondrichthyans, but their assignment to Igdabatis indicus is doubtful and requires more detailed study.

3.2. Plant fossil biostratigraphy of Deccan Trap-associated deposits

Coulthard (1833) reported fossil wood from the northern part of the DTVP, in Sagar, Madhya Pradesh, representing the first plant fossil from Deccan intertrappean beds. Megafloral remains consisting of fruits, seeds, leaves, roots, and woods were first reported some twenty years later from intertrappean sediments exposed near Nagpur in central India (Hislop and Hunter, 1854). In the early twentieth century, Birbal Sahni and coworkers initiated the study of silicified megafloral remains from Deccan intertrappean sediments, including petrified fossil wood (Sahni, 1931; Rode, 1933a, 1934a, 1936), fruits (Rode, 1933b; Sahni and Rode,

1937; Sahni, 1943), palm root (Rode, 1934b), and dicot leaf impressions (Rode, 1935). Sahni (1941) and Sahni and Rao (1943) also recorded diverse aquatic mega- and microfloral remains represented by *Azolla* (Salviniaceae), *Massulites* (an extinct aquatic water fern), micro- and megaspores of aquatic fern *Regnellidium*, filamentous algae (*Ulothrix*), fungal spores, and the charophyte *Chara sausari* from the Sausar intertrappean beds of central India. Over the last two decades, many megafloral fossil remains represented by wood, leaves, fruits, seeds, and flowers have been recorded and taxonomically described from the intertrappean sediments of central India (compiled by Kapgate, 2005; Bonde, 2008; Smith et al., 2015; Wheeler et al., 2017).

3.2.1. Palynomorphs

Palynofloral records from the Deccan intertrappean sediments are relatively recent in comparison. Sahni and Rao (1943) reported pteridophytic spores in a thin section of a cut and polished chert sample from the Sausar intertrappean sediments of central India. S. D. Chitaley (1950, 1951) initiated the study of microflora from Deccan intertrappean sediments by maceration of chert samples, a technique that has been applied to study new palynomorph-bearing intertrappean sites in the DTVP (Fig. 1).

Palynomorphs were first used as a tool to assess age of the intertrappean sediments following recovery of a palynofloral assemblage from a dug well in Padwar village, some 30 km east of Jabalpur and 4 km from the Ranipur intertrappean (Prakash et al., 1990; Mathur and Sharma, 1990). The Padwar palynoflora, which includes Azolla cretacea, Gabonisporis vigourouxii, Aquilapollenites bengalensis, Diporoconia sp., and other taxa, is similar to palynofloras of Upper Cretaceous subsurface marine-to-shallow marine sediments of the Bengal Basin (Baksi and Deb, 1980), the Cauvery Basin (Venkatachala and Sharma, 1974a, 1974b), and the Krishna-Godavari Basin (Venkatachala and Sharma, 1984). The presence of Upper Cretaceous marker palynomorphs plus the presence of titanosaur dinosaur fossil bones at the neighboring Ranipur intertrappean locality led Sahni et al. (1996) to contradict the prevailing opinion of an Eocene age for intertrappean beds based on megaflora (see Sahni, 1937; Prakash, 1960; Bande et al., 1988). This inference was corroborated later by the discovery of additional intertrappean localities associated with Maastrichtian palynomorphs and dinosaur fossils, such as Mohgaon Kalan in Chhindwara (Srinivasan, 1996; Kar and Srinivasan, 1997; Kumaran et al., 1997), Anjar in Kutch (Bajpai et al., 1990; Dogra et al., 2004), and Bagwanya in the Malwa Plateau (Mohabey et al., 2019; Samant et al., 2020a).

Ongoing palynological studies in the DTVP (Samant and Mohabey, 2014; Thakre et al., 2017) and in subsurface Upper Cretaceous (Maastrichtian) sediments of the Krishna-Godavari, Cauvery (Prasad and Pundeer, 2002), and Bengal (Baksi and Deb, 1980) basins indicate that the Maastrichtian palynoflora is characterized by Azolla cretacea, Ariadnaesporites spp., Farabeipollis spp., Jiangsupollis spp., Scollardia conferta, and Triporoletes reticulatus. In DTVP-associated sediments, pollen grains of Aquilapollenites bengalensis and Gabonisporis vigourouxii are predominant in the Maastrichtian and rare in the Paleocene. However, these taxa disappear before or at the KPB in the Krishna-Godavari, Cauvery (Prasad and Pundeer, 2002), and Bengal (Baksi and Deb, 1980) basins.

In contrast to the numerous Maastrichtian palynomorph-bearing intertrappean beds in the DTVP, only three intertrappean localities are interpreted as Paleocene in age (Fig. 1): Ninama, in the western part of the DTVP (Samant et al., 2014), Lalitpur, in the northernmost part of the DTVP (Singh and Kar, 2002), and Surli, in the southern part of the Mandla Lobe (Thakre et al., 2016). The Paleocene age of the Ninama and Lalitpur intertrappean localities is based solely on the palynoflora, but the age of the Surli intertrappean locality is also based on volcanostratigraphy, magnetostratigraphy, and its stratigraphic occurrence above the P1a (Paleocene) foraminifera-bearing intertrappean (Keller et al., 2009; Thakre et al., 2016).

3.2.2. New data: palynomorphs of the Naskal intertrappean

Seven samples from intertrappean sediments from Naskal were macerated for palynological and other microfossil studies. Four of these samples came from the 2016 Naskal site, NSK-A section (Fig. 5), with three samples from two chert strata being productive: a chert with banded silicified shale (NSKAP-3 and NSKAP-4) and a black, massive chert (NSKAP-1). The sample from the gray-to-yellow, very finely laminated shale (NSKAP-2) was unproductive. In addition to palynomorphs, NSKAP-3 and -4 also contained impressions of small fossil wood fragments and leaves and abundant charophytes. Two samples were collected from a gray-to-yellow finely laminated silty shale of the NSK-B section but were unproductive, and a sample from the white marlstone at the GSI Naskal quarry yielded only frustules of the centric diatom *Aulacoseira* and sponge spicules (Fig. 5).

For the extraction of palynomorphs from the Naskal and Rangapur samples, we used standard maceration techniques, including treatment with hydrochloric acid, hydrofluoric acid, nitric acid, and potassium hydroxide (Traverse, 2007); however, concentration and duration of the chemical treatment varied from sample to sample. Maceration was followed by sieving with 10–15 µm sieves and preparation of slides using polyvinyl alcohol and Canada balsam. Optical slides were scanned under a Olympus BX 51 microscope and photographs were taken under a DP25 Olympus camera. For Scanning Electron Microscopy (SEM), the sieved residue was observed under the light microscope, and the desired pollen grains were transferred to a SEM stub using a hair attached to a dissecting needle. The sample stubs were then coated with gold/palladium (Au/Pd) and studied under the SEM at Jawaharlal Nehru Aluminium Research Development and Design Centre, Nagpur, India. Slides and SEM stubs are housed in the museum of the Department of Geology, RTM Nagpur University, India.

The palynoflora from the NSK-A section (Fig. 5) is represented by algae (2 genera), pteridophytes (4 genera), and angiosperms (9 genera). Algal remains include Kachiisporis bivalvusYi, 1997 (Fig. 7J) of Zygnemataceae, the green colonial alga Actinastrum sp., and some unidentified algal spores. Pteridophytes are represented by spores of Cingulatisporites sp., Crybelosporites intertrappea (Samant et al., 2020b; Fig. 7B), Cyathidites australisCouper, 1953, Gabonisporis vigourouxiiBoltenhagen, 1967, and Gabonisporis sp. (Fig. 7A). Angiosperms are represented by Aesculipollis sp. (Fig. 7C), Echimonocolpites sp., Echistephanocolpites meghalayensisRao et al., 1985 (Fig. 7L), Margocolporites sp. (Fig. 7E), Mulleripollis bolpurensisBaksi and Deb, 1976 (Fig. 7G-I), Palmaepollenites neyveliiRamanujam, 1966, Sparganiaceaepollenites sp. (Fig. 7D), Striacolporites striatusSah and Kar, 1970 (Fig. 7F), Tricolpites reticulatusCouper, 1953 (Fig. 7K), and many tricolporate pollen grains. Mulleripollis bolpurensis and Sparganiaceaepollenites predominate in NSKAP-3 and -4, constituting about 40% of the total pollen assemblage. Quantitatively, the palynoflora from both NSKAP-3 and -4 is more diverse than that of NSKAP-1, which is predominated by algal spores. In addition, fungal spores and a good concentration of grass phytoliths, especially of Oryza (Oryzeae), are commonly recorded from both samples. At both these levels, the grass phytoliths are represented by wellpreserved cuticles as well as dispersed phytolith grains; the phytolith assemblage will be described in a separate paper.

The biostratigraphic distributions of the palynomorphs recorded at Naskal and other intertrappean localities in India are shown in Fig. 8. The predominant palynotaxa from Naskal are *Sparganiaceaepollenites* and *Mulleripollis bolpurensis. Sparganiaceaepollenites* is a long-ranging taxon known from Maastrichtian to Paleogene sediments (ongoing work), whereas *Mulleripollis bolpurensis* has a more restricted distribution. From terrestrial sections of the DTVP, it is known from the Surli intertrappean that occurs above the Paleocene P1a foraminifera-bearing intertrappean in the Mandla Lobe (Keller et al., 2009; Thakre et al., 2016). However, in the subsurface sections of the Krishna-Godavari and Cauvery basins (Prasad and Pundeer, 2002), its first appearance is in the upper most Maastrichtian, but its acme is in the upper part of the Paleocene. Therefore, Prasad and Pundeer (2002) divided the Paleocene

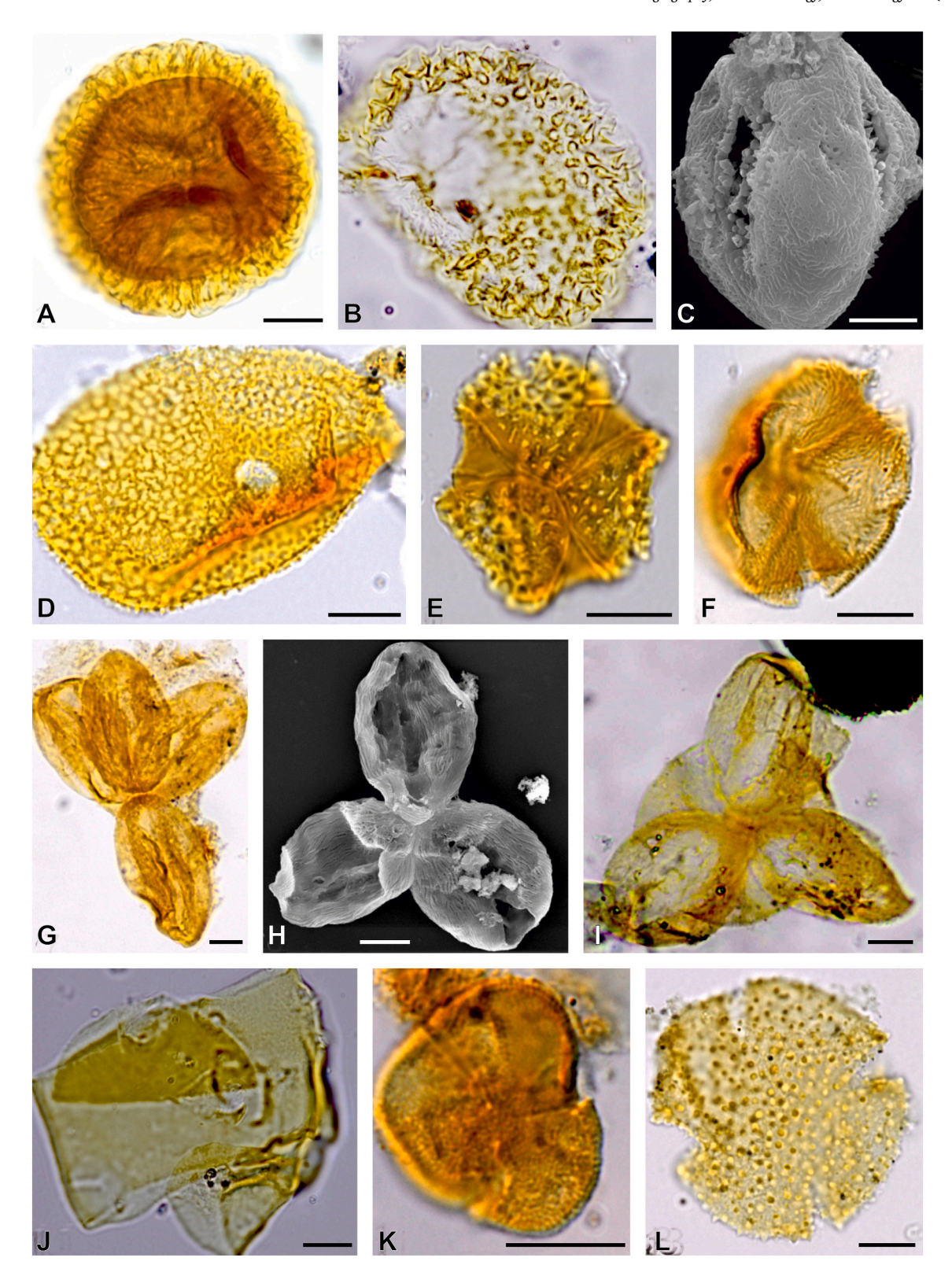


Fig. 7. Palynomorphs from the Naskal intertrappean sampled from the 2016 Naskal site. Images are transmitted light micrographs of palynomorphs unless noted otherwise. A, *Gabonisporis* sp. (slide no. PGNU/NSK/SL-1, EF G-33); B, *Crybelosporites intertrappea* (slide no. PGNU/NSK/SL-2, EF S-50); C, *Aesculipollis* sp. in equatorial view (SEM photograph); D, *Sparganiaceaepollenites* sp. (slide no. PGNU/NSK/SL-3, EF H-56/2); E, *Margocolporites* sp. (slide no. PGNU/NSK/SL-3, EF M-51/1); F, *Striacolporites striatus* (slide no. PGNU/NSK/SL-4, EF L-26/1); G, I, *Mulleripollis bolpurensis* (slide nos. PGNU/NSK/SL-1, EF F-43/4; PGNU/NSK/SL-5, EF K-36/2); H, *Mulleripollis bolpurensis* (SEM photograph); J, *Kachiisporis bivalvus* (slide no. PGNU/NSK/SL-6, EF O-52/3); K, *Tricolpites reticulatus* (slide no. PGNU/NSK/SL-3, EF L-52/4); L, *Echistephanocolpites meghalayaensis* (slide no. PGNU/NSK/SL-5, EF W53/2). "EF" represents England Finder reading of slide. Scale bar equals 10 microns. All slides accessioned to RTMNU.

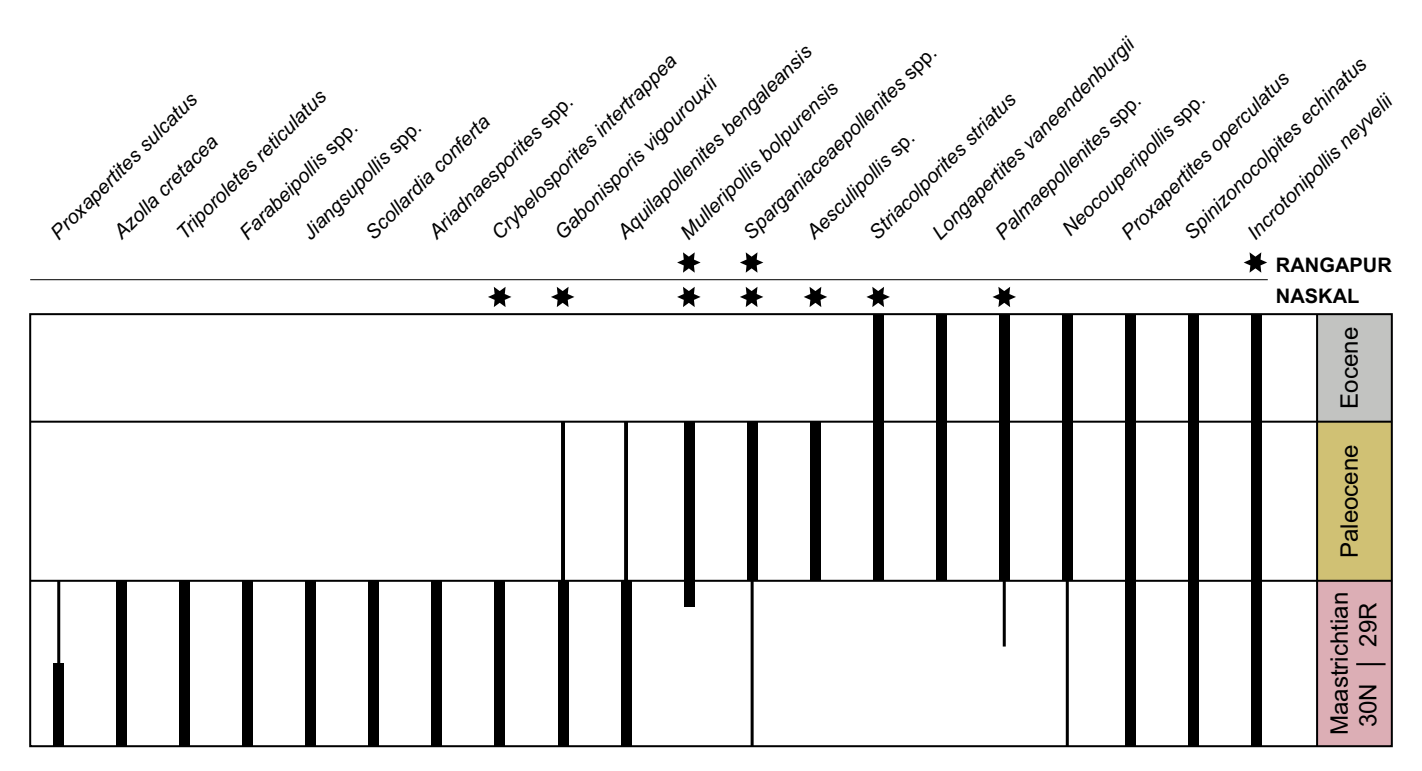


Fig. 8. Range chart of age marker palynomorphs from the Deccan Trap-associated intertrappean and subsurface sediments of the Krishna-Godavari, Cauvery, and Bengal basins of India. The presence of each marker palynomorph in the Naskal and Rangapur intertrappean beds is indicated by a filled star. Thickness of the vertical line represents the relative abundances (thick represents dominance and thin represents rarity).

into two biozones in the Krishna-Godavari and Cauvery basins: the lower one as the *Racemonocolpites romanus* biozone and the upper one as the *Mulleripollis bolpurensis* biozone. In contrast, in the Bengal Basin, *Mulleripollis bolpurensis* predominantly occurs in the uppermost biozone of the Upper Cretaceous (Baksi and Deb, 1980). The palynozonation of the Krishna-Godavari and Cauvery basins is more precise than that of the Bengal Basin because it is calibrated with dinoflagellates, foraminifera, and calcareous nanoplankton events in these basins.

Two rarely recorded but chronologically significant taxa from the Naskal intertrappean are *Crybelosporites intertrappea* and *Gabonisporis vigourouxii*. *Crybelosporites intertrappea* is known only from Maastrichtian intertrappean sediments (Samant et al., 2020b), and *Gabonisporis vigourouxii* is predominantly recorded from Maastrichtian intertrappean sediments, although occasionally from the Paleocene. Other associated palynotaxa from Naskal are otherwise known only from Paleocene sediments, namely *Striacolporites striatus*, *Echistephanocolpites meghalayensis*, *Palmaepollenites neyvelii*, and *Aesculipollis* (Saxena, 1991; Pocknall and Nichols, 1996; Mehrotra et al., 2005; Saxena and Trivedi, 2006).

About 1.5 km northwest of the Prasad Naskal site (Prasad and Sahni, 1988), Sahni et al. (1996) reported a palynomorph-bearing section that contains the Maastrichtian taxa Ariadnaesporites and Gabonisporis vigourouxii. From this intertrappean site, Singh et al. (2006) later reported Maastrichtian marker palynomorphs, such as Ariadnaesporites intermedius, Azolla cretacea, Gabonisporis vigourouxii, Triporoletes reticulatus, Mulleripollis bolpurensis, and Minerisporites triradiatus (Singh et al., 2006). This site and the 2016 Naskal site share only three palynotaxa in common: Cyathidites australis, Gabonisporis vigourouxii, and Mulleripollis bolpurensis.

Most of the Maastrichtian marker palynomorphs, such as *Azolla cretacea*, *Ariadnaesporites spiralis*, *Jiangsupollis* spp., and *Farabeipollis* spp., are absent at the 2016 Naskal site. These palynomorph markers are recorded in varying concentrations from most intertrappean sites that have been interpreted as Maastrichtian on the basis of volcanostratigraphy and magnetostratigraphy, including those in the Nand-

Dongargaon Basin and adjoining areas of the Sahyadri Group (Samant and Mohabey, 2009, 2014, 2016), the Bharudpura and Bagwanya localities in the Malwa Plateau (Mohabey et al., 2018, 2019; Samant et al., 2020a), and the Ranipur and Mohgaon Kalan localities in the Mandla Lobe (Mathur and Sharma, 1990; Kar and Srinivasan, 1997; Kumaran et al., 1997; Thakre et al., 2017).

The Naskal palynoflora has limited similarity with that of the Paleocene intertrappean sites of Surli (Samant and Mohabey, 2016), Ninama (Samant et al., 2014), and Lalitpur (Singh and Kar, 2002). Surli and Naskal have four taxa in common (Cyathidites australis, Gabonisporis vigourouxii, Mulleripollis bolpurensis, Sparganiaceaepollenites), whereas Ninama and Naskal have only two taxa in common (Cyathidites australis, Striacolporites striatus). The palynoflora of the Lalitpur intertrappean site is distinct, and only one taxon (Cyathidites australis) is shared with Naskal. The palynotaxa Cyathidites australis and Sparganiaceaepollenites have limited stratigraphic significance because both are long ranging (Cretaceous–Paleocene).

The palynofloral composition of the Naskal intertrappean (Fig. 8) is unique because it contains a Maastrichtian taxon (*Crybelosporites intertrappea*), Maastrichtian–Paleocene taxa (*Gabonisporis vigourouxii*, *Mulleripollis bolpurensis*), and Paleocene taxa (*Striacolporites striatus*, *Echistephanocolpites meghalayaensis*, *Palmaepollenites neyvelii*, *Aesculipollis*). This unique palynofloral composition suggests that the Naskal intertrappean might have been deposited during the K/Pg transition, during which the Maastrichtian palynoflora was in decline and a new floral community was establishing itself under changed environmental conditions.

3.2.3. New data: palynomorphs of the Rangapur intertrappean

Palynological samples were collected from four stratigraphic levels, although only the upper black chert yielded palynomorphs (RNGP-2, Fig. 6). The lower black-to-gray chert yielded only biodegraded organic matter (Fig. 6). The palynoflora of RNGP-2 is predominated by *Sparganiaceaepollenites* and *Mulleripollis bolpurensis* pollen grains, which constitute about 98% of the total assemblage. The remaining taxa are in

minor concentrations (*Cyathidites australis, Incrotonipollis neyvelii*, and tricolporate pollen grains and fungal spores). The Rangapur sediments are devoid of Maastrichtian palynomorph markers except *Mulleripollis bolpurensis*, which is a Maastrichtian–Paleocene taxon (Fig. 8). Spores of the Maastrichtian taxon *Crybelosporites intertrappea*, which are present in the Naskal intertrappean, are not recorded from the Rangapur intertrappean; accordingly, we cannot rule out that the sample from Rangapur is younger than those from Naskal.

3.2.4. New paleoenvironmental assessment: palynomorphs from the Naskal and Rangpur intertrappeans

Although both the Naskal and Rangapur intertrappeans are bracketed by Flows 3a/b and 4, a precise lateral correlation cannot be established. It is not known if these intertrappeans represent two separated depositional environments or a continuous surface, nor whether one was deposited prior to the other. The sediments in the lower part of the Naskal section (Fig. 5) are dominated by finely laminated, fine siliciclastics with no bioturbation and sandy clays, consistent with calm deposition in an open freshwater lake. The palynomorphs of Caesalpiniaceae (Striacolporites striatus, Margocolporites), Sapindaceae (Aesculipollis), Malvaceae (Malvacipolloides), and Arecaceae (Palmaepollenites) in the NSKAP-3 and -4 assemblage are consistent with this interpretation. Later in the history of Naskal, a closed-lake system developed, as indicated by presence of mostly aquatic forms like algal spores (Kachiisporis of Zygnemataceae; Actinastrum of Chlorellaceae), aquatic to semiaquatic pteridophytes (Crybelosporites and Gabonisporis of Marsileaceae) and angiosperms (Sparganiaceaepollenites, of Sparganiaceae/ Typhaceae), in the NSKAP-1 assemblage. The uppermost deposits represent comparatively dry and more evaporative conditions with increased alkalinity as indicated by presence of carbonate-dominated sediments (Fig. 5, NSK-A section). Unlike Naskal, the Rangapur sediments are dominated by carbonates, mainly marls and limestone associated with some diagenetic chert, which strongly suggest deposition under alkaline conditions with minimal non-calcareous siliciclastic sedimentation, consistent with a closed-lake system. The open-lake system at Naskal favored growth of diverse flora, in contrast to the closed lake at Rangapur, which shows reduced floral diversity and an absence of arboreal plants.

3.3. Flow-wise mapping of Basalts

The complicated architecture of continental flood basalt provinces has been recognized and discussed elsewhere (e.g., Thordarson and Self, 1998; Jerram, 2002; Single and Jerram, 2004; Jerram and Widdowson, 2005).

3.3.1. Eruptive architecture

Volcanostratigraphic architecture can be described using three hierarchical categories: flow lobe, lava flow, and flow field (e.g., Self et al., 1997). A flow lobe is an individual part of a lava flow formed by internal inflation, bounded top and bottom by a glassy rind or selvage. A lava flow is the product of a single outpouring of lava (i.e., eruptive unit), although it is entirely possible for an eruption to form two or more lava flows simultaneously. A flow field is the aggregate product from a single eruption or vent and is built up of one or more lava flows. Flow fields can be recognized where they are bounded between two weathering horizons, sometimes marked by red soils (i.e., 'boles') or contemporaneous sedimentation. The presence of boles implies that sufficient time would have elapsed between successive eruptions at a given locality to permit at least minor weathering to occur.

Basalts at the southern and southeastern limit of the DTVP commonly lie directly upon the Archean–Proterozoic granitic basement, although patchy, fossiliferous, Upper Cretaceous–lower Paleogene lacustrine sediments occasionally intervene between the basalts (i.e., intertrappeans) or between them and basement (i.e., infratrappeans). The source vent areas that fed the DTVP have not yet been unequivocally

identified, but they are likely to have existed on its western margin, originally near or beyond the current Western Ghats escarpment where the thickest successions are recorded (Deshmukh, 1988; Widdowson and Cox, 1996; Kale et al., 2020). Further to the east these successions progressively thin, with fewer flow fields having extended to these greater distances. The succession eventually terminates at its eastward extreme in the areas between Hyderabad and Nagpur. In the southeastern DTVP, this eruptive thinning becomes especially important because these peripheral areas are likely to have witnessed lava encroachment during only the most volumetrically effusive phases of the later Deccan episode; the succession there represents selective sampling of the stratigraphy most fully represented in the classic sections of the Western Ghats. Accordingly, long hiatuses must have occurred between these singular eruptive events, which allowed establishment of weathering horizons and sedimentary deposits, including ponds and extensive shallow lakes. Evidence of these is now preserved as both infratrappean deposits and intertrappean deposits such as those at the Naskal and Rangapur sites.

The flow-wise mapping of the southeastern DTVP by the Geological Survey of India established a stratigraphy for the exposed volcanic successions on the basis of physical mapping of individual eruptive units on a scale of 1:63,360 (1 inch $=1\,$ mile) or 1:50,000 (2 cm $=1\,$ km). Mapping criteria included physico-volcanological features of lava flows, presence of marker units (e.g., giant plagioclase basalts), petrological and petrogenetic studies, and presence of intertrappeans and boles between flows.

3.3.2. New data: flows at Naskal and Rangapur

The mammal-bearing intertrappean sections at Naskal and Rangapur are geographically separated by ~6 km (Fig. 3). There, nine recognizable, stacked eruptive units (henceforth termed flows) are exposed, each having thicknesses between 7-30 m. Intertrappean beds occur at five stratigraphic levels. The uppermost flows, Flows 8 and 9, are usually weathered to a deep lateritic profile in the area, and even Flows 6 and 7 are lateritized to the east and northeast of Rangapur. An intertrappean horizon is positioned between Flows 5 and 6 at the Somangurti locality near Naskal. Stratigraphically below this, Flows 3a/b and 4 (see Section 2) bracket the intertrappean beds at both Naskal and Rangapur. At both these localities, the base of the intertrappean section occurs at an elevation of nearly 624 m above mean sea level (Fig. 3B). Flow 2 is the most extensive regionally, overlying the Precambrian granites and infratrappean sediments at adjacent localities such as Gingurti, which has yielded numerous sauropod eggshells of Megaloolithus affinity. A red bole horizon approximately 1 m thick is present between the Flows 1 and 2 in a quarry section near Guttimukla village (Fig 3A-B).

3.4. Chemostratigraphy of the Deccan Traps

Lava successions in large igneous provinces are complex (Jerram and Widdowson, 2005), and flow mapping in the DTVP has proven challenging. Efforts towards building a workable basalt flow stratigraphy have taken advantage of the changing chemistries of lava eruptions, using them to establish successive 'chemotypes' that each represent a unique stage in the petrogenetic evolution of the magma source and/or degree of crustal contamination during surfaceward magma ascent prior to its emplacement. These lava packages of recognizable chemical affinity have been given the status of formations, and a chemostratigraphy for the Main DTVP has been established from detailed investigation of multiple exposed sections in the Western Ghats and corroborated with extensive traverses inland (Beane et al., 1986; Cox and Hawkesworth, 1984, 1985; Devey and Lightfoot, 1986; Mitchell and Widdowson, 1991; Jay and Widdowson, 2008). The resulting chronological succession is consistent with, and in some cases provides greater stratigraphic resolution than, the C30N-C29R-C29N magnetostratigraphy that encapsulates the whole of the Deccan succession.

The chemostratigraphy of the Main DTVP (Table 1) was developed

Table 3
Wai Subgroup chemostratigraphy. Element and isotopic characteristics of individual criteria are used to define the magma types and different formations in the DTVP (modified after Cox and Hawkesworth, 1984; Devey and Lightfoot, 1986)

Formation	Sr	Ba	Ba/Y	Zr/Nb	87Sr/86Sr
Panhala	<200	<90	<3	>13	0.7045-0.7055
Mahabaleshwar	>250	>100	>4	<10.5	>0.7050
Ambenali	200-250	<100	< 3.5	10.5-15	< 0.7050
Poladpur	<240	>100	>3.5	15-20	0.7050-0.7130

on the basis of field mapping and analyses of geochemical characteristics of successions exposed along the Western Ghats undertaken in the 1980s and 1990s (Beane et al., 1986; Cox and Hawkesworth, 1984, 1985; Devey and Lightfoot, 1986; Mitchell and Widdowson, 1991). The lava succession is now divided into three subgroups containing 11 formations (Table 1), of which the Wai Subgroup is the most widely exposed. Within the Wai Subgroup, formation boundaries are based on changes of ⁸⁷Sr/⁸⁶Sr ratios, Sr and Ba concentrations, and Ba/Y and Zr/Nb ratios (e. g., Devey and Lightfoot, 1986; Table 3). The ⁸⁷Sr/⁸⁶Sr data provide very clear breaks at formation boundaries across an interface between successive flow field units, whereas the element and element ratio values change over a number of such units and therefore often show 'transitional boundaries.' These diagnostic elemental criteria (Table 3) provide an easily acquired, accurate classification of single eruptive units and a successional chronology.

The current study explores intertrappeans exposed in the south-eastern corner of the main DTVP (Fig. 1), where they lie directly on peripheral basement (Jay and Widdowson, 2008). Ambenali-type flows are the most predominant and widespread chemotype in the current study area and typically, but not exclusively, represent the youngest eruptive succession in the Deccan Traps stratigraphy in this southeastern region (Jay and Widdowson, 2008:fig. 3). The order of these southeastern DTVP chemostratigraphic units exactly follows the type sections of the Western Ghats, thus indicating that these represent comparable relative chronologies of eruption (Jay and Widdowson, 2008).

The samples described below were classified according to the chemostratigraphic trace element criteria (e.g., Beane et al., 1986; Cox and Hawkesworth, 1984, 1985; Devey and Lightfoot, 1986; Mitchell and Widdowson, 1991).

3.4.1. New data: Naskal chemostratigraphy

The Naskal intertrappean sites lie between Flows 3a and 4 (NAS19-1 and NAS 19-2, respectively). Flows 1–5 are consistent with an Ambenali Formation classification (Table S1). In ascending order, samples NAS19-7, NAS19-1, NAS19-2, and NAS19-5 all show strong Ambenali-type chemistries. Slightly elevated Zr/Nb in the lowermost flows (NAS19-7 and NAS19-1) may indicate a transition from the preceding Poladpurtype chemistry. By contrast, the uppermost Flow 6 (NAS19-6) yields an unequivocally characteristic Mahabaleshwar-type chemistry, consistent with flows at the highest elevations in this area and extending to around Gurmatka (Jay and Widdowson, 2008).

The C29R–C29N reversal is placed just above the first two or three Mahabaleshwar-type flow fields in the type succession of the Western Ghats (Jay et al., 2009) and thus postdates the KPB by ca. 330 kyr. If the Mahabeleshwar-type flows capping the Ambenali-type succession at Naskal were synchronous with those in the Western Ghats, then we would expect that the uppermost Flows 5 and 6 are just below or at the C29R-C29N reversal horizon (65.724 \pm 0.013 Ma; Sprain et al., 2018). However, our date for Flow 6 (sample NAS19-6) is ca. 250,000 years older than this (65.976 \pm 0.065 Ma), implying a disconnect between the

Table 4

Similarity matrix for geochemistry of Naskal (NAS) and Rangapur (RAN) samples. Values shown are the average normalized root mean square of element concentration differences between each combination of the lavas bracketing the intertrappean beds. Concentrations are normalized to an anhydrous basis using the Loss on Ignition values. Values used are weight-% oxides for the major elements (Table S1a) plus Zr, Y, Nb and the rare earth elements in ng/g (Table S1b). Low values indicate similarity; hence, among our samples, the RAN19-2 and NAS19-2 flows (the overlying flows at each site) are the most similar, and RAN19-1 and NAS19-1 (the underlying flows at each site) are the least similar.

	RAN19-1	RAN19-2		
NAS19-1	0.612	0.207		
NAS19-2	0.247	0.047		

local chemostratigraphy and chronostratigraphy (e.g., Kale et al., 2020; Sheth et al., 2014).

3.4.2. New data: Rangapur chemostratigraphy

The Rangapur intertrappean is between Flows 3b and 4 (samples RAN19-1 and RAN19-2, respectively), which are similarly consistent with an Ambenali Formation succession (Table S1). In ascending order, samples RAN19-1 and RAN19-2 show strong Ambenali-type chemistries; again, a slightly elevated Zr/Nb in the lowermost RAN19-1 may indicate a lower Ambenali succession unit indicative of a transition from those of the preceding Poladpur-type chemistry.

Based on geochemical comparison between the upper and lower lavas at the Naskal and Rangapur intertrappean sites, we conclude that the upper flows at each site represent the same flow field. However, the basalt flows immediately underlying each site are sufficiently different geochemically (see Table 4) that we consider that it is highly improbable that these two lavas are from the same flow field. We cannot determine the lateral relationship between the flows underlying the two sites due to poor exposure between the two sections. This relationship is perhaps unsurprising because at any instance during the development of a large igneous province its exposed surface will consist of flow fields of differing ages. Successive eruptions are unlikely to uniformly and wholly cover over pre-existing flow fields. Accordingly, successive later eruptions will extend over a range of earlier flow fields each representing differing eruptive events (Jay et al., 2009:figs. 4 and 7) and leading to local complexities at the flow and flow-field level of succession.

The chemostratigraphy of the Naskal and Rangapur basalt flow successions are remarkably similar, consisting of Ambenali-type flow fields. In both cases, flows with marginally elevated Zr/Nb form the succession immediately beneath the intertrappean, and wholly Ambenali-type units immediately overlie it. This chemostratigraphy would accord with lower Ambenali units forming topographic 'substrate' prior to the development of the Naskal and Rangapur lakes, which were then overwhelmed by lavas of the later Ambenali-type flow fields. At Naskal, this succession was additionally subsequently covered with Mahabaleshwar-type flows that indicate a time horizon before the C29R-C29N transition, and thus place a robust youngest age limit on the date for the key intertrappeans preserved in the successions immediately beneath. Greater precision to this age bracket is provided by high-resolution ⁴⁰Ar/³⁹Ar dating in Section 3.6.1.

3.5. Magnetostratigraphy of the Deccan Traps

Magnetostratigraphy of Deccan basalt sequences historically have been used in conjunction with $^{40}\text{K}/^{40}\text{Ar}$ and $^{40}\text{Ar}/^{39}\text{Ar}$ datasets to constrain the overall duration of eruptions, largely on successions

exposed in the flow sequences from the Western Ghats (Vandamme et al., 1991; Chenet et al., 2009; Jay et al., 2009). Accordingly, it was asserted that the bulk of the DTVP was erupted over the course of three polarity chrons, with most eruptions taking place during C29R (Duncan and Pyle, 1988; Courtillot et al., 1988; Vandamme et al., 1991; Baksi, 1994; Hofmann et al., 2000).

3.5.1. New data: magnetostratigraphy of the Naskal and Rangapur area

At the Naskal-Rangapur area, three oriented blocks samples from Flows 2, 3a/b, and 4 were collected using standard methods (see Collinson, 1983). Flow 2 is the most widely exposed in the area, and rests on either the Precambrian basement, infratrappean sediments, or Flow 1. Flow 3a was sampled near the GSI Naskal quarry/2016 Naskal site, Flow 4 was sampled at Rangapur, and Flow 2 was sampled at the Guttimukla quarry, where a red bole horizon separates Flows 1 and 2. These flows were also sampled for $^{40} \mathrm{Ar}/^{39} \mathrm{Ar}$ age dating (see Section 3.6.1). Table 2 presents the summary of the data, which clearly depict reverse polarity for all the samples from Flows 2, 3a/b, and 4, suggesting their magnetization during C29R.

Samples were selected to widely represent the lava flow outcrop at the site. After coring, standard cylindrical specimens (2.5 cm in diameter x 2.2 cm in length) were cut, cleaned, and kept in a low-field environment for about one week. Representative samples were analyzed for routine rock magnetic studies to ascertain abundance of stable single domain grains in these samples Isothermal Remanent Magnetization and Anhysteretic Remanent Magnetization analyses. Detailed paleomagnetic analyses were conducted using thermal and alternating field demagnetizers (MMTD-80, Magnetic Measurement, UK and LDA 3A AGICO, Czech) to study the behavior of remanent magnetization in these samples. Characteristic Remanent Magnetization directions were obtained from trends on orthogonal demagnetization (Zijderveld) plots, and site mean Fisher statistics were computed using the common software of CEMP, Puffin Plots, and IAPD 2014.

3.6. Geochronology of the Deccan Traps

The first widely published DTVP basalt ages utilizing the 40K/40Ar system suggested an extended eruptive duration lasting roughly 5 million years (e.g., Wellman and McElhinny, 1970; Kaneoka and Haramura, 1973; Alexander, 1981). More precise radioisotopic 40Ar/39Ar dates from exposures in the Western Ghats revealed a much more rapid emplacement centered around the KPB (Pande et al., 1988; Duncan and Pyle, 1988; Courtillot et al., 1988). Modern applications of the 40 Ar/ 39 Ar method on multi-grain plagioclase separates from Western Ghats basalts have shown that more than 90% of the presently exposed volume erupted over an interval less than 1 million years, with a volumetric majority of the eruptions occurring after the KPB (e.g., Renne et al., 2015; Sprain et al., 2019). The overall rapid emplacement of Western Ghats lavas around the KPB was corroborated by an alternative geochronologic method that models eruptive rates using U/Pb zircon age distributions from interpreted tephras in bole horizons between lavas (Schoene et al., 2015; Schoene et al., 2019).

The U/Pb method applied to zircon is not generally directly applicable to basalt, because basalts lack sufficient Zr and SiO₂ to precipitate zircon. The version of this method applied by Schoene et al. (2019) requires the presence of silicic tephra components of red bole horizons, which we did not observe in either the Naskal or Rangapur sections. Hence the $^{40}\text{Ar}/^{39}\text{Ar}$ method was used for this study.

3.6.1. New data: geochronology of the Naskal and Rangapur area

We report five 40 Ar/ 39 Ar ages from discrete flows within the Naskal area and two 40 Ar/ 39 Ar ages from discrete flows within the Rangapur area (Fig. 9, Table 5). Samples were measured in step-heating experiments that include four to eight multi-grain aliquots of plagioclase for each flow. Information about methods and facilities can be found in Sprain et al. (2019) and Renne et al. (2015). Samples were closely

bracketed by co-irradiated neutron fluence monitors (Fish Canyon sanidine; see Renne et al., 2011) to achieve the highest possible precision. Four of the five Naskal samples were collected from a coherent section, which include the basalt flows directly above and below the intertrappean localities and correspond to Flows 3a, 4, 5, and 6 (Fig. 3). The stratigraphically lowest flow sampled was collected from the Guttimukla quarry, which is 4.9 km northwest of the GSI Naskal quarry/2016 Naskal site and corresponds to Flow 2 (Fig. 3). The two samples from the Rangapur area come from the flows directly below and above the intertrappean locality and correspond to Flows 3b and 4, respectively (Fig. 3).

The samples analyzed had Ca/K ratios >100, typical of plagioclase from lavas of the Wai Subgroup in the Western Ghats (Renne et al., 2015; Sprain et al., 2019) and consequently are challenging for high-precision dating. All the samples analyzed from both the Naskal and Rangapur sections yielded multiple age plateaus that are mutually indistinguishable and indistinguishable from the age of the KPB, at the 95% confidence level as shown in Fig. 9.

The ⁴⁰Ar/³⁹Ar ages for the lava flows bracketing the intertrappean sites at Naskal and Rangapur are insufficiently precise to permit correlation between the two sites on the basis of age alone. To facilitate such correlation, we compared the geochemistry of lava samples collected above and below each site. As shown in Table 4, the flows overlying the two sites (i.e., samples NAS19-2 and RAN19-2) are very similar geochemically. We infer that they are from the same lava flow field (i.e., Flow 4), and thus that the upper age limit for the two sites is identical within given error. By contrast, the eruptive units underlying the two intertrappean sites (i.e., samples NAS19-1 and RAN19-1) are geochemically dissimilar (Table 4), and we conclude that they represent distinct eruptive events or flow fields (i.e., Flows 3a and 3b, respectively). This requires that the lower flows at the two sites had restricted extent and that the neo-formed surface that formed the substrate for deposition of the intertrappeans presented itself as a mosaic of intertwining flow fields. The difference in elevation between the two intertrappeans is effectively negligible, given the shallow dip and/or billowed surface topographies observed in modern lava fields. We conclude, therefore, that they were emplaced onto a neo-formed volcanic surface having some topography and represent deposition during the same volcanic hiatus, but we cannot unequivocally determine whether the onset of sedimentation at the two sites was synchronous or whether the two were originally physically connected.

Because the samples from lava immediately overlying the two sites unambiguously represent the same flow field and are therefore synchronous on a time scale of decades or less, we combined the results from RAN19-2 and NAS19-2 to obtain a weighted mean age of 66.100 ± 0.067 Ma for the upper (younger) bound on the age of the GSI Naskal quarry/2016 Naskal site and the Rangapur intertrappean site (Fig. 10). Permissible age ranges for the two intertrappean sites were determined using Monte Carlo simulation applied to the Bayesian constraint that any plausible age must be younger than the lower bounding flow and older than the overlying one. Ages were generated randomly from a normal distribution for the overlying and underlying flows, and the difference computed. The result was rejected if the result for older flow minus younger flow was negative (i.e., a violation of the Bayesian constraint). This procedure was iterated 3,000 times for each pair of dates, and the averages for the older and younger flows that satisfied the Bayesian constraint were used to define the range of plausible ages at the 68% confidence level. This approach cannot determine the distribution of ages within the intertrappean interval, rather it constrains the possible age of any horizon within this interval. The Rangapur intertrappean interval is constrained to occur between 66.184 and 66.075 Ma, and the Naskal intertrappean interval is constrained between 66.136 and 66.056 Ma, at 68% confidence. Accordingly, both sites are most likely latest Maastrichtian, within 100 kyr of the KPB (66.052 ± 0.008 Ma; Sprain et al., 2019), or less likely earliest Paleocene. Because all dates compared herein are based on the 40Ar/39Ar method using the same

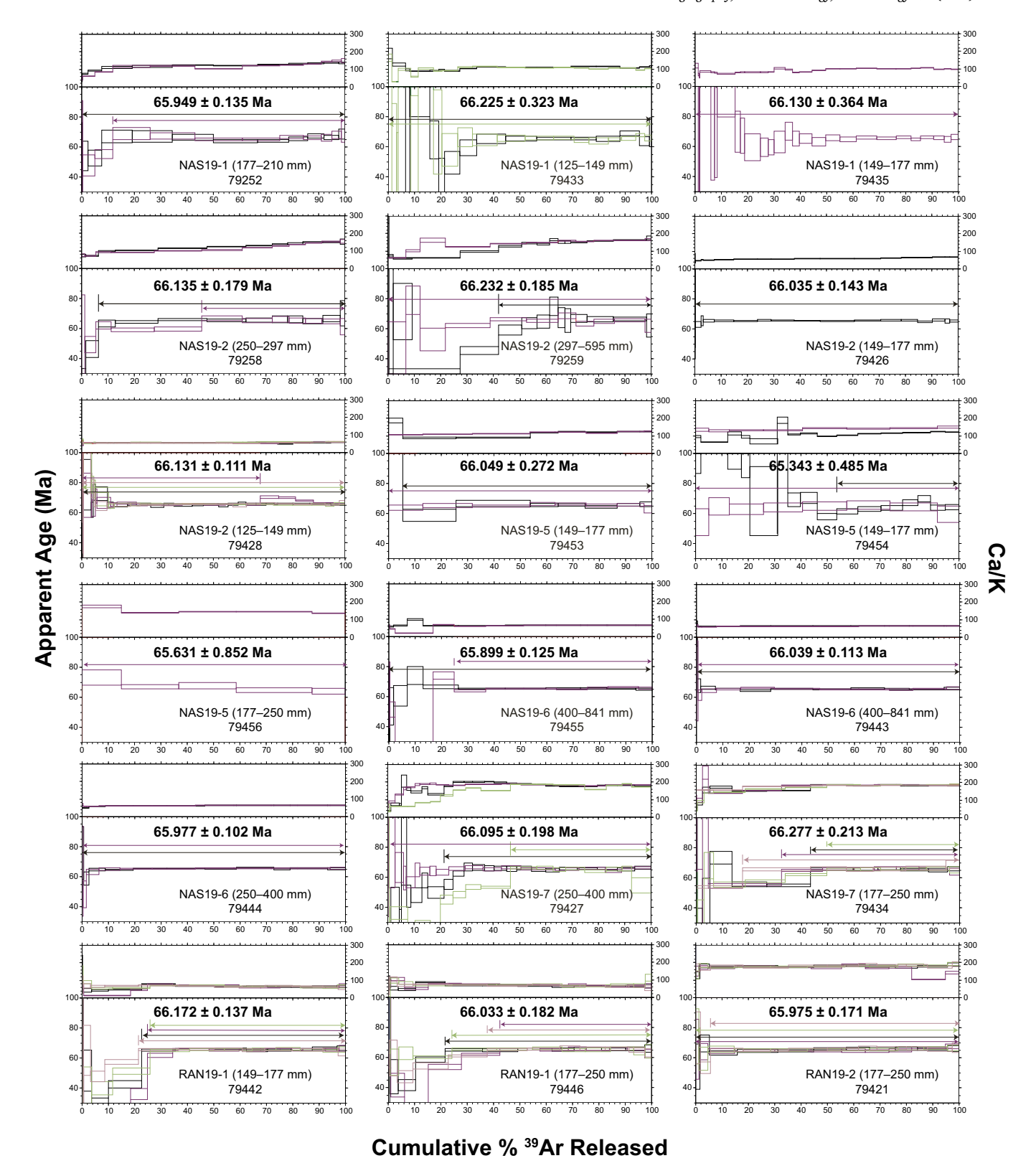


Fig. 9. 40 Ar/ 39 Ar age spectra for samples from basalt flows near Naskal and Rangapur. Each plot shows 1–4 age spectra (lower panel) from step-heating analyses of sample aliquots from a given irradiation position, coinciding with a unique neutron fluence parameter (J-value), as indicated by the laboratory identification number (LID#) shown underneath the sample number. The upper panel of each plot shows the Ca/K spectrum matched by color to the corresponding age spectrum. Colors serve only to distinguish distinct step-heating analyses. The steps defining plateau ages are indicated by color-coded horizontal bars with arrows above the age spectra. For each LID#, the weighted mean of all plateau ages is shown with 1σ uncertainty limits that include only analytical sources (c.f. systematic sources). Grain size fractions in micrometers (μ m) for each sample are indicated.

Table 5
Summary of 40Ar/39Ar plateau age data. Notes: (a) Lab ID# specifies a unique neutron fluence parameter (J-value). (b) R is the 40Ar/39Ar ratio of the sample relative to the interpolated value for the standards at this irradiation position. (c) uncertainty (standard deviation) of the age excluding systematic sources. (d) uncertainty (standard deviation) of the age including systematic sources.

		Size (µm)	R^b	$\pm R$	Age (Ma)	$\pm 1\sigma^{c}$ (Ma)	$\pm 1\sigma \text{ syst}^{d}$ (Ma)
NAS19-1	79252	177–210	2.355360	0.004920	65.949	0.135	
NAS19-1	79433	125-149	2.365390	0.011757	66.225	0.323	
NAS19-1	79435	149-177	2.361941	0.013220	66.130	0.364	
NAS19-1	Coml	bined	2.357391	0.004293	66.005	0.118	0.126
NAS19-2	79258	250-297	2.362120	0.006524	66.135	0.179	
NAS19-2	79259	297-595	2.365638	0.006732	66.232	0.185	
NAS19-2	79426	149-177	2.358465	0.005195	66.035	0.143	
NAS19-2	79428	125-149	2.361981	0.004033	66.131	0.111	
NAS19-2	Coml	bined	2.361659	0.002634	66.123	0.073	0.083
NAS19-5	79453	149-177	2.358992	0.009906	66.049	0.272	
NAS19-5	79454	149-177	2.333308	0.017645	65.343	0.485	
NAS19-5	79456	177-250	2.380151	0.031015	66.631	0.852	
NAS19-5	Coml	bined	2.354803	0.008321	65.934	0.229	0.232
NAS19-6	79455	400-841	2.353522	0.004528	65.899	0.125	
NAS19-6	79443	400-841	2.358614	0.004098	66.039	0.113	
NAS19-6	79444	250-400	2.356374	0.003703	65.977	0.102	
NAS19-6	Coml	bined	2.356342	0.002349	65.976	0.065	0.078
NAS19-7	79427	250-400	2.360660	0.007205	66.095	0.198	
NAS19-7	79434	177-250	2.367285	0.007748	66.277	0.213	
NAS19-7	Coml	bined	2.363733	0.005276	66.180	0.145	0.155
RAN19-1	79442	149-177	2.363453	0.004967	66.172	0.137	
RAN19-1	79446	177-250	2.358407	0.006642	66.033	0.183	
RAN19-1	Coml	bined	2.361643	0.003978	66.122	0.111	0.119
RAN19-2	79421	177-250	2.356298	0.006206	65.975	0.171	0.178
RAN19-2 & NAS	19-2 combined		2.360841	0.002425	66.100	0.067	0.078

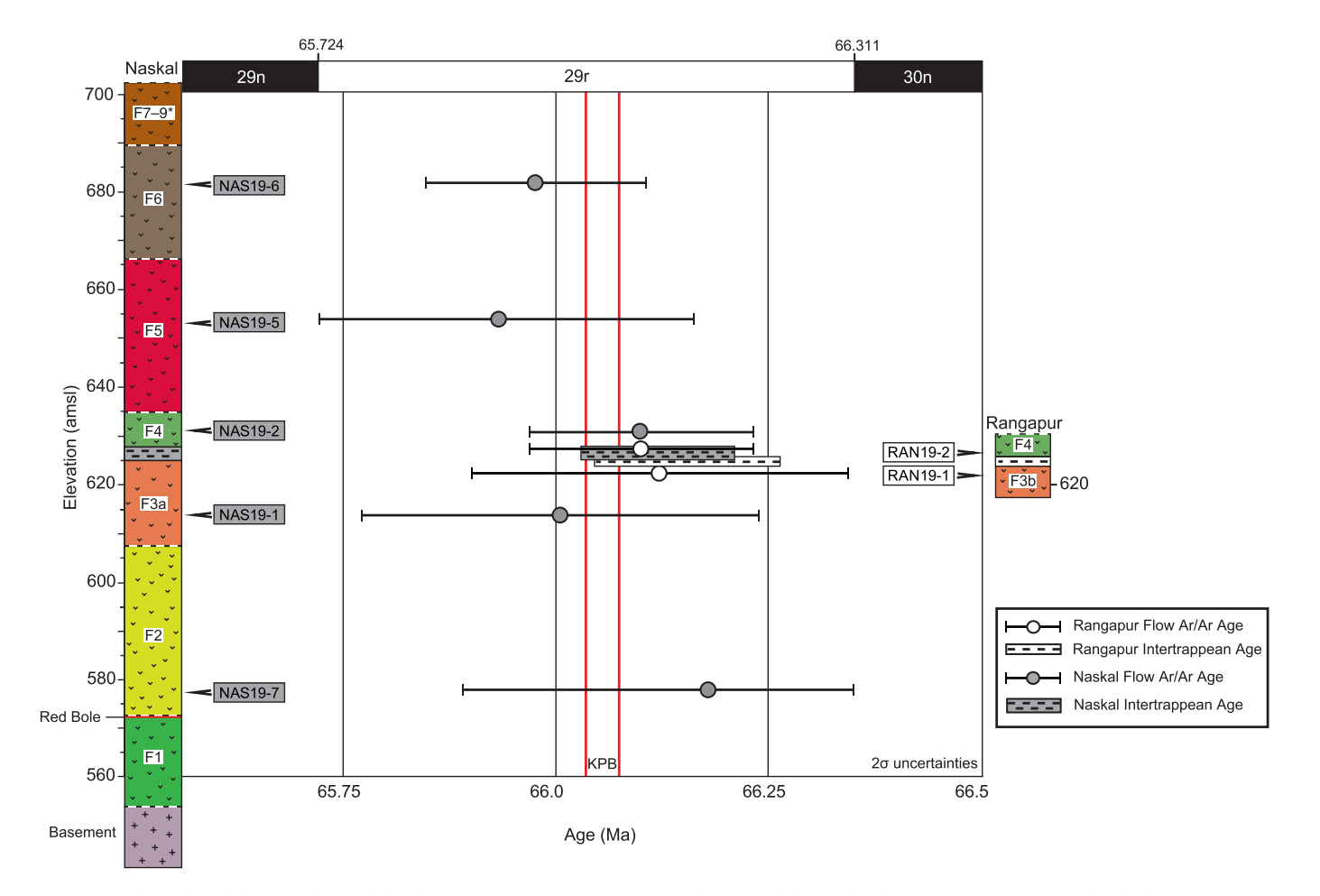


Fig. 10. Geochronological data for the Naskal and Rangapur interptrappean sites and associated flows. Plot shows composite stratigraphic thickness (in meters) versus age for basalt flows and sediments at Naskal (left, gray symbols) and Rangapur (right, white symbols). All ages are plotted with 2σ uncertainties. Magnetochron boundaries follow Sprain et al. (2018). Abbreviations: KPB, Cretaceous-Paleogene Boundary; NAS, Naskal; RAN, Rangapur.

calibration, systematic sources of uncertainty (e.g., due to decay constants or the isotopic composition of the standard) are neglected.

4. Systematic Paleontology

MAMMALIA Linnaeus, 1758 EUTHERIA Gill, 1872 INCERTAE SEDIS

4.1. Indoclemensia, gen. nov.

4.1.1. Etymology

Indo refers to the Indian subcontinent, and *Clemens* honors the late Professor William A. Clemens, who had a major influence on the study of early mammals and facilitated early scholarly exchange between researchers in the U.S. and at the Geological Survey of India, Southern Region.

4.1.2. Type species

Indoclemensia naskalensis sp. nov.

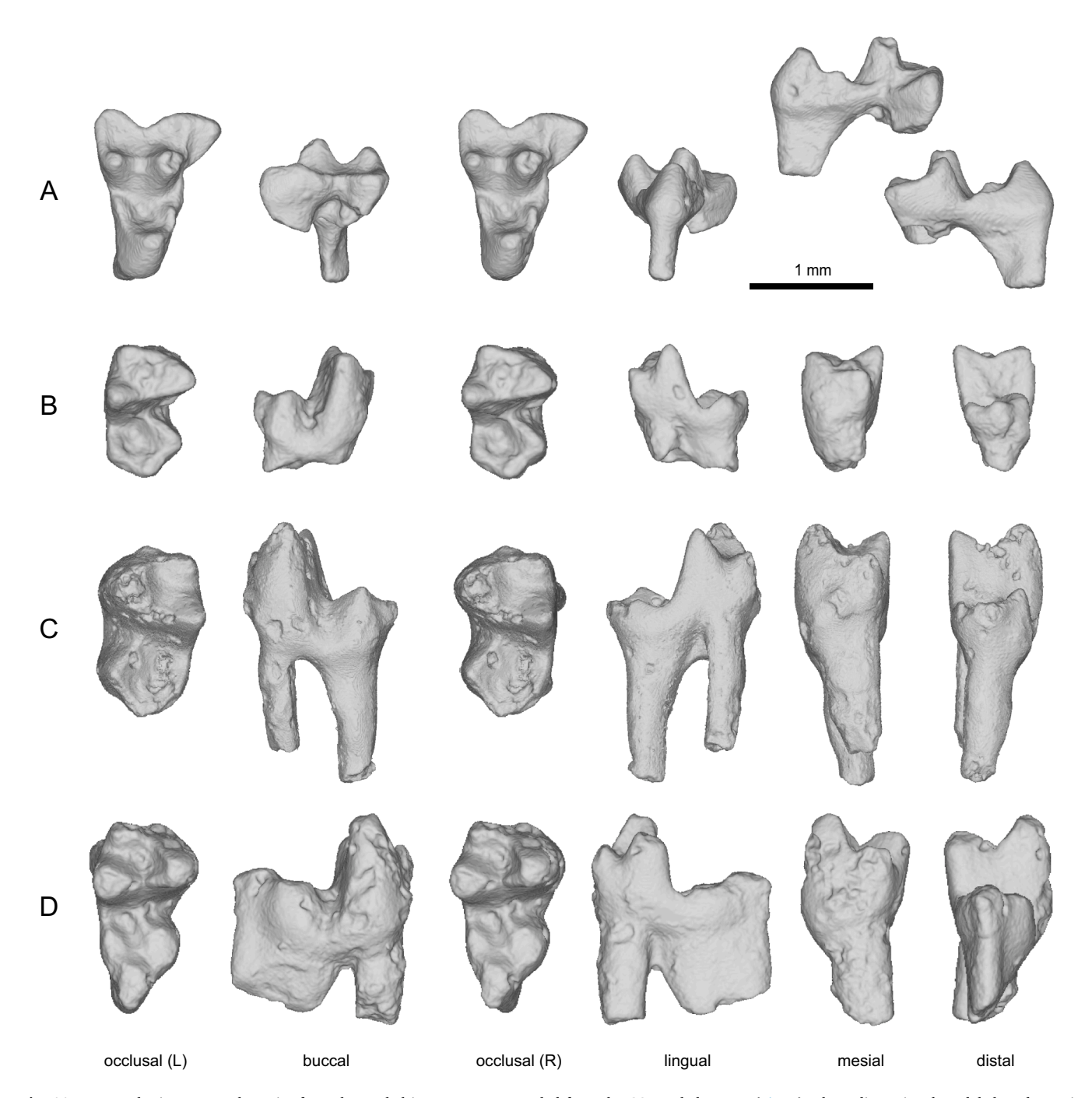


Fig. 11. New eutherian mammal species from the Naskal intertrappean sampled from the GSI Naskal quarry (Fig. 5). Three-dimensional models based on microcomputed tomography of the original specimens. A–B, *Indoclemensia naskalensis*, gen. et sp. nov., GSI/SR/PAL-N031 (holotype), right M2, and GSI/SR/PAL-N011, right m2, respectively. C–D, *Indoclemensia magnus*, sp. nov., GSI/SR/PAL-N043 (holotype), left m2, and GSI/SR/PAL-N019, right m3, respectively. Views from left to right: stereo occlusal left, buccal, stereo occlusal right, lingual, mesial, and distal. Scale bar equals 1 mm.

4.1.3. Diagnosis

Indoclemensia differs from both Deccanolestes and Sahnitherium in having upper molars with lower, more conical (less mesiobuccally compressed) buccal cusps with more rounded apices, a smaller stylar shelf, lower and shorter postmetacrista and preparacrista, a less bowed and less well-developed paracingulum that terminates mesial to the paracone, weaker conules and internal crests, and a lower, narrower (mesiodistally), and less lingually expanded protocone. Indoclemensia further differs from Deccanolestes in having upper molars with a less prominent stylocone and parastyle and lower molars with more rounded cusps and cristids, a smaller paraconid, a greater trigonid height:talonid height ratio, a higher trigonid basin, a more mesiodistally compressed trigonid, and a narrower talonid basin. Indoclemensia further differs from Sahntherium in having upper molars that are more expanded transversely, possess a stylocone, and lack a "C" cusp on the postmetacrista.

4.2. Indoclemensia naskalensis, sp. nov.

(Fig. 11A-B, Table 6)

4.2.1. Etymology

Naskal refers to the village of Naskal near the holotypic locality.

4.2.2. Holotype

GSI/SR/PAL-N031, right M2.

4.2.3. Referred specimens

GSI/SR/PAL-N011, right m2 from the holotypic locality.

4.2.4. Locality and horizon

The holotypic locality is near Naskal, Telangana, India (Figs. 1 and 3; $17^{\circ}~15^{\circ}~N,~77^{\circ}~50^{\circ}~E$). Fossils were found in the white marlstone to mudstone below the dark clay with sandy lenses and clasts and above the loose, yellowish, shaly/carbonate mudstone to marlstone at the GSI Naskal quarry (see Fig. 5). Application of Monte Carlo methods and Bayesian constraint to $^{40}\text{Ar}/^{39}\text{Ar}$ ages of the bounding lavas (see Section 3.6.1) indicates that the permissible age range of the Naskal intertrappean is between 66.136 and 66.056 Ma, at 68% confidence. Additional data are available from the GSI.

4.2.5. Diagnosis

Indoclemensia naskalensis is similar in size to Deccanolestes hislopi, D. narmadensis, and Sahnitherium rangapurensis; it is smaller than D. robustus and the other new species Indoclemensia magnus (see below).

4.2.6. Description

The holotypic specimen, GSI/SR/PAL-N031, is a well-preserved right M2 with its lingual root and the bases of its two buccal roots intact (Fig. 11A). The crown is relatively unworn, and its enamel surface lacks the pitting typical of many teeth from the Naskal locality (Prasad and

Sahni, 1988; Prasad et al., 1994; Khajuria and Prasad, 1998).

In occlusal outline, the crown has a long, narrow triangular shape (Fig. 11A). Its buccolingual width (MW and DW, Table 6) is greater than its mesiodistal length at the buccal margin (BL) and considerably greater than its mesiodistal length at the level of the conules (PRL). For description of measurement protocols, conventions, and abbreviations, see Section 1.2 and Fig. 2. Both the paracone and metacone are conical in shape with rounded apices. Despite damage to its apex, the paracone is taller than the metacone, which has a distally deflected apex. The base of the paracone is both buccally and lingually broader than the base of the metacone, and medially the bases of these cusps are fused ventral to the level of the stylar shelf (moderate zalambdodonty) to form a broad, V-shaped centrocrista in buccal view (Fig. 11A). In occlusal view, the wear facet on the centrocrista is buccolingually wide but does not extend to the apices of the cusps. Near the base of the paracone on its mesiobuccal aspect, a low, broad preparacrista extends mesiobuccally terminating in a distinct swelling on the ectocingulum, the stylocone. The stylocone is separated from a low parastyle by a shallow groove for the protoconid. The preparastylar region has a straight, not hook-like, buccal margin. It is also broad lingual to the stylocone, suggesting the presence of a preparastyle but none is evident; it might have been lost to wear or merged with the parastyle though wear. From the distobuccal aspect of the metacone apex, a broad postmetacrista (with no evidence of cusp "C") extends in an almost entirely buccal direction to join the distal end of the ectocingulum (Fig. 11A); a metastyle is not evident at the junction. The low but distinct ectocingulum traces the buccal margin of the crown forming a broad, nearly symmetrical, V-shaped ectoflexus in occlusal view. Together, the ectocingulum, preparacrista, postmetacrista, and centrocrista enclose a broad, dorsobuccally sloped stylar shelf.

The paraconule is a mesiodistally compressed swelling that is discernible as a slight ventral deflection of the preprotocrista. A preparaconule crista extends buccally beyond the lingual base of the paracone but does not flare mesially to form a broad paracingulum; it terminates at the mesial base of the paracone lingual to the preparastylar region. The postparaconule crista is a faint ridge that extends buccally a short distance to the lingual base of the paracone. The metaconule is also mesiodistally compressed and nearly indistinguishable from the postprotocrista. A premetaconule crista is not evident. The postmetaconule crista does not extend beyond the lingual base of the metacone. The trigon basin is mesiodistally narrow but deep and contained within the walls formed by the pre- and postprotocrista. The wall of the preprotocrista is slightly taller than that of the postprotocrista and, as a result, the paraconule is slightly taller than the metaconule (Fig. 11A). The protocone is mesiodistally narrow and only slightly lingually expanded at its base. The buccal aspect of the protocone slopes steeply into the trigon basin. The apex of the protocone is blunt from slight wear and is slightly mesiodistally recumbent.

Referred specimen GSI/SR/PAL-N011 is a well-preserved right m2 with portions of both roots intact (Fig. 11B). The apex of the protoconid

Table 6Dental measurements of *Indoclemensia naskalensis* and *I. magnus*. Measurements follow the schematic in Fig. 2. All measurements are in millimeters, except the trigonid angle (TR∠) is in degrees. Abbreviations are explained in the caption for Fig. 2. Holotypic specimens are indicated by an asterisk (*).

Taxon	Measurements (mm)									
Indoclemensia naskalensis										
	BL	PRL	MW	DW	PRW	PAH	MEH	PRH		
GSI/SR/PAL-N031*, R M2	1.01	0.54	1.36	1.37	0.65	0.56	0.53	0.45		
	BL	TRL	TAL	TRW	TAW	TR∠	PADH	MDH	PDH	TAH
GSI/SR/PAL-N011, R m2	0.97	0.51	0.46	0.64	0.54	32°	0.69	0.85	0.80	0.48
Indoclemensia magnus										
	BL	TRL	TAL	TRW	TAW	TR∠	PADH	MDH	PDH	TAH
GSI/SR/PAL-N043*, L m2	1.51	0.77	0.74	0.91	0.79	42°	0.97	1.23	1.35	0.82
GSI/SR/PAL-N019, R m3	1.61	0.71	0.90	0.96	0.73	33°	0.94	1.08	1.24	0.76

is slightly chipped, and a few fine sediment grains are lodged in the trigonid basin. Otherwise, the crown is relatively unworn, and its enamel surface is not pitted.

The trigonid of GSI/SR/PAL-N011 is considerably taller and slightly wider than the talonid (MDH vs. TAH and TAW vs. TRW, Table 6). The trigonid is mesiodistally compressed, such that in occlusal view the apices of the main cusps (paraconid-protoconid-metaconid) form an acute angle of 37° (TR,, Table 6). The trigonid basin is high above the base of the crown. The apices of the main cusps are rounded rather than sharp and pyramidal as in Deccanolestes; this is interpreted as a morphological rather than a preservational feature. The metaconid is the tallest cusp, but based on the size of its base, the protoconid was probably as tall or taller prior to breakage. The paraconid is small and lies buccal to the mesiodistal line formed by the metaconid and entoconid; it is positioned nearly along the mesiodistal line from the hypoconulid. The protoconid is slightly mesial relative to the metaconid, such that the distal aspect of the trigonid is slightly oblique to the buccolingual line. The paraconid and protoconid are connected by a rounded paracristid that in mesial view forms a broad, asymmetrical, V-shaped apex (Fig. 11B). The metaconid and protoconid are connected by a tall, rounded protocristid that in distal view forms what is now a broad, Vshaped apex; prior to breakage of the protoconid, the angle of the protocristid apex was probably less obtuse (Fig. 11B). In lingual view, the paraconid and metaconid bases meet to form a shallow V-shaped valley; however, a distinct metacristid is not evident. A slight swelling near the base of the mesial aspect of the trigonid below the paracristid notch is the only evidence of a precingulid (Fig. 11B). The mesial and distal aspects of the trigonid are nearly perpendicular to the horizontal plane (see Section 1.2).

The talonid basin is small but deep and contained by the walls formed by the cristid obliqua, the entocristid, and the postcristid. The talonid notch is deep. The cristid obliqua is taller than the entocristid and contacts the base of the distal aspect of the trigonid slightly lingual to the protocristid notch (Fig. 11B). A faint trace of a distal metacristid is evident. The hypoflexid is well excavated and forms an acute angle in occlusal view. The hypoconulid is slightly closer to the entoconid than it is to the hypoconid, but the cusps are not twinned. The hypoconid is slightly mesial relative to the entoconid. The hypoconid is the largest and tallest of the talonid cusps; the entoconid and hypoconulid are subequal in height. In distal view, the talonid is lingually canted relative to the dorsoventral line, and neither the buccal nor lingual base of the crown is inflated (Fig. 11B).

4.2.7. Comments

Lower molar GSI/SR/PAL-N011 is referred to *Indoclemensia naskalensis* on the basis of several features that suggest a possible functional occlusal relationship with the holotypic upper molar (GSI/SR/PAL-N031). The size of the referred lower molar specimen is consistent with the size of the holotypic upper molar; indeed, the talonid length of GSI/SR/PAL-N011 is identical to the protocone shelf length of the holotype. The detailed morphology of the talonid basin of GSI/SR/PAL-N011 is also consistent with the morphology of the protocone of the holotype. The protocone has a blunt apex, a steep buccal slope, and lacks a lingually expanded base; the talonid is buccolingually narrow but has a deep and well excavated basin. The tall, buccolingually wide protocristid of GSI/SR/PAL-N011 also matches the transversely wide preprotocrista on the holotype. The crowns of both specimens lack the inflation typical of *Deccanolestes* and have cusps that are conical with rounded rather than sharply pointed, pyramidal apices.

4.3. Indoclemensia magnus, sp. nov.

(Fig. 11C-D, Table 6)

4.3.1. Etymology

Magnus refers to the larger size of this species relative to the type

species.

4.3.2. Holotype GSI/SR/PAL-N043, left m2.

4.3.3. Referred specimens GSI/SR/PAL-N019, right m3.

4.3.4. Locality and horizon

The holotypic locality is from the intertrappean beds near Naskal, Telangana, India (Figs. 1 and 3; 17° 15' N, 77° 50' E). Fossils were found in the white marlstone to mudstone below the dark clay with sandy lenses and clasts and above the loose, yellowish, shaly/carbonate mudstone to marlstone at the GSI Naskal quarry (see Fig. 5). Application of Monte Carlo methods and Bayesian constraint to 40 Ar/ 39 Ar ages of the bounding lavas (see Section 3.6.1) indicates that the permissible age range of the Naskal intertrappean is between 66.136 and 66.056 Ma, at 68% confidence. Additional data are available from the GSI.

4.3.5. Diagnosis

Indoclemensia magnus is similar in size to Deccanolestes robustus and is larger than D. hislopi, D. narmadensis, I. naskalensis, and Sahnitherium rangapurensis.

4.3.6. Description

The holotypic specimen, GSI/SR/PAL-N043, is a left m2 with complete mesial and distal roots (Fig. 11C). The crown has slight pitting on its enamel surface.

The trigonid of GSI/SR/PAL-N043 is significantly taller and wider than the talonid (PDH vs. TAH and TAW vs. TRW, Table 6), and it is slightly mesiodistally compressed (Fig. 11C). The floor of the trigonid basin is high above the base of the crown (Fig. 11C). The main cusps of the trigonid are somewhat rounded and pyramidal rather than sharp and angular. The protoconid is the tallest trigonid cusp, followed by the metaconid and the paraconid. The paraconid is slightly buccal to the mesiodistal line formed by the metaconid and entoconid. The protoconid is mesial relative to the metaconid and nearly level with the halfway point between the metaconid and paraconid; as a result, the distal aspect of the trigonid is oblique to the buccolingual line. The paracristid is a sharp ridge above the level of the trigonid basin that extends horizontally from the paraconid to the paracristid notch and then steeply ascends the protoconid. In distal view, the protocristid forms a broad, shallow V-shaped apex (Fig. 11C). The sharpness of the protocristid is difficult to judge due to pitting in the vicinity. In lingual view, the paraconid and metaconid bases meet to form a shallow, asymmetrical V-shaped valley; a metacristid is not evident (Fig. 11C). At the mesial base of the trigonid, directly below the paracristid notch, a small precingulid is present. The mesial and distal aspects of the trigonid are nearly perpendicular to the horizontal plane (Fig. 11C).

The talonid basin is narrow, shallow, and ventrolingually sloping. The hypoconid is distinct, whereas the entoconid and hypoconulid are smaller and blend almost imperceptibly with the entocristid and post-cristid, respectively. The hypoconid is slightly mesial relative to the entoconid (Fig. 11C). The hypoconulid is slightly closer to the entoconid than it is to the hypoconid. The cristid obliqua contacts the distal aspect of the trigonid directly below the protocristid notch and continues as a faint distal metacristid a very short distance up the trigonid. The hypoflexid is shallow. The entocristid extends nearly horizontally from the entoconid to the distal aspect of the trigonid, such that a talonid notch is very shallow (Fig. 11C). In distal view, the buccal and lingual aspects of the crown are uninflated and form nearly vertical faces (Fig. 11C).

Referred right m3 GSI/SR/PAL-N019 is well-preserved with two complete roots intact (Fig. 11D). The distal root is more robust than the mesial root and is directed ventrodistally. The enamel surface of the crown is not pitted, but there is some apical wear on the cusps.

Like the holotype, the trigonid of referred m3 GSI/SR/PAL-N019 is taller and significantly wider than the talonid (PDH vs. TAH and TAW vs. TRW, Table 6). The trigonid basin is high above the base of the crown (Fig. 11D). The trigonid cusps are pyramidal with rounded apices. The protoconid is the tallest cusp, followed by the metaconid and paraconid. The paraconid is positioned buccally relative to the mesiodistal line formed by the metaconid and entoconid (Fig. 11D). The protoconid is positioned mesially relative to the metaconid, but not to the same degree as in the holotype. As a result, the distal aspect of the trigonid forms a slightly oblique angle with the buccolingual line. The trigonid is more mesiodistally compressed than it is in the holotype. Both differences likely reflect the relative positions in the molar series of the two specimens, not taxonomic differences. The paracristid and protocristid are similar to those in the holotype; the lack of pitting on GSI/SR/PAL-N019 reveals that the protocristid is a distinct ridge near the notch but becomes rounded towards the apices of the protoconid and metaconid. The paraconid and metaconid bases meet as in the holotype. A small precingulid is present in a position similar to that in the holotype (Fig. 11D). The mesial and distal aspects of the trigonid are nearly perpendicular to the horizontal plane.

The talonid of referred m3 GSI/SR/PAL-N019 differs from that of the holotype in features that are related to position in the molar series and degree of wear. The talonid of GSI/SR/PAL-N019 is longer and narrower than it is in the holotype (TRL vs TAL, Table 6). The talonid basin is narrow, shallow, and mesioventrally sloping (Fig. 11D). The hypoconid and hypoconulid have broad, inflated bases; the latter is also distally elongate, as expected for an m3. The hypoconulid is the tallest of the talonid cusps; the entoconid is discernible as a worn oval-shaped facet on the entocristid. The hypoconulid is slightly closer to the entoconid than it is to the hypoconid. The cristid obliqua contacts the distal aspect of the trigonid directly below the protocristid notch. A distal metacristid is not evident. A small talonid notch is evident. In distal view, the buccal and lingual aspects of the crown form nearly vertical faces and are not inflated (Fig. 11D).

4.3.7. Comments

Although they represent different positions in the molar series, GSI/ SR/PAL-N043 and GSI/SR/PAL-N019 are similar in size and general morphology to each other, such that we attribute them to the same taxon. We compared them to the lower molars of the new genus Indoclemensia and to those of Deccanolestes. Sahnitherium is only known from an upper molar, so we could not make direct comparisons to that taxon. GSI/SR/PAL-N043 and GSI/SR/PAL-N019 both differ from the lower molars of Decccanolestes in having a taller trigonid relative to talonid (PDH vs. TAH, Table 6), a more mesiodistally compressed trigonid (TRL), a narrower talonid (TAW), and a smaller, less projecting paraconid. These features are consistent with those that distinguish Indoclemensia from Deccanolestes. Because the m2 (GSI/SR/PAL-N043) is more than 50% larger (BL) than the m2 of holotype species I. naskalensis, we chose to erect a new species for these specimens.

4.4. Phylogenetic affinities

Dental traits of the new genus Indoclemensia reflect an insectivorous diet, which is common among small-bodied eutherians from the Cretaceous and Paleocene. Because dental adaptations to insectivory are similar across multiple groups, inferring phylogenetic relationships from a small sample of isolated teeth alone is challenging. Some dental traits of Indoclemensia are plesiomorphic among eutherians. The upper molar has a wide stylar shelf, lacks strong conules and conular cristae, lacks mesiodistal or lingual expansion of the protocone, and lacks a hypocone or cingula (Kielan-Jaworowska et al., 2004). The lower molars do not have an extreme trigonid:talonid height differential (large or small) or a talonid basin as wide as the trigonid. Other dental traits of Indoclemensia are derived relative to those of Early Cretaceous eutherians such as Prokennalestes, Murtoilestes, and Bobolestes. On the upper molar, the

paracone and metacone are in a buccal position relative to the midwidth of the crown, the preparastyle is reduced or absent, and the preparaconule crista extends beyond the lingual base of the paracone. On the lower molars, the paraconid is somewhat reduced, the trigonid is slightly mesiobuccally compressed, and the cristid obliqua contacts the distal aspect of the trigonid below the protocristid notch (not more lingually).

Indoclemensia differs from Late Cretaceous and Paleocene "zhelestids," archaic ungulates, gypsonictopids, and plesiadapiforms, which all trend toward omnivory. It lacks the reduction of both molar cusp height and trigonid:talonid height differential, the inflation of molar cusps (particularly the protocone), and the development of molar cingula, and the trigonid width is greater than the talonid width (Kielan-Jaworowska et al., 2004). Indoclemensia also differs in these ways from the adapisoriculids such as the Indian genus Deccanolestes (Prasad et al., 2010), which has a distinct and mesially projecting paraconid. Indoclemensia differs from Late Cretaceous and Paleocene insectivorous asioryctitheres, zalamdalestids, cimolestids, and palaeoryctids in several ways. The upper molar is not as transversely wide and the conules are not as developed, not on the same mesiodistal line, and closer to the protocone than to the paracone and metacone. It further differs from palaeoryctids in that the upper molar paracone and metacone are not tightly appressed to each other; it further differs from cimolestids in not having the extreme trigonid:talonid height differential.

In sum, we consider the phylogenetic affinities of Indoclemensia as indeterminate within Eutheria, until a larger sample of specimens of our new genus is available for a robust phylogenetic analysis.

4.5. Faunal summary

We treat the Naskal and Rangapur mammalian fossil assemblages as a single local fauna due to their close geographic proximity (6 km) and strongly overlapping temporal constraints. This combined Naskal-Rangapur local fauna (Table 7) now includes 51 published specimens that represent seven species (Prasad and Sahni, 1988; Prasad et al., 1994; Prasad and Godinot, 1994; Rana and Wilson, 2003; Prasad et al., 2007b; Wilson et al., 2007; Boyer et al., 2010; this paper). Four of those specimens (8%) represent the sudamericid gondwanatherian Bharrattherium bonapartei; the remaining 47 specimens (92%) are eutherian mammals.

5. Discussion

The Naskal intertrappean localities are the most prolific mammalbearing sites in India (Prasad and Sahni, 1988; Prasad et al., 1994, 2007b; Wilson et al., 2007; this paper). Ever since the first mammals were recorded from there, its age was accepted to be latest Cretaceous (Maastrichtian). This assignment was in part based on paleomagnetic

Table 7 Taxonomic summary of the Naskal-Rangapur local fauna based on the 51 pub-

lished specimens (Prasad and Sahni, 1988; Prasad et al., 1994; Prasad and Godinot, 1994; Rana and Wilson, 2003; Prasad et al., 2007b; Wilson et al., 2007; Boyer et al., 2010; this paper).

Naskal-Rangapur local fauna		
Gondwanatheria		
	Sudamericidae	
		Bharrattherium bonapartei
Eutheria	A dtt11.d	
	Adapisoriculidae	
		Deccanolestes hislopi
		Deccanolestes robustus
		Deccanolestes narmadensis
	Incertae sedis	
		Sahnitherium rangapurensis
		Indoclemensia naskalensis
		Indoclemensia magnus

data and biostratigraphic indicators (non-avian dinosaurs and the ray *Igdabatis indicus*); the latter were poorly documented from the site or were documented from other intertrappean localities inferred to correlate with Naskal.

Our new paleomagnetic, radioisotopic, geochemical, and palynological data from the Naskal and Rangapur sites provide the most robust evaluation to date of the age of these important fossil localities. These data constrain the age of both sites to within 100 kyr of the KPB; standard error of the radioisotopic ages constrain the sites to either the very latest Cretaceous or very earliest Paleocene (Fig. 10). Below, we discuss the implications of both the new fossils and the refined age of the Naskal and Rangapur intertrappean sites for our understanding of the Deccan chemostratigraphy and Deccan volcanism, K/Pg mass extinction, Indian mammalian faunal evolution, and the timing of the origin of placental mammals.

5.1. Implications for Deccan chemostratigraphy and Deccan volcanism

The basalts bracketing the mammal-bearing intertrappean sediments at Naskal have geochemical affinity with those of the Ambenali and Poladpur formations of the Wai Subgroup in the Western Ghats (e.g., Beane et al., 1986). Despite this similarity, the ⁴⁰Ar/³⁹Ar ages reported here for the Naskal basalts contrast with the Paleocene ⁴⁰Ar/³⁹Ar ages reported by Sprain et al. (2019) for the Wai Subgroup basalts in the Western Ghats. Although the analytical uncertainty of the ages reported here render it possible (albeit improbable) that the lavas dated at Naskal and Rangapur are actually Paleocene, our results imply geochemically defined formation contacts are not synchronous at the ± 100 kyr level over the entire DTVP, a conclusion that has been suggested previously (e.g., Kale et al., 2020). An additional implication is that the volcanological and geochemical transition at the base of the Wai Subgroup in the Western Ghats (i.e., Richards et al., 2015; Renne et al., 2015) was not everywhere synchronous, which would be inconsistent with the impact trigger hypothesis of Richards et al. (2015). Resolution of these questions must await additional sampling and higher precision geochronology.

5.2. Implications for the Cretaceous-Paleogene mass extinction

High-precision ages of fossil assemblages before and after the KPB are critical to testing hypotheses related to the K/Pg mass extinction and subsequent biotic recovery. The new age data presented in this paper constrain the Naskal and Rangapur sites to within 100 kyr of the KPB. To our knowledge, no other non-marine locality outside of North America is as tightly constrained with respect to the KPB. Moreover, although earliest Paleocene fossil localities in North America have been bracketed by geochronological data to within 25–80 kyr of the KPB (Smith et al., 2018; Sprain et al., 2018; Wilson Mantilla et al., 2021), those from the latest Cretaceous have only been constrained to within 259 kyr of the KPB (i.e., between the age of the C30N-C29R boundary and the KPB; Sprain et al., 2015, 2018).

The age model described above (Section 3.6.1) suggests that a latest Cretaceous age is more likely than an earliest Paleocene age for the Naskal and Rangapur sites. A latest Cretaceous age for both localities would be significant considering the distinctive nature of their vertebrate fossil and palynofloral assemblages. Despite large vertebrate microfossil samples size (e.g., several thousand specimens from Naskal), only a single dinosaur specimen has been reported from these sites. Its taxonomic identification is dubious; it was never figured, described, nor compared with non-dinosaur taxa reported from the same horizon. Likewise, the palynoflora is distinct from other definitively older Maastrichtian intertrappean palynofloras (Thakre et al., 2017; Samant et al., 2020a). This would imply that the terrestrial fauna and flora had undergone significant turnover and modifications in community structure prior to the bolide impact at the KPB, as has been suggested previously for India (Samant and Mohabey, 2009; Mohabey and Samant,

2013). This taxonomic pattern contrasts with that from contemporaneous latest Cretaceous (Lancian) vertebrate fossil assemblages from North America, which do show changes in mammalian evenness (Wilson, 2014) and dinosaur relative abundances (Horner et al., 2011) but do not show declining dinosaur richness or major palynofloral turnover in the last hundreds of thousands of years of the Cretaceous (Fastovsky and Bercovici, 2016). Palynological data from Naskal and Rangapur and other Maastrichtian intertrappeans of the DTVP show the disappearance of the majority of Maastrichtian palynoflora (Azolla cretacea, Ariadnaesporites spp., Farabeipollis spp., Jiangsupollis spp., Scollardia conferta and Triporoletes reticulatus) before the KPB. This palynofloral change contrasts with the changes observed in Western Interior of North America, where the major extinction event of Cretaceous "K taxa" occurs at the KPB and earliest Paleocene as marked by the so-called "fern spike" (Nichols and Johnson, 2008; Bercovici et al., 2009). One potential driver of such change is the Deccan volcanic eruptions and the associated environmental changes (e.g., late Maastrichtian event; Nordt et al., 2003; Hull et al., 2020). To robustly test this hypothesis, additional temporally constrained and well-sampled fossil localities from the latest Cretaceous and early Paleocene of India are needed.

Although less likely, a very early Paleocene age for the Naskal and Rangapur sites cannot be ruled out. The upper bound of the standard deviation of the radioisotopic age model indicates that the localities may be as young as 66.031 Ma (Naskal) and 66.046 Ma (Rangapur), which are 21 kyr and 6 kyr younger, respectively, than the KPB (95% confidence). In this case, Naskal and Rangapur would represent the first early Paleocene mammal localities from India. A very earliest Paleocene age would also mean that the vertebrate faunas and palynofloras from these sites provide our first look at K/Pg survivorship. The mammalian local faunas would be contemporaneous with or perhaps even slightly older than early Puercan (Pu1) local faunas from western North America (Lofgren et al., 2004; Wilson, 2013, 2014), which typically are low in species richness, highly uneven, and predominated by small-bodied insectivores. This would also substantially alter our Cretaceous record of mammals from India and call into question the Maastrichtian age for other intertrappean mammal-bearing localities, such as Kisalpuri and Gokak (Prasad et al., 2007a; Wilson et al., 2007). (Although Khosla et al., 2004 reported the presence of dinosaur eggshell at Kisalpuri, the material was not described or illustrated in their paper, and our samples from the same site have not yielded any dinosaur material.) Accordingly, Deccanolestes would either represent a K/Pg survivor (if Kisalpuri is still latest Cretaceous in age) or it would no longer be a latest Cretaceous mammal (if Kisalpuri is also Paleocene in age). We also cannot reject the possibility that deposition at Naskal, Rangapur, or both sites spanned the KPB and that palynofloral or vertebrate microfossil collections together represent a mix of Maastrichtian and Paleocene forms.

5.3. Implications for mammalian faunal evolution

Previous discussions of India's Late Cretaceous mammalian fauna were based on a composite sample, taken from across the subcontinent with little temporal constraint. Here, the combined Naskal-Rangapur local fauna provides a more precise spatiotemporal lens through which to evaluate mammalian faunal evolution in India. This local fauna, which is from within 100 kyr of the KPB, consists of one gondwanatherian and six eutherian species (Table 7), with the eutherians comprising 92% of all mammalian specimens. In comparison, wellsampled latest Cretaceous (Lancian) mammalian local faunas from North America, such as those from the Hell Creek Formation, typically have 25-30 species and a much lower relative abundance of eutherians (<20%; e.g., Wilson, 2014). The only other Cretaceous local faunas in which eutherians predominate are those from the late Turonian of Central Asia (Cifelli, 2000). Well-sampled earliest Paleocene (early Puercan) mammalian local faunas from North America often have low species richness (10-20 spp.) but moderate-to-high relative abundance of eutherians (~40%; e.g., Wilson, 2014), which is closer to but still less

than in the Naskal-Rangapur local fauna.

The ecological composition of the Naskal-Rangapur local fauna also differs from that of contemporaneous North American sites. The gondwanatherian Bharrattherium bonapartei, which has hypsodont molariforms, is likely herbivorous (Wilson et al., 2007), and the six eutherians, all of which have tribosphenic molars with greater shearing than crushing/grinding capacity, are insectivorous. The prevalence of insectivory is typical among both latest Cretaceous and earliest Paleocene mammalian local faunas of North America, whereas omnivory and herbivory only became common among eutherians during the early Paleocene (Wilson, 2013; Grossnickle and Newham, 2016; Wilson Mantilla et al., 2021; but see Harper, 2011). The most abundant mammalian taxon from Naskal-Rangapur, and Indian intertrappeans more broadly, is Deccanolestes, which is interpreted to be arboreal or scansorial based on the morphology of referred postcranial elements (Prasad and Godinot, 1994; Boyer et al., 2010). Arboreality has been inferred among Late Cretaceous stem marsupials and multituberculates (e.g., Chester et al., 2012; Chen and Wilson, 2015), but it has not been confirmed among other Late Cretaceous eutherians (Szalay and Decker, 1974; DeBey and Wilson, 2017; Hughes et al., 2021), although this may be due in part to the sparse postcranial fossil record of eutherians. Aboreality became more common among eutherians, particularly plesiadapiform primates, during the early Paleocene (e.g., Chester et al.,

The body-size distribution of the Naskal-Rangapur mammalian local fauna is also distinctive. The gondwanatherian *Bharrattherium bonapartei* has an inferred body size on par with medium-sized multituberculates (e.g., ~300 g, *Cimolomys gracilis*; Wilson, 2013), but the Naskal-Rangapur eutherians, which again make up 92% of all specimens, are all comparable to or smaller than the smallest mammals from the latest Cretaceous and earliest Paleocene local faunas from North America (e.g., 5–10 g, *Batodon tenuis*; Wilson, 2013). Prasad and Sahni (1999) also recognized the skewed body-size distribution and suggested that it might be reflective of a body-size filter for 'island hopping,' perhaps from Asia or Africa. Alternatively, this body-size distribution could reflect the greater survivorship of small-bodied mammalian taxa across the KPB in northeastern Montana reported by Wilson (2013).

In summary, the Naskal-Rangapur local fauna is distinctive in its richness, relative abundance structure, ecological traits, and body-size distribution. In comparison to mammalian local faunas from North America, it more closely resembles those from the early Paleocene, rather than those of the latest Cretaceous. This might reflect either a true Paleocene age for the Naskal and Rangapur sites, a relatively advanced stage of faunal evolution, paleoenvironmental differences, or differences in the timing and pattern of the K/Pg mass extinction in India. Moreover, the Kisalpuri local fauna, which includes an archaic ungulate with omnivorous dental morphology (Kharmerungulatum; Prasad et al., 2007a), has an even slightly younger Paleocene-aspect than does the Naskal-Rangapur local fauna. Nevertheless, we acknowledge that the Naskal-Rangapur local fauna is still only known by 51 published specimens and the Kisalpuri local fauna by even fewer compared to the thousands of specimens for latest Cretaceous and earliest Paleocene local faunas in North America (Lofgren et al., 2004), so our faunal interpretations must be considered preliminary until more robust samples are available.

5.4. Implications for the timing of the origin of placental mammals

A central focus in the study of mammalian evolution has been the timing of the origin of Placentalia (crown group eutherians) and its extant orders (see review in Upham et al., 2021). Debate on this topic persists because molecular divergence estimates—although they have migrated toward the KPB—have consistently placed the origins of placentals and some extant orders in the Cretaceous (e.g., Springer et al., 2003; Bininda-Emonds et al., 2007; Meredith et al., 2011; dos Reis et al., 2012); whereas fossil evidence and analyses of fossil sampling biases do

not unambiguously support the origin of placentals or extant orders before the KPB (Archibald, 2003; Archibald et al., 2011; Davies et al., 2017; Foote et al., 1999; O'Leary et al., 2013; Wible et al., 2007; Wilson Mantilla et al., 2021).

Deccanolestes, which is the most abundant mammalian taxon in the Naskal-Rangapur local fauna and other intertrappean local faunas, has been among the most pivotal fossil taxa in this debate (Prasad, 2009). Phylogenetic studies have variously placed it (i) within Placentalia (Upham et al., 2021), (ii) more deeply nested within Placentalia in the supraordinal clade Euarchonta (e.g., Prasad and Godinot, 1994; Boyer et al., 2010; Smith et al., 2010), or (iii) outside Placentalia as a closely related stem placental (e.g., Wible et al., 2007; Goswami et al., 2011; Manz et al., 2015). Whereas additional morphological data are needed to help resolve this phylogenetic uncertainty, our results further constrain the age of Deccanolestes to within 100 kyr of the KPB. Despite this refinement to the ages of the Naskal and Rangapur sites, we still are not able to unambiguously support a model in which the K/Pg mass extinction triggered the origin and diversification of placentals ("hard explosive" model) versus a model in which a few placental lineages survived the K/Pg mass extinction to ignite the early Paleocene diversification ("soft explosive" model; Phillips and Fruciano, 2018). Notably, Deccanolestes, as well as another possible placental Kharmerungulatum, is also known from the Kisalpuri site; thus, geochronological data from this locality would provide critical information to discriminate between these models.

6. Conclusions

The first-discovered Cretaceous mammal site in India is now recognized as one of the last of the Cretaceous or first of the Paleocene. ⁴⁰Ar/³⁹Ar dating of the lavas bracketing the Naskal and Rangapur sites indicate that these intertrappeans were deposited between 66.210 and 66.031 Ma (Naskal) and between 66.264 and 66.046 Ma (Rangapur) at 95% confidence. This indicates that a latest Maastrichtian age for both sites is most likely, although a Paleocene age for either or both is possible, but much less probable. Thus, Naskal and Rangapur represent 'transitional' intertrappeans, whose fauna and palynoflora are distinctive in the absence of dinosaurs, the presence of mostly small-bodied eutherian mammals, and palynomorphs typical of the Maastrichtian (Crybelosporites intertrappea), Maastrichtian-Paleocene (Gabonisporis vigourouxii, Mulleripollis bolpurensis), and Paleocene (Striacolporites striatus, Echistephanocolpites meghalayensis, Palmaepollenites neyvelii, Aesculipollis sp.). These 'transitional' intertrappeans can be distinguished from typical Maastrichtian intertrappeans, such as those at Ranipur, Takli, Anjar, and Ukala, which contain dinosaur remains and Maastrichtian palynomorphs including Gabonisporis bacricumulus, Aquilapollenites indicus (Anjar; Dogra et al., 2004) or Azolla cretacea, Triporoletes reticulatus, Pulcheripollenites cauveriana, and Hemicorpus group (Ranipur; Mathur and Sharma, 1990). Our results suggest that the Kisalpuri and Upparhati (Gokak) sites, both of which are geographically adjacent and biotically similar to Naskal and Rangapur, might also be 'transitional' intertrappeans, but this requires additional testing.

The prevailing notion that there are two superimposed sedimentary horizons associated with the Deccan Traps Volcanic Province—"infratrappeans" and "intertrappeans"—has been demonstrated to be incorrect and misleading based on previous magnetostratigraphic results and the new geochronological data presented in this paper. Not only are there infratrappean horizons that are younger than intertrappean horizons, a finer breakdown of DTVP-associated sediments is beginning to emerge. Our results combined with previous work on fossiliferous sites in the DTVP (Hansen et al., 2005; Mohabey and Samant, 2013; Mohabey et al., 2019) suggest the presence of at least six distinct groups of localities: C30N infratrappeans (e.g., Rahioli), 30N intertrappeans (e.g., Mohgaon Kalan, Bagwanya, Bharudpura, Ukala), C30N-C29R infratrappeans (e.g., Dongargaon), C29R Maastrichtian infratrappeans (e.g., Bara Simla), C29R Maastrichtian intertrappeans (e.g., Bara Simla), C29R Maast

g., Ranipur, Takli, Anjar), and C29R 'transitional' intertrappeans (e.g., Naskal, Rangapur, ?Kisalpuri, ?Upparhati). These temporally distinct sites and associated biota force reconsideration of simplistic lumping of fossils from infratrappean and intertrappean localities in faunal discriminatory analyses (e.g., Halliday et al., 2018, 2020).

Supplementary data to this article can be found online at https://doi.org/10.1016/j.palaeo.2022.110857.

Declaration of Competing Interest

The authors declare no competing interests.

Acknowledgements

This research was conducted under the auspices of a Memorandum of Understanding between BS (RTMNU) and JAWM (UM) and between SA and DCDS (formerly GSI/PAL/SR) and GPWM (UW). We thank A. Marzoli, K. Goram, R. Patel, D. Kumar, D. DeMar, Jr., L. Weaver, GSI/ PAL/SR crews, and Naskal locals for assistance in the field. We thank Prof. S. Sangode, Department of Geology, SP Pune University, Pune, India for analysis of samples for paleomagnetic studies. BS is grateful to Head, Department of Geology, RTMNU, Nagpur, India for providing working facilities and Jawaharlal Nehru Aluminium Research Development and Design Centre, Nagpur, India for help in SEM study of palynomorphs. We thank the late William A. Clemens for his support and guidance of this project. We thank S. Santana for access to the Santana Lab μCT scanner, B. Hovatter for μCT scanning, H. Fulghum for μCT processing, post-processing, and construction of specimen plates, and M. Holland for reproduction of 3D print casts. We also thank Dr. M. Mahajan, Director, Palaeontology Division, Geological Survey of India, Hyderabad and former Director Dr. K. Ayyassami for facilitating our visit to GSI to examine the mammalian fossil collection. This research was supported by a grant from the National Science Foundation to co-PIs PRR (EAR-1736737), TST (EAR-1736792), GPWM (EAR-1736787), and JAWM (EAR-1736606), grants from UCMP Welles Fund, the National Geographic Society, and the UW Royalty Research Fund to GPWM, and grants from the Ministry of Earth Science, New Delhi (No. MoES/PO (GEOSCI)/49/2015) and Science and Engineering Research Board, New Delhi (CRG/2020/001339) to BS and DMM.

References

- Ahluwalia, A.D., 1990. Geological map and detailed field observations on the Cretaceous mammal bearing locality, Hyderabad District, Andhra Pradesh, India. In: Sahni, A., Jolly, A. (Eds.), Cretaceous Event Stratigraphy and the Correlation of the Indian Nonmarine Strata, A Seminar cum Workshop IGCP 216 and 245, Chandigarh, pp. 120–122.
- Alexander, P.O., 1981. Age and duration of Deccan volcanism: K-Ar evidence. Mem. Geol. Soc. India 3, 244–258.
- Anantharaman, S., Das Sarma, D.C., 1997. Palaeontological studies on the search of micromammals in the infra and intertrappean sediments of Karnatak. Rec. Geol. Surv. India 130, 239–240.
- Anantharaman, S., Wilson, G.P., Das Sarma, D.C., Clemens, W.A., 2006. A possible Late Cretaceous "Haramiyidan" from India. J. Vertebr. Paleontol. 26, 488–490.
- Archibald, J.D., 1982. A study of Mammalia and geology across the Cretaceous-Tertiary boundary in Garfield County, Montana. Univ. California Publicat. Geol. Sci. 122, 1–286.
- Archibald, J.D., 2003. Timing and biogeography of the eutherian radiation: fossils and molecules compared. Mol. Phylogenet. Evol. 28, 350–359.
- Archibald, J.D., Averianov, A.O., Ekdale, E.G., 2001. Late Cretaceous relatives of rabbits, rodents, and other extant eutherian mammals. Nature 414, 62–65.
- Archibald, J.D., Zhang, Y., Harper, T., Cifelli, R.L., 2011. Protungulatum, confirmed Cretaceous occurrence of an otherwise eutherian (placental?) mammal. J. Mamm. Evol. 18, 153–161.
- Arratia, G., López-Arbarello, A., Prasad, G.V.R., Parmar, V., Kriwet, J., 2004. Late Cretaceous-Paleocene percomorphs from India early radiation of Perciformes; pp. In: Arratia, G., Wilson, M.V.H., Cloutier, R. (Eds.), Recent Advances in the Origin and Early Radiation of Vertebrates. Verlag Dr. Friedrich Pfeil, München, Germany, pp. 635–663.
- Bajpai, S., Sahni, A., Jolly, A., Srinivasan, S., 1990. Kachchh intertrappean biotas: affinities and correlation. In: Sahni, A., Jolly, A. (Eds.), Cretaceous Event Stratigraphy and the Correlation of the Indian Nonmarine Strata, A Seminar cum Workshop IGCP 216 and 245 Chandigarh, pp. 101–105.

- Baksi, A.K., 1994. Geochronological studies on whole rock basalts, Deccan Traps, India: evaluation of the timing of volcanism relative to the K-T boundary. Earth Planet. Sci. Lett. 121, 43–56.
- Baksi, S.K., Deb, U., 1976. On Mulleripollis bolpurensis gen. et sp. nov. from the Upper Cretaceous of Bengal Basin. Rev. Palaeobot. Palynol. 22, 73–77.
- Baksi, S.K., Deb, U., 1980. Palynostratigraphic zonation of the Upper Cretaceous-Paleogene sequences of Bengal Basin. Geophytology 10, 199–224.
- Bande, M.B., Chanda, A., Venkatachala, B.S., Mehrotra, R.C., 1988. Deccan traps floristics and their stratigraphic implications. In: Proceedings of the Symposium on Palaeocene of India: Limits and Subdivision (Indian Association of palynostratigraphers, Lucknow), pp. 83–123.
- Beane, J.E., Turner, C.A., Hooper, P.R., Subbarao, K.V., Walsh, J.A., 1986. Stratigraphy, composition and form of the Deccan Basalts, Western Ghats, India. Bull. Volcanol. 48, 61–83.
- Bercovici, A., Pearson, D., Nichols, D.J., Wood, J., 2009. Biostratigraphy of selected K/T boundary sections in southwestern North Dakota, USA: toward a refinement of palynological identification criteria. Cretac. Res. 30, 632e658.
- Bilgrami, S.Z., 1999. A reconnaissance geological map of eastern part of the Deccan Traps (Bidar-Nagpur). In: Subbarao, K.V. (Ed.), Deccan Volcanic Province. Memoirs of the Geological Society of India 43, pp. 219–232.
- Bininda-Emonds, O.R.P., Cardillo, M., Jones, K.E., MacPhee, R.D.E., Beck, R.M.D., Grenyer, R., Price, S.A., Vos, R.A., Gittleman, J.L., Purvis, A., 2007. The delayed rise of present-day mammals. Nature 446, 507–512.
- Blanco, A., 2019. *Igdabatis marmii* sp. nov. (Myliobatiformes) from the lower Maastrichtian (Upper Cretaceous) of north-eastern Spain: an Ibero-Armorican origin for a Gondwanan batoid. J. Syst. Palaeontol. 17, 865–879.
- Blanford, W.T., 1867a. Traps and intertrappean beds of western and central India. Mem. Geol. Soc. India 1, 295–330.
- Blanford, W.T., 1867b. On the traps and intertrappean beds of Western and Central India. Mem. Geol. Surv. India 6, 137–162.
- Boltenhagen, E., 1967. Spore and pollen of the Upper Cretaceous of Gabon. Pollen Spores 9, 335–339.
- Bonaparte, J.F., Novas, F.E., Coria, R.A., 1990. *Carnotaurus sastrei* Bonaparte, the horned, lightly built carnosaur from the Middle Cretaceous of Patagonia. Contribut. Sci. 416, 1–42.
- Bonde, S.D., 2008. Indian fossil monocotyledons: current status, recent developments and future directions. Palaeobotanist 57, 141–164.
- Borkar, V.D., 1973. Fossil fishes from the inter-trappean beds of Surendranagar District, Saurashtra. Proceed. Indian Acad. Sci. Section B 78, 181–193.
- Bown, T.M., Kraus, M.J., 1979. Origin of the tribosphenic molar and metatherian and eutherian dental formulae; pp. In: Lillegraven, J.A., Kielan-Jaworowska, Z., Clemens, W.A. (Eds.), Mesozoic Mammals: The First Two-Thirds of Mammalian History. University of California Press, Berkeley, pp. 172–181.
- Boyer, D.M., Prasad, G.V.R., Krause, D.W., Godinot, M., Goswami, A., Verma, O., Flynn, J.J., 2010. New postcrania of *Deccanolestes* from the Late Cretaceous of India and their bearing on the evolutionary and biogeographic history of euarchontan mammals. Naturwissenschaften 97, 365–377.
- Buffetaut, E., 1987. On the age of the dinosaur fauna from the Lameta Formation (Upper Cretaceous of Central India). Newsl. Stratigr. 18, 1–6.
- Butler, P.M., 1990. Early trends in the evolution of tribosphenic molars. Biol. Rev. 65, 529–552.
- Cappetta, H., 1972. Les poissons crétacés et tertiaires du bassin des Iullemmeden (République du Niger). Palaeovertebrata 5, 179–225.
- Carrano, M.T., Sampson, S.D., Forster, C., 2002. The osteology of Masiakasaurus knopfleri, a small abelisauroid (Dinosauria:Theropoda) from the Late Cretaceous of Madagascar. J. Vertebr. Paleontol. 22, 510–534.
- Chatterjee, S., 1978. *Indosuchus* and *Indosaurus*, Cretaceous carnosaurs from India. J. Paleontol. 52, 570–580.
- Chen, M., Wilson, G.P., 2015. A multivariate approach to infer locomotor modes in Mesozoic mammals. Paleobiology 41, 280–312.
- Chenet, A.-L., Courtillot, V., Fluteau, F., Gérard, M., Quidelleur, X., Khadri, S.F.R., Subbarao, K.V., Thordarson, T., 2009. Determination of rapid Deccan eruptions across the Cretaceous-Tertiary boundary using paleomagnetic secular variation: 2. Constraints from analysis of eight new sections and synthesis for a 3500-m-thick composite section. J. Geophys. Res. Solid Earth 114, 1–38.
- Chester, S.G., Sargis, E.J., Szalay, F.S., Archibald, J.D., Averianov, A.O., 2012. Therian femora from the Late Cretaceous of Uzbekistan. Acta Palaeontol. Pol. 57, 53–64.
- Chester, S.G., Bloch, J.I., Boyer, D.M., Clemens, W.A., 2015. Oldest known euarchontan tarsals and affinities of Paleocene *Purgatorius* to Primates. Proc. Natl. Acad. Sci. 112, 1487–1492.
- Chiappe, L.M., Salgado, L., Coria, R.A., 2001. Embryonic skulls of titanosaur sauropod dinosaurs. Science 293, 2444–2446.
- Chitaley, S.D., 1950. Microflora of the Deccan intertrappean cherts, Paleobotany in India, VII. J. Indian Bot. Soc. 29, 30.
- Chitaley, S.D., 1951. Fossil megaflora from the Mahagaon Kalan beds of the Madhya Pradesh, India. Proceed. Nat. Inst. Sci. India 17, 373–383.
- Cifelli, R.L., 2000. Cretaceous mammals of Asia and North America. Paleontol. Soc. Korea Special Publication 4, 49–84.
- Collinson, D.W., 1983. Methods in Rock Magnetism and Palaeomagnetism: Techniques and Instrumentation. Chapman and Hall, New York, p. 503.
- Coulthard, H., 1833. The trap formation of the Sagar District, and those districts westward of it, as far as Bhopalpur, on the banks of river Newas, in Omatwara. Asiatic Res. 18, 47–81.
- Couper, R.A., 1953. Upper Mesozoic and Cenozoic spores and pollen grains from New Zealand. New Zealand Geol. Surv. Paleontol. Bull. 22, 1–77.

- Courtillot, V., Besse, J., Vandamme, D., Montigny, R., Jaeger, J.-J., Cappetta, H., 1986.
 Deccan flood basalts at the Cretaceous/Tertiary boundary? Earth Planet. Sci. Lett.
 80. 361–374.
- Courtillot, V., Feraud, G., Maluski, H., Vandamme, D., Moreau, M.G., Besse, J., 1988.
 Deccan flood basalts at the Cretaceous/Tertiary boundary. Nature 333, 843–845.
- Cox, K.G., Hawkesworth, C.J., 1984. Relative contribution of crust and mantle to flood basalt magmatism, Mahabaleshwar area, Deccan Traps. Philos. Trans. R. Soc. Lond. A 310, 627–641.
- Cox, K.G., Hawkesworth, C.J., 1985. Geochemical stratigraphy of the Deccan Traps at Mahabaleshwar, Western Ghats, India, with implications for open system magmatic processes. J. Petrol. 26, 355–377.
- Cripps, J.A., Widdowson, M., Spicer, R.A., Jolley, D.W., 2005. Coastal ecosystem responses to late stage Deccan Trap volcanism: the post K-T boundary (Danian) palynofacies of Mumbai (Bombay), west India. Palaeogeogr. Palaeoclimatol. Palaeoecol. 216, 303–332.
- Das Sarma, D.C., Anantharaman, S., Vijayasarathi, G., Nath, T.T., Rao, C.V., 1995.Palaeontological studies for the search of micromammals in the infra- and intertrappean horizons of Andhra Pradesh. Rec. Geol. Surv. India 128, 223.
- Davies, T.W., Bell, M.A., Goswami, A., Halliday, T.J., 2017. Completeness of the eutherian mammal fossil record and implications for reconstructing mammal evolution through the Cretaceous/Paleogene mass extinction. Paleobiology 43, 521–536.
- de Broin, Lapparent, De, F., Chirio, L., Bour, R., 2020. The oldest erymnochelyine turtle skull, *Ragechelus sahelica* n. gen., n. sp., from the Iullemmeden basin, Upper Cretaceous of Africa, and the associated fauna in its geographical and geological context. In: Steyer, J.-S., Augé, M.L., Métais, G. (Eds.), Memorial Jean-Claude Rage: A Life of a Paleo-Herpetologist. Geodiversitas, 42, pp. 455–484.
- DeBey, L.B., Wilson, G.P., 2017. Mammalian distal humerus fossils from eastern Montana, USA with implications for the Cretaceous-Paleogene mass extinction and the adaptive radiation of placentals. Palaeontol. Electron. 20 (3), 1–92.
- Deshmukh, S.S., 1988. Petrographic variations in compound flows of Deccan Traps and their significance. In: Subbarao, K.V. (Ed.), Deccan Flood Basalts of India: Geological Society of India Memoir, 10, pp. 305–319.
- Devey, C.W., Lightfoot, P.C., 1986. Volcanological and tectonic control of stratigraphy and structure in the Western Deccan Traps. Bull. Volcanol. 48, 195–207.
- Dingus, L.J., Clarke, G.R., Scott, C.C., Swisher, L.M., Chiappe, and R. A. Coria., 2000. Stratigraphy and magnetostratigraphic/faunal constraints for the age of sauropod embryo-bearing rocks in the Neuquén Group (Late Cretaceous, Neuquén Province, Argentina). Am. Mus. Novit. 3290, 1–11.
- Dogra, N.N., Raghumani, Y., Singh, R.Y., 2004. Palynological assemblage from the Anjar intertrappean, Kachchh district, Gujarat: age implication. Curr. Sci. 86, 1596–1597.
- dos Reis, M., Inoue, J., Hasegawa, M., Asher, R.J., Donoghue, P.C., Yang, Z., 2012. Phylogenomic datasets provide both precision and accuracy in estimating the timescale of placental mammal phylogeny. Proc. R. Soc. Lond. B Biol. Sci. 279 (1742), 3491–3500.
- Duncan, P.M., 1865. A description of Echinodermata from the strata of the south-eastern coast of Arabia, and at Bagh on the Nerbudda, in the collection of the Geological Society. Q. J. Geol. Soc. Lond. 21, 349–363.
- Duncan, R.A., Pyle, D.G., 1988. Rapid eruption of the Deccan flood basalts at the Cretaceous/Tertiary boundary. Nature 333, 833–841.
- Dutt, N.V.B.S., 1975. Deccan traps of the western part of Hyderabad District, Andhra Pradesh. Rec. Geol. Surv. India 106, 114–126.
- Fastovsky, D.E., Bercovici, A., 2016. The Hell Creek Formation and its contribution to the Cretaceous–Paleogene extinction: A short primer. Cretac. Res. 57, 368–390.
- Foote, M., Hunter, J.P., Janis, C.M., Sepkoski Jr., J.J., 1999. Evolutionary and preservational constraints on origins of biologic groups: Divergence times of eutherian mammals. Science 283, 1310–1314.
- Garcia, G., Marivaux, L., Pélissié, T., Vianey-Liaud, M., 2006. Earliest Laurasian sauropod eggshells. Acta Palaeontol. Pol. 51, 99–104.
- Goswami, A., Prasad, G.V.R., Upchurch, P., Boyer, D.M., Seiffert, E.R., Verma, O., Gheerbrant, E., Flynn, J.J., 2011. A radiation of arboreal basal eutherian mammals beginning in the Late Cretaceous of India. Proc. Natl. Acad. Sci. 108, 16333–16338.
- Grossnickle, D.M., Newham, E., 2016. Therian mammals experience an ecomorphological radiation during the Late Cretaceous and selective extinction at the K–Pg boundary. Proc. R. Soc. Lond. B Biol. Sci. 283, 20160256.
- Halliday, T.J.D., Prasad, G.V.R., Goswami, A., 2018. Faunal similarity in Madagascan and South Indian Late Cretaceous vertebrate faunas. Palaeogeogr. Palaeoclimatol. Palaeoecol. 468, 70–75.
- Halliday, T.J., Holroyd, P.A., Gheerbrant, E., Prasad, G.V.R., Scanferla, A., Beck, R.M.D., Krause, D.W., Goswami, A., 2020. Leaving Gondwana: the changing position of the Indian Subcontinent in the global faunal network; pp. In: Prasad, G.V.R., Patnaik, R. (Eds.), Biological Consequences of Plate Tectonics: New Perspectives on Post-Gondwana Break-up—A Tribute to Ashok Sahni. Vertebrate Paleobiology and Paleoanthropology Series. Springer Nature, Switzerland, pp. 227–249.
- Hansen, H.J., Toft, P., Mohabey, D.M., Sarkar, A., 1996. Lameta age: dating the main pulse of Deccan Trap volcanism. Gondwana Geol. Mag. Special 2, 365–374.
- Hansen, H.J., Mohabey, D.M., Lojen, S., Toft, P., Sarkar, A., A., 2005. Orbital cycles and stable carbon isotopes of sediments associated with Deccan volcanic suite, India: implications for the stratigraphic correlation and Cretaceous/Tertiary boundary. Gondwana Geological Magazine, pp. 5–28. Special Volume 8.
- Harper, A.M., 2011. Three-dimensional analysis of large scale dental wear in Late Cretaceous eutherians, Dzharakuduk region Uzbekistan. Master thesis. (San Diego State University, San Diego).
- Hislop, S., Hunter, R., 1854. On the geology and fossils of the neighbourhood of Nágpur, Central India. Q. J. Geol. Soc. 11, 345–383.

- Hofmann, C., Féraud, G., Courtillot, V., 2000. 40Ar/39Ar dating of mineral separates and whole rocks from the Western Ghats lava pile: further constraints on duration and age of the Deccan traps. Earth Planet. Sci. Lett. 180, 13–27.
- Hora, S.L., 1937. Geographical distribution of Indian freshwater fishes and its bearing on the probable land connections between India and adjacent countries. Curr. Sci. 7, 351–356.
- Hora, S.L., 1938. On the age of the Deccan Trap as evidenced by fossil fish-remains. Curr. Sci. 8, 370–372.
- Horner, J.R., Goodwin, M.B., Myhrvold, N., 2011. Dinosaur census reveals abundant *Tyrannosaurus* and rare ontogenetic stages in the Upper Cretaceous Hell Creek Formation (Maastrichtian), Montana, USA. PLoS One 6, e16574.
- Huene, F.V., Matley, C.A., 1933. Cretaceous Saurischia and Ornithischia of the Central Provinces of India. Palaeontologica Indica 21, 1–74.
- Hughes, J.J., Berv, J.S., Chester, S.G., Sargis, E.J., Field, D.J., 2021. Ecological selectivity and the evolution of mammalian substrate preference across the K–Pg boundary. Ecol. Evolut. 11, 14540–14554.
- Hull, P.M., Bornemann, A., Penman, D.E., Henehan, M.J., Norris, R.D., Wilson, P.A.,
 Blum, P., Alegret, L., Batenburg, S.J., Bown, P.R., Bralower, T.J., Cournede, C.,
 Deutsch, A., Donner, B., Friedrich, O., Jehle, S., Kim, H., Kroon, D., Lippert, P.C.,
 Loroch, D., Moebius, I., Moriya, K., Peppe, D.J., Ravizza, G.E., Röhl, U., Schueth, J.
 D., Sepúlveda, J., Sexton, P.F., Sibert, E.C., Sliwinska, K.K., Summons, R.E.,
 Thomas, E., Westerhold, T., Whiteside, J.H., Yamaguchi, T., Zachos, J.C., 2020. On
 impact and volcanism across the Cretaceous-Paleogene boundary. Science 367,
 266–272.
- Jain, S.L., Sahni, A., 1983. Some Upper Cretaceous vertebrates from central India and their palaeogeographic implications; pp. In: Maheshwari, H.K. (Ed.), Indian Association of Palynostratigraphers Symposium on Cretaceous of India, Lucknow, 1983. Birbal Sahni Institute of Palaeobotnay, Lucknow, Uttar Pradesh, pp. 66–83.
- Jay, A.E., Widdowson, M., 2008. Stratigraphy, structure and volcanology of the SE Deccan continental flood basalt province: implications for eruptive extent and volumes. J. Geol. Soc. 165, 177–188.
- Jay, A.E., MacNiocaill, C., Widdowson, M., Self, S., Turner, W., 2009. New paleomagnetic data from the Mahabaleshwar plateau, Deccan Flood Basalt Province, India: implications on volcanostratigraphic architecture of continental flood basalt provinces. J. Geol. Soc. 166, 13–24.
- Jerram, D.A., 2002. Volcanology and facies architecture of flood basalts. Special Paper Geol. Soc. Am. 362, 119–132.
- Jerram, D.A., Widdowson, M., 2005. The anatomy of continental flood basalt provinces: geological constraints on the processes and products of flood volcanism. Lithos 79, 385–405.
- Kale, V.S., Dole, G., Shandilya, P., Pande, K., 2020. Stratigraphy and correlations in Deccan Volcanic Province, India: quo vadis? Geol. Soc. Am. Bull. 132, 588–607.
- Kaneoka, I., Haramura, H., 1973. K/Ar ages of successive lava flows from the Deccan Trans. India. Earth Planet. Sci. Lett. 18, 229–236.
- Kapgate, D.K., 2005. Megafloral analysis of intertrappean sediments with focus on diversity and abundance of flora of Mohgaonkalan, Mandla and adjoining areas of Madhya Pradesh. Gondwana Geol. Mag. 20, 31–45.
- Kar, R.K., Srinivasan, S., 1997. Late Cretaceous palynofossils from the Deccan intertrappean beds of Mohagaon Kalan, Chhindwara District, Madhya Pradesh. Geophytology 27, 17–22.
- Keller, G., Adatte, T., Bajpai, S., Mohabey, D.M., Widdowson, M., Khosla, A., Sharma, R., Khosla, S.C., Fleitmann, D., Sahni, A., 2009. K-T transition in Deccan Traps of central India marks major marine seaway across India. Earth Planet. Sci. Lett. 282, 10–23.
- Khajuria, C.K., Prasad, G.V.R., 1998. Taphonomy of a Late Cretaceous mammal-bearing microvertebrate assemblage from the Deccan inter-trappean beds of Naskal, peninsular India. Palaeogeogr. Palaeoclimatol. Palaeoecol. 137, 153–172.
- Khajuria, C.K., Singh, B.P., 1992. Geochemistry of the infratrappean beds of Marepalli and intertrappean beds of Naskal, Rangareddy District, Andhra Pradesh. Proceed. Indian Nat. Sci. Acad. 58, 69–82.
- Khosla, A., Prasad, G.V.R., Verma, O., Jain, A.K., Sahni, A., 2004. Discovery of a micromammal-yielding Deccan intertrappean site near Kisalpuri, Dindori District, Madhya Pradesh. Curr. Sci. 87, 380–383.
- Kielan-Jaworowska, Z., Cifelli, R.L., Luo, Z.-X., 2004. Mammals from the Age of Dinosaurs: Origins, Evolution, and Structure. Columbia University Press, New York, p. 630.
- Krause, D.W., Prasad, G.V.R., Koenigswald, W.V., Sahni, A., Grine, F.E., 1997. Cosmopolitanism among Gondwanan Late Cretaceous mammals. Nature 390, 504–507.
- Kumaran, K.P.N., Bonde, S.D., Kanitkar, M.D., 1997. An Aquilapollenites associated palynoflora from Mohagaonkalan and its stratigraphic implications for age and stratigraphic correlation of Deccan intertrappean beds. Curr. Sci. 72, 590–592.
- Lofgren, D.L., Lillegraven, J.A., Clemens, W.A., Gingerich, P.D., Williamson, T.E., 2004.
 Paleocene biochronology: The Puercan through Clarkforkian land mammal ages. In:
 Woodburne, M.O. (Ed.), Late Cretaceous and Cenozoic Mammals of North America:
 Biostratigraphy and Geochronology. Columbia University Press, New York, pp. 43–105.
- Lydekker, R., 1877. Notices of new and other vertebrata from Indian tertiary and secondary rocks. Rec. Geol. Soc. India 10, 30–42.
- Manz, C.L., Chester, S.G., Bloch, J.I., Silcox, M.T., Sargis, E.J., 2015. New partial skeletons of palaeocene nyctitheriidae and evaluation of proposed euarchontan affinities. Biol. Lett. 11, 20140911.
- Mathur, N. S., and S. D. Sharma. 1990. Palynofossils and age of the Ranipur intertrappean beds, Gaur River, Jabalpur, M.P. 58–59 A. Sahni and A. Jolley Cretaceous event Stratigraphy and Correlation of Indian Non-Marine Strata, Chandigarh. International Geological Correlation Project 216-245.

- Mathur, S.C., Gour, S.D., Loyal, R.S., Tripathi, A., Sisodia, M.S., 2005. Spherules from the Late Cretaceous phosphates of the Fatehgarh Formation, Barmer Basin, India. Gondwana Res. 8 (4), 579–584.
- Mathur, S.K., Mathur, S.C., Loyal, R.S., 2006. First microvertebrate assemblage from the Fatehgarh Formation (Cretaceous), Barmer District, Western Rajasthan. J. Geol. Soc. India 67, 759–769.
- Matley, C.A., 1921. On the stratigraphy, fossils and geological relationships of the Lameta beds of Jubbulpore. Rec. Geol. Surv. India 53, 142–164.
- Medlicott, H.B., 1872. Note on the Laméta or Infra-trappan Formation of Central India. Rec. Geol. Surv. India 5, 115–119.
- Mehrotra, N.C., Venkatachala, B.S., Kapoor, P.N., 2005. Palynology in hydrocarbon exploration (the Indian scenario). Mem. Geol. Soc. India 61, 1–128.
- Meredith, R.W., Janečka, J.E., Gatesy, J., Ryder, O.A., Fisher, C.A., Teeling, E.C., Goodbla, A., Eizirik, E., Simão, T.L., Stadler, T., Rabosky, D.L., Honeycutt, R.L., Flynn, J.J., Ingram, C.M., Steiner, C., Williams, T.L., Robinson, T.J., Burk-Herrick, A., Westerman, M., Ayoub, N.A., Springer, M.S., Murphy, W.J., 2011. Impacts of the Cretaceous terrestrial revolution and KPg extinction on mammal diversification. Science 334, 521–524.
- Mitchell, C., Widdowson, M., 1991. Geological maps of the southern Deccan Traps, India and its structural implications. J. Geol. Soc. 148, 495–505.
- Mohabey, D.M., Samant, B., 2013. Deccan continental flood basalt eruptions terminated Indian dinosaurs before Cretaceous-Palaeocene boundary. Geol. Soc. India, Special 1, 260–267.
- Mohabey, D.M., Samant, B., Kumar, D., Dhobale, A., Rudra, A., Dutta, S., 2018. Record of charcoal from early Maastrichtian intertrappean lake sediments of Bagh valley of Madhya Pradesh: palaeofire proxy. Curr. Sci. 114, 1540–1544.
- Mohabey, D.M., Samant, B., Dhobale, A., Kumar, D., 2019. Reptilian vertebrates from Deccan volcanic associated sediments of Malwa Plateau in context to reptiles across Maastrichtian-Paleocene volcanic eruptions in Main Deccan Volcanic Province, India. Global Geol. 22, 250–257.
- Molnar, R.E., 1990. Problematic Theropoda: "Carnosaurs;" pp. In: Weishampel, D.B., Dodson, P., Osmólska, H. (Eds.), The Dinosauria. University of California Press, Berkeley, pp. 306–317.
- Moody, R.T.J., Sutcliffe, P.J.C., 1991. The Cretaceous deposits of the Iullemmeden Basin of Niger, central West Africa. Cretac. Res. 12, 137–157.
- Nessov, L.A., Archibald, J.D., Kielan-Jaworowska, Z., 1998. Ungulate-like mammals from the Late Cretaceous of Uzbekistan and a phylogenetic analysis of Ungulatomorpha, in C. Beard and M. Dawson (eds.), Dawn of the Age of Mammals in Asia. Bull. Carnegie Museum Nat. Hist. 34, 40–88.
- Nichols, D.J., Johnson, K.R., 2008. Plants and the K-T Boundary. Cambridge University Press. p. 280.
- Nolf, D., Rana, R.S., Prasad, G.V.R., 2008. Late Cretaceous (Maastrichtian) fish otoliths from the Deccan Intertrappean Beds, India: a revision. In: Steurbaut, E., Jagt, J.W.M., Jagt-Yazykova, E.A. (Eds.), Annie V. Dhondt Memorial Volume. Bulletin de l'Institut Royal des Sciences Naturelles de Belgique, Sciences de la Terre 78, pp. 239–259.
- Nordt, L., Atchley, S., Dworkin, S., 2003. Terrestrial evidence for two greenhouse events in the latest Cretaceous. GSA Today 13, 4–9.
- O'Leary, M.A., Bloch, J.I., Flynn, J.J., Gaudin, T.J., Giallombardo, A., Giannini, N.P., Goldberg, S.L., Kraatz, B.P., Luo, Z.-X., Meng, J., Ni, X., Novacek, M.J., Perini, F.A., Randall, Z.S., Rougier, G.W., Sargis, E.J., Silcox, M.T., Simmons, N.B., Spaulding, M., Velazco, P.M., Weksler, M., Wible, J.R., Cirranello, A.L., 2013. The placental mammal ancestor and the post–K-Pg radiation of placentals. Science 339, 662–667.
- Pande, K., Venkatesan, T.R., Gopalan, K., Krishnamurthy, P., Macdougall, J.D., 1988. 40Ar–39Ar ages of alkali basalts from Kutch, Deccan volcanic province, India. Mem. Geol. Soc. India 10, 145–150.
- Phillips, M.J., Fruciano, C., 2018. The soft explosive model of placental mammal evolution. BMC Evol. Biol. 18, 1–13.
- Pocknall, D.T., Nichols, D.J., 1996. Palynology of coal zones of the Tongue River Member (upper Paleocene) of the Fort Union Formation, Powder River Basin, Montana and Wyoming. Am. Associat. Stratigr. Palynolog. Contribut. Ser. 32, 1–58.
- Prakash, U., 1960. A survey of the Deccan Intertrappean flora of India. J. Paleontol. 34 (5), 1027–1040.
- Prakash, T., Singh, R.Y., Sahni, A., 1990. Palynofloral assemblage from the Padwar Deccan intertrappean (Jabalpur) M.P., pp. 68–69. In: Sahni, A., Jolly, A. (Eds.), Cretaceous Event Stratigraphy and Correlation of Indian Non Marine Strata, Chandigarh, International Geological Correlation Project, pp. 216–245.
- Prasad, G.V.R., 1989. Vertebrate fauna from the infra- and inter-trappean beds of Andhra Pradesh: age implications. J. Geol. Soc. India 34, 161–173.
- Prasad, G.V.R., 2009. Divergence time estimates of mammals from molecular clocks and fossils: Relevance of new fossil finds from India. J. Biosci. 34, 649–659.
- Prasad, G.V.R., 2012. Vertebrate biodiversity of the Deccan volcanic province of India: a review. Bulletin de la Société géologique de France 183, 597–610.
- Prasad, G.V.R., Cappetta, H., 1993. Late Cretaceous selachians from India and the age of the Deccan Traps. Palaeontology 36, 231–248.
- Prasad, G.V.R., de Lapparent de Broin, F., 2002. Late Cretaceous crocodile remains from Naskal (India): comparisons and biogeographic affinities. Annales de Paléontologie 88. 19–71.
- Prasad, G.V.R., Godinot, M., 1994. Tarsal bones from the Late Cretaceous of India. J. Paleontol. 68, 892–902.
- Prasad, G.V.R., Khajuria, C.K., 1990. A record of microvertebrate fauna from the intertrappean beds of Naskal, Andhra Pradesh. J. Palaeontol. Soc. India 35, 151–161.
- Prasad, B., Pundeer, B.S., 2002. Palynological events and zones in Cretaceous-Tertiary boundary sediments of Krishna-Godavari and Cauvery basins, India. Palaeontographica 262, 39–70.
- Prasad, G.V.R., Sahni, A., 1988. First Cretaceous mammal from India. Nature 332, 638–640.

- Prasad, G.V.R., Sahni, A., 1999. Were there size constraints on biotic exchanges during the northward drift of the Indian plate? PINSA 65, 377–396.
- Prasad, G.V.R., Sahni, A., 2014. Vertebrate fauna from the Deccan volcanic province: response to volcanic activity. Geol. Soc. Am. Spec. Pap. 505, 505–509.
- Prasad, G.V.R., Jaeger, J.J., Sahni, A., Gheerbrant, E., Khajuria, C.K., 1994. Eutherian mammals from the Upper Cretaceous (Maastrichtian) intertrappean beds of Naskal, Andhra Pradesh, India. J. Vertebr. Paleontol. 14, 260–277.
- Prasad, G.V.R., Verma, O., Sahni, A., Parmar, V., Khosla, A., 2007a. A Cretaceous hoofed mammal from India. Science 318, 937.
- Prasad, G.V.R., Verma, O., Gheerbrant, E., Goswami, A., Khosla, A., Parmar, V., Sahni, A., 2010. First mammal evidence from the Late Cretaceous of India for biotic dispersal between India and Africa at the KT transition. Comptes Rendus Palevol 9 (1-2), 63-71.
- Prasad, G.V.R., Verma, O., Sahni, A., Krause, D.W., Khosla, A., Parmar, V., 2007b. A new Late Cretaceous gondwanatherian mammal from central India. Proc. Indian Natl. Sci. Acad. 73, 17–24.
- Ramanujam, C.G.K., 1966. Palynology of the Miocene lignite from south Arcot district, Madras, India. Pollen Spores 8, 149–203.
- Rana, R.S., 1988. Freshwater fish otoliths from the Deccan Trap associated sedimentary (Cretaceous-Tertiary transition) beds of Rangapur, Hyderabad, District, Andhra Pradesh, India. Geobios 21, 465–493.
- Rana, R.S., 1990a. Alligatorine teeth from the Deccan Intertrappean beds near Rangapur, Andhra Pradesh, India: further evidence of Laurasiatic elements. Curr. Sci. 59, 49–51.
- Rana, R.S., 1990b. Palaeontology and palaeoecology of the intertrappean (Cretaceous-Tertiary transition) beds of the peninsular India. J. Palaeontol. Soc. India 35, 105–120.
- Rana, R.S., 1996. Additional fish otoliths from the Deccan Trap associated sedimentary beds exposed near Rangapur, Rangareddi District, Andhra Pradesh. In: Pandey, J., Azmi, R.J., Bhandari, A., Dave, A. (Eds.), Contributions to the XV Indian Colloquium on Micropalaeontology and Stratigraphy, Dehra Dun, 1996, pp. 477–490.
- Rana, R.S., 2005. Lizard fauna from intertrappean (Late Cretaceous-Early Palaeocene) beds of peninsular India. Gondwana Geol. Mag. 8, 123–132 (Special Volume).
- Rana, R.S., Wilson, G.P., 2003. New Late Cretaceous mammals from the intertrappean beds of Rangapur, India and paleobiogeographic framework. Acta Palaeontol. Pol. 48, 331–348.
- Rana, R.S., Kumar, K., Singh, H., 2006. Paleocene vertebrate fauna from the Fatehgarh Formation of Barmer District, Rajasthan, Western India; pp. In: Sinha, D.K. (Ed.), Micropaleontology: Application in Stratigraphy and Paleoceanography. Narosa Publishing House, New Delhi, pp. 113–130.
- Rao, M.R., Saxena, R.K., Singh, H.P., 1985. Palynology of the Barail (Oligocene) and Surma (Lower Miocene) sediments exposed along Sonapur–Badarpur Road Section, Jaintia Hills (Meghalaya) and Cachar (Assam). Part 4. Angiospermous pollen grains. Geophytology 15, 7–23.
- Renne, P.R., Balco, G., Ludwig, K.R., Mundil, R., Min, K., 2011. Response to the comment by WH Schwarz et al. on "Joint determination of 40K decay constants and 40Ar*/ 40K for the Fish Canyon sanidine standard, and improved accuracy for 40Ar/39Ar geochronology" by PR Renne et al. (2010). Geochim. Cosmochim. Acta 75 (17), 5097–5100.
- Renne, P.R., Cassata, W.S., Morgan, L.E., 2009. The isotopic composition of atmospheric argon and $^{40}\text{Ar}/^{39}\text{Ar}$ geochronology: time for a change? Quat. Geochronol. 4, 288–298. https://doi.org/10.1016/j.quageo.2009.02.015.
- Renne, P.R., Sprain, C.J., Richards, M.A., Self, S., Vanderkluysen, L., Pande, K., 2015. State shift in Deccan volcanism at the Cretaceous-Paleogene boundary, possibly induced by impact. Science 350, 76–78.
- Richards, M.A., Alvarez, W., Self, S., Karlstrom, L., Renne, P.R., Manga, M., Sprain, C.J., Smit, J., Vanderkluysen, L., Gibson, S.A., 2015. Triggering of the largest Deccan eruptions by the Chicxulub impact. Geol. Soc. Am. Bull. 127, 1507–1520.
- Rode, K.P., 1933a. Petrified palm from the Deccan intertrappean beds I. Quart. J. Geol. Min. Metall. Soc. India 5, 75–88.
- Rode, K.P., 1933b. A note on fossil angiospermous fruit from the Deccan intertrappean beds of central province. Curr. Sci. 2, 171–172.
- Rode, K.P., 1934a. A note on the petrified palms from Mohgaon Kalan, District Chhindwara. In: C.P. Proceedings of the 21st Indian Science Congress, Bombay, 3, p. 349.
- Rode, K.P., 1934b. On *Rhizopaloxylon penchiensis* sp. nov. a fossil palm root from Mohgaon Kalan, District Chhindwara. In: C.P. Proceedings of the 21st Indian Science Congress, Bombay, 3, pp. 349–350.
- Rode, K.P., 1935. On a dicotyledonous leaf impression: *Phyllites mohgaonsis* sp. nov. from the Deccan intertrappean beds of Chhindwara district. In: C.P. Proceedings of the 22nd Indian Science Congress, Calcutta, 3, p. 209.
- Rode, K.P., 1936. A silicified dicotydonous wood: *Dryoxylon mohgaoense* sp. nov. from the Deccan intertrappean beds of India. J. Indian Bot. Soc. 15, 131–138.
- Rogers, A., 1869. A few remarks on the geology of the country surrounding the Gulf of Cambay, in western India. Q. J. Geol. Soc. 26, 118–124.
- Sah, S.C.D., Kar, R.K., 1970. Palynology of the Laki sediments in Kutch-3. Pollen from the bore-holes around Jhularai, Baranda and Panandhro. Palaeobotanist 18, 127–142.
- Sahni, B., 1931. Material for the monograph of the Indian petrified palms. Proceed. Indian Acad. Sci. India 1, 140–144.
- Sahni, B., 1937. General discussion. In: The age of the Deccan Traps. Proceedings of the 24th Indian Science Congress, Hyderabad, pp. 464–467.
- Sahni, B., 1941. Indian silicified plants I Azolla intertrappea Sah and Rao. Proceed. Indian Acad. Sci. India, Section B 14, 489–501.
- Sahni, B., 1943. *Enigmocarpon parijai*, a silicified fruit from the Deccan, with a review of the fossil history of the Lythraceae. Proceed. Indian Acad. Sci. Section B 17, 59–96.

- Sahni, A., 1984. Cretaceous-Paleocene terrestrial faunas of India: lack of endemism during drifting of the Indian Plate. Science 226, 441–443.
- Sahni, B., Rao, H.S., 1943. A silicified flora from the intertrappean cherts around Sausar in the Deccan. Proceed. Nat. Acad. Sci. India 13, 36–75.
- Sahni, B., Rode, K.P., 1937. Fossil plants from the intertrappean beds of Mohgaon Kalan, in the Deccan, with a sketch of the geology of the Chhindwara district. Proceed. Nat. Acad. Sci. India 7, 165–174.
- Sahni, A., Tandon, S.K., Jolly, A., Bajpai, S., Sood, A., Srinivasan, S., 1994. Cretaceous dinosaur eggs and nesting sites from the Deccan volcano-sedimentary province of peninsular India. In: Carpenter, K., Hirsch, K., Horner, J. (Eds.), Dinosaur Eggs and Babies. Cambridge University Press, New York, pp. 204–226.
- Sahni, A., Venkatachala, B.S., Kar, R.K., Rajanikanth, A., Prakash, T., Prasad, G.V.R., Singh, R.Y., 1996. New palynological data from the Deccan Intertrappean beds: implications for the latest record of dinosaurs and synchronous initiation of volcanic activity in India. Mem. Geol. Soc. India 37, 267–283.
- Samant, B., Mohabey, D.M., 2009. Palynoflora from Deccan volcano-sedimentary séquence (Cretaceous-Paleocene transition) of central India: implications for spatiotemporal correlation. J. Biosci. 34, 811–823.
- Samant, B., Mohabey, D.M., 2014. Deccan volcanic eruptions and their impact on flora: palynological evidence. Geol. Soc. Am. Spec. Pap. 505, 171–191.
- Samant, B., Mohabey, D.M., 2016. Tracking temporal palynofloral changes close to Cretaceous-Paleogene boundary in Deccan volcanic associated sediments of eastern part of central Deccan volcanic province. Global Geol. 19, 205–215.
- Samant, B., Mohabey, D.M., Srivastava, P., Thakre, D., 2014. Palynology and clay mineralogy of the Deccan volcanic associated sediments of Saurashtra, Gujarat: age and paleoenvironment. J. Earth Syst. Sci. 123, 219–232.
- Samant, B., Kumar, A., Mohabey, D.M., Humane, S., Kumar, D., Dhoble, A., Priya, P., 2020a. Centropyxis aculeata (testate lobose amoebae) and associated diatoms from the intertrappean lacustrine sediments (Maastrichtian) of central India: implications in understanding paleolake ecology. Palaeontol. Electron. 23, a60.
- Samant, B., Yadav, D., Mohabey, D.M., Kapgate, D.K., Manchester, S.R., Patil, S.K., 2020b. Palynoflora from intertrappean localities in southeastern part of Deccan volcanic province: taxonomic composition, age and paleogeographic implications. Palaeoworld 29, 161–175.
- Saxena, R.K., 1991. A Catalogue of Fossil Plants from India. Part 5, A, B, Cenozoic (Tertiary). A, Spores and Pollen; B, Fungi. Birbal Sahni Institute of Paleobotany, Lucknow, p. 147.
- Saxena, R.K., Trivedi, G.K., 2006. A Catalogue of Tertiary spores and Pollen from India. Birbal Sahni Institute of Paleobotany, Lucknow, p. 221.
- Schneider, C.A., Rasband, W.S., Eliceiri, K.W., 2012. NIH Image to ImageJ: 25 years of image analysis. Nat. Methods 9, 671–675.
- Schoene, B., Samperton, K.M., Eddy, M.P., Keller, G., Adatte, T., Bowring, S.A., Gertsch, B., 2015. U-Pb geochronology of the Deccan Traps and relation to the end Cretaceous mass extinction. Science 347, 182–184.
- Schoene, B., Eddy, M.P., Samperton, K.M., Keller, C.B., Keller, G., Adatte, T., Khadri, S.F. R., 2019. U-Pb constraints on pulsed eruption of the Deccan Traps across the end-Cretaceous mass extinction. Science 363, 862–866.
- Self, S., Thordarson, T., Keszthelyi, L.P., 1997. Emplacement of continental flood basalt lava flows. In: Mahoney, J.J., Coffin, M.F. (Eds.), Large Igneous Provinces: Continental, Oceanic, and Planetary Flood Volcanism, DC 100. American Geophysical Union, Washington, pp. 381–410.
- Sheth, H.C., Zellmer, G.F., Demonterova, E.I., Ivanov, A.V., Kumar, R., Patel, R.K., 2014. The Deccan tholeitte lavas and dykes of Ghatkopar-Powai area, Mumbai, Panvel flexure zone: geochemistry, stratigraphic status and tectonic significance. J. Asian Earth Sci. 84, 69–82.
- Singh, R.S., Kar, R., 2002. Paleocene palynofossils from the Lalitpur intertrappean beds, Uttar Pradesh. J. Geol. Soc. India 60, 213–216.
- Singh, R.S., Kar, R., Prasad, G.V.R., 2006. Deccan intertrappean beds of Naskal, Rangareddi district, Andhra Pradesh. Curr. Sci. 90, 1281–1285.
- Single, R., Jerram, D.A., 2004. The 3-D facies architecture of flood basalt provinces and their internal heterogeneity: examples from the Palaeogene Skye lava field. J. Geol. Soc. 161, 911–926.
- Sleeman, W.H., 1844. Rambles and Recollections of an Indian Official. J. Hatchard and Son, London vol. 1, 478 pp.
- Smith, T., De Bast, E., Sigé, B., 2010. Euarchontan affinity of Paleocene Afro-European adapisoriculid mammals and their origin in the late Cretaceous Deccan Traps of India. Naturwissenschaften 97, 417–422.
- Smith, S.Y., Manchester, S.R., Samant, B., Mohabey, D.M., Wheeler, E.A., Baas, P., Kapgate, D., Srivastava, R., Sheldon, N.D., 2015. Integrating paleobotanical, paleosol, and stratigraphic data to study critical transitions: a case study from the Late Cretaceous–Paleocene of India. In: Polly, P.D., Head, J.J., Fox, D.L. (Eds.), Earth-Life Transitions: Paleobiology in the Context of Earth System Evolution, The Paleontological Society Papers 21, pp. 137–166.
- Smith, S.M., Sprain, C.J., Clemens, W.A., Lofgren, D.L., Renne, P.R., Wilson, G.P., 2018. Early mammalian recovery after the end-Cretaceous mass extinction: a high-resolution view from McGuire Creek area, Montana, USA. Geol. Soc. Am. Bull. 130 (11–12), 2000–2014.
- Soler-Gijón, R., López-Martínez, N., 1998. Sharks and rays (Chondrichthyes) from the Upper Cretaceous red beds of the south-central Pyrenees (Lleida, Spain): indices of an India-Eurasia connection. Palaeogeogr. Palaeoclimatol. Palaeoecol. 141, 1–12.
- Sprain, C.J., Renne, P.R., Clemens, W.A., Wilson, G.P., 2018. Calibration of chron C29r: new high-precision geochronologic and paleomagnetic constraints from the Hell Creek region, Montana. GSA Bull. 130, 1615–1644.
- Sprain, C.J., Renne, P.R., Vanderkluysen, L., Pande, K., Self, S., Mittal, T., 2019. The eruptive tempo of Deccan volcanism in relation to the Cretaceous-Paleogene boundary. Science 363, 866–870.

- Sprain, C.J., Renne, P.R., Wilson, G.P., Clemens, W.A., 2015. High-resolution chronostratigraphy of the terrestrial Cretaceous-Paleogene transition and recovery interval in the Hell Creek region, Montana. Geol. Soc. Am. Bull. 127 (3–4), 393–409.
- Springer, M.S., Murphy, W.J., Elzirik, E., O'Brien, S.J., 2003. Placental mammal diversification and the Cretaceous-Tertiary boundary. Proceed. Nat. Acad. Sci. U.S.A 100, 1056–1061.
- Srinivasan, S., 1996. Late Cretaceous eggshells from the Deccan volcano-sedimentary sequences of central India. In: Sahni, A. (Ed.), Cretaceous Stratigraphy and Environment. Rama Rao Volume. Memoir of the Geological Society of India 37, pp. 321–336.
- Szalay, F.S., Decker, R., 1974. Origins, evolution, and function of the tarsus in Late Cretaceous Eutheria and Paleocene primates. Primate Locomot. 1, 223–259.
- Tantawy, A.A., Keller, G., Adatte, T., Stinnesbeck, E.S., Kassab, A., Schulte, P., 2001. Maastrichtian to Paleocene depositional environment of the Dakhla Formation, Western Desert, Egypt: sedimentology, mineralogy, and integrated micro- and macrofossil biostratigraphies. Cretac. Res. 22, 795–827.
- Thakre, D., Samant, B., Mohabey, D.M., 2016. Palynology and magnetostratigraphy of Deccan volcanic associated sedimentary sequence of Amarkantak Group in Central India: age and paleoenvironment. In: Dzyuba, O.S., Pestchevitskaya, E.F., Shurygin, B.N. (Eds.), Short papers for the Fourth International Symposium of International Geoscience Programme IGCP Project 608. Russian Academy of Science, Novosibirsk, Russia, pp. 101–102.
- Thakre, D., Samant, B., Mohabey, D.M., Sangode, S., Srivastava, P., Kapgate, D.K., Mahajan, R., Upretii, N., Manchester, S.R., 2017. A new insight into age and environments of intertrappean beds of Mohgaon Kalan, Chhindwara District, M. P. using palynology, megaflora, magnetostratigraphy and clay mineralogy. Curr. Sci. 112, 2193–2197.
- Thordarson, T., Self, S., 1998. The Roza Member, Columbia River Basalt Group; a gigantic pāhoehoe lava flow field formed by endogenous processes? J. Geophys. Res. B, Solid Earth Planets 103, 27411–27445.
- Traverse, A., 2007. Paleopalynology, 2nd edition. Springer, p. 772.
- Upham, N.S., Esselstyn, J.A., Jetz, W., 2021. Molecules and fossils tell distinct yet complementary stories of mammal diversification. Curr. Biol. 31, 4195–4206.
- Vandamme, D., Courtillot, V., Besse, J., Montigny, R., 1991. Paleomagnetism and age determinations of the Deccan Traps (India): results of a Nagpur-Bombay traverse and review of earlier work. Rev. Geophys. 29, 159–190.
- Venkatachala, B.S., Sharma, K.D., 1974a. Palynology of the Cretaceous sediments from the subsurface of Pondicherry area (Cauvery Basin). New Botanist 1, 170–200.
- Venkatachala, B.S., Sharma, K.D., 1974b. Palynology of the Cretaceous sediments from the subsurface of Vridhachalam area, Cauvery Basin. Geophytology 4, 151–183.
- Venkatachala, B.S., Sharma, K.D., 1984. Palynological zonation in subsurface sediments in Narsapur well No. 1, Godavari–Krishna Basin, India. In: Proceedings of the X Indian Colloquium on Micropalaeontology and Stratigraphy, pp. 445–466.
- Venkatesan, T.R., Pande, K., Gopalan, K., 1993. Did Deccan volcanism pre-date the Cretaceous/Tertiary transition? Earth Planet. Sci. Lett. 119, 181–189.
- Venugopal Rao, C.H., 1987. Final report on the palaeontological studies on the intertrappean sediments of Andhra Pradesh. Unpublished Report of Geological Survey of India. Palaeontology Division, Southern Region, Hyderabad, pp. 1–21.
- Verma, O., Khosla, A., Kaur, J., Prashanth, M., 2017. Myliobatid and pycnodont fish from the Late Cretaceous of central India and their paleobiogeographic implications. Hist. Biol. 29, 253–265.
- Walker, A.D., 1964. Triassic reptiles from the Elgin area: Ornithosuchus and the origin of carnosaurs. Philosophical Transactions of the Royal Society of London. Series B, Biol. Sci. 248, 53–134.
- Wellman, P., McElhinny, M.W., 1970. K–Ar Age of the Deccan Traps, India. Nature 227, 595–596.
- Wheeler, E.A., Srivastava, R., Manchester, S.R., Bass, P., 2017. Surprisingly modern Latest Cretaceous—earliest Paleocene woods of India. IAWA J. 38, 456–542.
- Wible, J.R., Rougier, G.W., Novacek, M.J., Asher, R.J., 2007. Cretaceous eutherians and Laurasian origin for placental mammals near the K/T boundary. Nature 447, 1003–1006.
- Widdowson, M., Cox, K.G., 1996. Uplift and erosional history of the Deccan Traps, India: Evidence from laterites and drainage patterns of the Western Ghats and Konkan Coast. Earth Planet. Sci. Lett. 137, 57–69.
- Wilson, G.P., 2013. Mammals across the K/Pg boundary in northeastern Montana, U.S. A.: dental morphology and body-size patterns reveal extinction selectivity and immigrant-fueled ecospace filling. Paleobiology 39, 429–469.
- Wilson, G.P., 2014. Mammalian extinction, survival, and recovery dynamics across the Cretaceous-Paleogene Boundary in northeastern Montana, USA. Geol. Soc. Am. Spec. Pap. 503, 365–392.
- Wilson Mantilla, G.P., Chester, S.G., Clemens, W.A., Moore, J.R., Sprain, C.J., Hovatter, B.T., Mitchell, W.S., Mans, W.W., Mundil, R., Renne, P.R., 2021. Earliest Palaeocene purgatoriids and the initial radiation of stem primates. R. Soc. Open Sci. 8, 210050.
- Wilson, J.A., Upchurch, P., 2003. Revision of *Titanosaurus*, the first dinosaur genus with a "Gondwanan" distribution. J. Syst. Palaeontol. 1, 125–160.
- Wilson, G.P., Das Sarma, D.C., Anantharaman, S., 2007. Late Cretaceous sudamericid gondwanatherians from India with paleobiogeographic consideration of Gondwanan mammals. J. Vertebr. Paleontol. 27, 521–531.
- Wilson, J.A., D'Emic, M.D., Curry Rogers, K.A., Mohabey, D.M., Sen, S., 2009. Reassessment of the sauropod dinosaur *Jainosaurus* (=Antarctosaurus) septentrionalis from the Upper Cretaceous of India. Contributions from the Museum of Paleontology, University of Michigan 32, 17–40.
- Wilson, J.A., Barrett, P.M., Carrano, M.T., 2011. An associated partial skeleton of Jainosaurus cf. septentrionalis (Dinosauria: Sauropoda) from the Late Cretaceous of Chhota Simla, central India. Palaeontology 54, 981–998.

- Wilson, G.P., Wilson, J.A., Mohabey, D.M., Samant, B., Tobin, T., Widdowson, M., Renne, P.R., 2019a. Mammalian faunas from the Deccan Volcanic Province and the Cretaceous-Paleogene transition in India. In: Droser, M.L., Hughes, N., Bonuso, N., Bottjer, D.J., Eernisse, D., Gaines, R., Hendy, A., Jacobs, D., Miller-Camp, J., Norris, R., Roy, K., Sadler, P., Springer, M., Wang, X., Vendrasco, M. (Eds.), 11th North American Paleontological Conference Program with Abstracts, PaleoBios, 36, pp. 370–371. Supplement 1.
- Wilson, J.A., Mohabey, D.M., Lakra, P., Bhadran, A., 2019b. Titanosaur (Dinosauria: Sauropoda) vertebrae from the Upper Cretaceous Lameta Formation of western and
- central India. Contributions from the Museum of Paleontology, University of Michigan 33, 1–27.
- Woodward, A.S., 1908. On some fish remains from the Lameta beds at Dongargaon, Central Provinces. Palaeontologia Indica 3, 1–6.
- Yi, S., 1997. Zygnematacean zygospores and other freshwater algae from the Upper Cretaceous of the Yellow Sea Basin, southwest coast of Korea. Cretac. Res. 18, 515–544.
- Zimbelman, J.R., Johnston, A.K., 2002. New precision topographic measurements of the Carrizozo and McCartys basalt flows, New Mexico. In: New Mexico Geological Society Guidebook, 53rd Field Conference, Geology of White Sands, pp. 121–127.